Infrastructureless Pedestrian Positioning

Infrastrukturloser Fußgängerpositionierung

Dissertation an der Universität Bremen, Studiengang Informatik

zur Erlangung des akademischen Grades Doktor-Ingenieur (Dr.-Ing)

vorgelegt von ***Stéphane Beauregard*** am 3. April 2009

(Finale Fassung 30. August 2009)

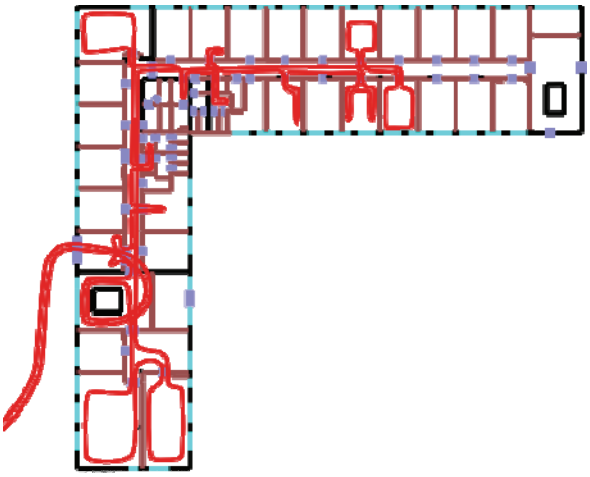

Erstgutachter: *Prof. Dr. Otthein Herzog*

Zweitgutachter: *Dr. Dirk Pesch, Cork Institute of Technology, Irland*

(Titelbildquelle: Mobile Research Center, Bremen)

Zusammenfassung der Dissertation

Es gibt viele Methoden zur Fußgänger-Navigation. So können GPS/ Galileo Satelliten Navigationssysteme in den meisten Fällen zufriedenstellende Positionsbestimmungen für Fußgänger liefern. Auch bestehende Kommunikationsinfrastrukturen wie Mobilfunknetze oder TV-Signale können für diesen Zweck herangezogen werden. Innerhalb von Gebäuden kann durch die Installation von Hochfrequenztechnik, Ultraschallsendern oder Lichtschranken für kleinere Räume und durch Transponder in großen Räumlichkeiten die Position bestimmt werden. Allerdings nutzen all diese Systeme Signale, deren exakter Wertebereich durch Schallschwächung, Blockierung, Reflektions- und Diffraktionseffekte erheblich reduziert oder verändert werden kann.

Inertialnavigationssysteme (INS) sind hingegen insofern „unabhängig“ als dass sie nicht auf extern übertragene Signale angewiesen sind. Daraus erklärt sich ihr großer Nutzen für Highend-Überwachung zu Land, Wasser und in der Luft sowie für Navigations- und Kontrollanwendungen, bei denen Abhängigkeit von externen Signalen entweder nicht umsetzbar ist oder riskant wäre. Leider ist die herkömmliche Inertialnavigation für die Fußgänger-Navigation ohne Anpassung nur von sehr begrenztem Nutzen. Für eine sinnvolle Obergrenze des Positionierungsfehlers im Meterbereich bei einigen Zehnerminuten unabhängiger Navigation wird ein hochgenaues INS oder sehr häufige zero-velocity-updates (ZUPTs) in Verbindung mit einem mindergenauen INS benötigt.

Diese Faktoren und die Tatsache, dass die Klasse der navigationsfähigen INS in der kommenden Dekade groß, teuer und energieintensiv bleiben werden, zeigt, dass die herkömmlichen Bauformen für die individuelle Navigation derzeit nicht einsetzbar sind.

Das Ziel dieser Arbeit ist zu untersuchen, wie mindergenaue, preisgünstige und energieeffiziente INS für die Fußgänger-Navigation und im Besonderen als Notrufsystem genutzt werden können.

Im ersten Schritt zeigt eine eingehende Betrachtung bisheriger Forschungsergebnisse die Vorzüge unterschiedlicher Technologien in Notfallszenarien und militärischen Anwendungen. Als nächstes wird eine Erweiterung der häufig beschrieben Fußgänger-Koppelnavigation (PDR) mit Beschleunigungssensoren im Kopfbereich und deren gute Leistung bei der Bestimmung der „Entfernung über Grund“ (DoG) gezeigt.

Da es bei einer Vielzahl von Bewegungsmustern nicht trivial ist, indirekte Schrittdetektion anzuwenden, wird das kurze Ruhen des Fußes beim Auftreten als eine Alternative analysiert. Mit einer am, später im, Schuhwerk installierten Inertial Measurement Unit (IMU) wird ein Sensor zur Bestimmung des omnidirektionalen Bewegungsmusters ermöglicht mit sehr guten DoG- und vertikal Schätzungen.

Unglücklicherweise werden bei einfachen Richtungsfiltern und durch magnetische Störungen innerhalb von Gebäuden große Sprünge in den Ausrichtungsangaben verursacht. Die vorliegende Arbeit zeigt, wie sich diese Ausrichtungsfehler modellieren und durch Mapfiltering mit bekannten Gebäudeinformationen reduzieren lassen.

Erklärung

Ich versichere hiermit, dass ich die vorliegende Arbeit selbstständig verfasst und keine anderen als die in Literaturverzeichnis angegebenen Quellen benutzt habe.

Stellen, die wörtlich oder sinngemäß aus veröffentlichten oder noch nicht veröffentlichten Quellen entnommen wurden, sind als solche kenntlich gemacht.

Die Zeichnungen oder Abbildungen in dieser Arbeit sind von mir selbst erstellt worden oder mit einen entsprechenden Quellennachweis versehen.

Diese Arbeit ist in gleicher oder ähnlicher Form bei keiner anderen Prüfungsbehörde eingereicht worden.

Bremen, den 3. April 2009

Stéphane Beauregard

Infrastructureless Pedestrian Positioning

Thesis submitted in partial fulfillment of the requirements of
the degree of Doktor-Ingenieur (Dr.-Ing) of the
Faculty of Mathematics and Informatics
University of Bremen, Bremen, Germany

by

Stéphane Beauregard

Submitted April 3, 2009
Final version July 30, 2009

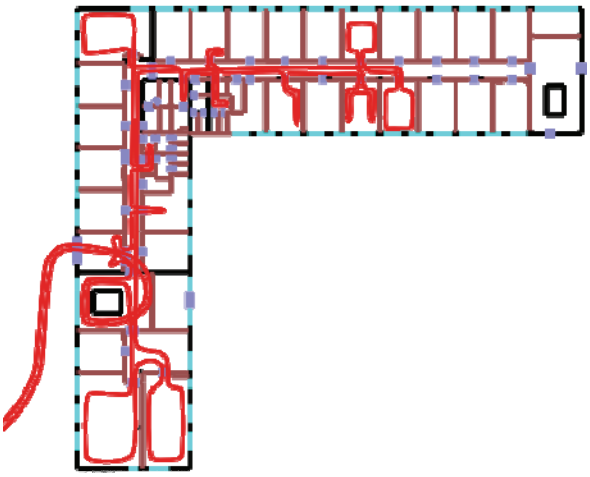

First reviewer: *Prof. Dr. Otthein Herzog*

Second reviewer: *Dr. Dirk Pesch, Cork Institute of Technology, Ireland*

(Title photo source: Mobile Research Center, Bremen)

Abstract

Many methods for pedestrian positioning exist. In outdoor environments, global satellite navigation systems such as GPS can give satisfactory positioning performance in many circumstances encountered by pedestrians. Pre-installed outdoor communication infrastructure, such as cellular networks or TV broadcast signals, can be leveraged for pedestrian uses. Specialized RF, ultrasound or light ranging beacons can also be installed indoors for positioning in spaces as small as individual rooms and networks of transponders can cover large installations. However, all these systems use transmitted signals that are subject to attenuation, blocking, reflection and diffraction effects, all of which can greatly reduce the accuracy and availability of range information.

In contrast, Inertial Navigation Systems (INS) are "sourceless" in that they do not rely on any external transmitted signals. This explains their great utility in high-end land, air, marine and space guidance, navigation and control systems, where depending on external signals for aiding purposes might be impractical or risky. Unfortunately, for pedestrian navigation, unaided traditional INSs are of limited use. If the upper limit to the position error is set to some reasonable value, say a few metres after some 10s of minutes of self-contained navigation, either a very accurate navigation-grade INS or very frequent zero velocity updates (ZUPTs) with a tactical-grade system are required. These realities, plus the fact that navigation-grade INSs will remain large, costly and power-hungry for at least another 10 years, means that traditional mechanization schemes for self-contained, personal navigation are currently impractical.

The overall objective of this thesis is to investigate how low-grade, low-cost, and low-power INSs can be exploited for pedestrian positioning and in particular for first responder scenarios. To begin, a thorough bibliography of past research permits the identification of the relative merits of various technologies that have been proposed for emergency, rescue and military operations. Next, an extension to the well-studied occurrential pedestrian dead reckoning (PDR) technique using headgear-mounted motion sensors is described and good distance over ground (DoG) estimation performance is demonstrated. Since it is not a simple matter to apply occurrential techniques to a large class of locomotion patterns, the foot-inertial technique is then explored as an alternative. With an IMU (Inertial Measurement Unit) attached to (and in the future, mounted in) footwear, simplified strapdown inertial navigation techniques allow for omnidirectional motion patterns, very good DoG estimates, and vertical excursion characterization. Unfortunately, large heading jumps occur indoors, caused by magnetic disturbances and by the use of a generic orientation filter. It is shown how these heading errors can be modeled and then mitigated via map filtering techniques running over minimal a priori building geometry information.

Acknowledgements

- I am very grateful to Prof. Dr. Otthein Herzog for his supervision as well as for providing me the financial means and intellectual freedom to pursue this topic within TZI.
- Prof. Dr. Michael Lawo's enthusiastic and positive outlook, regular high-level technical mentoring and other sound advice really kept me on course to the finish line. His tireless help with maddening administrative snafus mitigated many an apoplectic fit.
- Thanks go to Dr. Dirk Pesch, from the Cork Institute of Technology, who was kind enough to be the second reader of this thesis.
- I was very lucky to have Dr. Martin Klepal and Widyawan, also from Cork, as WearIT@Work project collaborators. It was a great pleasure working with them on the map filtering aspects of this thesis.
- Dr. Holger Kenn, the WearLab's post-doc, deserves a special mention for getting me into TZI and the WearIT@Work project in the first place. His well-meaning guidance will be fondly remembered.
- Financial support for this work came from the European Union via the FP6 IST WearIT@Work project (EC IST IP2003 0004216), managed by Prof. Dr. O. Herzog and Prof. Dr. M. Lawo.
- Prof. Bertrand Merminod of the TOPO lab at the *École Polytechnique Fédérale de Lausanne* is thanked for sponsoring a 3-month research visit by the author. It was great to learn from true navigation experts at the lab, in particular from Dr. Jan Skaloud.
- A preliminary phase of this work was funded in part by the BIS (Bremerhavener Gesellschaft für Innovationsförderung und Stadtentwicklung GmbH) within the T.i.M.E. program of the State of Bremen / Bremerhaven. It was overseen by Prof. Dr. Harald Haas while the author was at the International University Bremen (now Jacob's University). This support is hereby acknowledged.
- Last but not least, mega-bouquets to Mari Fernan for her life support during this ordeal.

Basic research is what I am doing when I don't know what I am doing.
Wernher von Braun, rocket scientist (1912 - 1977)

Relax, it's all been done before.
April Lavigne, pop singer (born 1984)

Table of Contents

List of Tables

Notation

Abbreviations and Acronyms

A-GPS	Assisted GPS
BPF	Backtracking Particle Filter
DARPA	Defense Advanced Research Projects Agency
DLR	Deutsches Zentrum für Luft- und Raumfahrt, the German center for air and space flight (research).
DoF	Degree of Freedom
DoG	Distance over Ground. For PDR experiments, the sum of the distance between successive footfalls.
DR	Dead Reckoning
EU	European Union
GNSS	Global Navigation Satellite System
GPS	Global Positioning System, a GNSS owned and operated by the U.S. Department of Defense. The official designation is the NAVSTAR GPS.
HDOP	Horizontal Dilution of Precision
HSGPS	High-sensitivity GPS
HUD	Heads-Up Display
IMES	Indoor MEssaging System. A pseudolite-like subsystem of the QZSS for indoor seamless positioning.
IMU	Inertial Measurement Unit. It is composed of 3 accelerometers and 3 (rate) gyros, sensing on orthogonal axes.
INS	Inertial Navigation System

ISM	Industrial, Scientific and Medical Band. Several bands are defined, the most used being centered at 2.45 GHz. Use is generally unlicensed.
LASER	Light Amplification by Stimulated Emission of Radiation
LORAN	LOng Range Aid to Navigation, a terrestrial radio navigation system using low frequency (100kHz) radio transmitters that uses multiple transmitters (multilateration) to determine location and/or speed of the receiver.
MCXO	Microprocessor-controlled Crystal Oscillator
MEMS	Microelectromechanical System
MF	Map Filtering
MOUT	Military Operations in Urban Terrain
NLOS	Non-Line-of-Sight
NN	Neural Network
PDR	Pedestrian Dead Reckoning
PF	Particle Filter
PL	Pseudolite, or pseudo-satellite. Ground-based GPS transmitters, originally used for testing.
PRN	Pseudo-random Number. Used in the GPS modulation scheme to uniquely identify individual satellites.
QZSS	Quasi-Zenith Satellite System. A Japanese GNSS.
RADAR	Radio Detection and Ranging
RF	Radio frequency
RFID	Radio-frequency Identification
RTK	Real-time Kinematic. A high-accuracy, carrier-phase-based GPS positioning method for moving platforms.
SLAM	Simultaneous Localization and Mapping
SONAR	Sound Navigation and Ranging
UKF	Unscented Kalman Filter
USAR	Urban Search and Rescue

UWB	Ultra-wideband. Radio communication technique using a large portion of the radio spectrum.
ZARU	Zero Attitude Rate Update
ZUPT	Zero Velocity Update

Symbols

g	Acceleration due to gravity at the Earth's surface, 9.8065 m/s^2
$\mathbf{R}_b^l$	Attitude matrix which does a rotation from body frame to local-level frame
$\mathbf{X}$	Bold, uppercase symbol indicates a matrix
$\mathbf{x}$	Bold, lowercase symbol indicates a vector
$\dot{x}$	First derivative
$\ddot{x}$	Second derivative

Chapter 1

Introduction

Many methods for pedestrian positioning exist. In outdoor environments, the GPS and Galileo satellite navigation systems can give satisfactory positioning performance in many circumstances encountered by pedestrians. Pre-installed outdoor communication infrastructure, such as cellular or TV broadcast signals, can be leveraged for pedestrian uses. Specialized RF, ultrasound or light ranging beacons can also be installed indoors for positioning in spaces as small as individual rooms and networks of transponders can cover large installations. However, all these systems use transmitted signals that are subject to attenuation, blocking, reflection and diffraction effects, all of which can greatly reduce the accuracy and availability of range information.

In contrast, Inertial Navigation Systems (INS) are "sourceless" in that they do not rely on any external transmitted signals. This explains their great utility in high-end land, air, marine and space guidance, navigation and control systems, where depending on external signals for aiding purposes might be impractical or risky. Unfortunately, for pedestrian navigation, unaided traditional INSs are of limited use. If the upper limit to the position error is set to some reasonable value, say a few metres after some tens of minutes of self-contained navigation, either a very accurate navigation-grade INS or very frequent zero velocity updates (ZUPTs) with a medium-grade system are required [38, 171]. These realities, plus the fact that navigation-grade INSs will remain large, costly and power-hungry for at least another 10 years, means that traditional mechanization schemes for self-contained, personal navigation are currently impractical. Low-cost INSs can be aided by GPS outdoors (and to a certain extent indoors by so-called "High-sensitivity GPS") but bridging reception outages beyond a few tens of seconds is very difficult [137, 246].

The overall objective of this thesis is to investigate how low-grade, low-cost, and low-power INSs can be exploited for pedestrian positioning and in particular for first responder scenarios. Meter-level accuracy, that is, localization at least to the level of specific rooms, is desired for this application domain.

1.1 The WearIT@Work Project

The research results presented in this document were developed in the context of the EU-funded WearIT@Work project (EC IST IP2003 0004216). Consequently, some motivational background is in order. The WearIT@Work project aimed to show that wearable computers are a viable technology concept for workers of the future [40]. In order for wearable computers to have pro-active capability and get the right information to the user at the right time (for example, a specific page of an assembly manual), the wearables must have "context awareness". That is, the wearables must be sensitive to general environmental conditions (ambient temperature, humidity, lighting) and to the user's physiological state (heart rate, stress level), current task (drilling, hammering) and body attitude. The location of the user, in absolute terms but more importantly relative to key landmarks, is a key context feature.

Within the WearIT@Work project, four different real-world scenarios were targeted for study. The goals of the wearable solution for each of the scenarios were as follows:

1. Emergency Response: Increase the safety of the firefighters via effective coordination and communication; Augment human senses

2. Production: Give permanent access to process and production information for the plant management, the service staff, and the assembly worker; Aggregate information; Integrate different and heterogeneous information sources

3. Maintenance: Support inspection, service and repair; Provide smart wearable manuals that are context sensitive and adaptive; Allow for authoring and gathering of information during maintenance

4. Healthcare: Coordinate the medical staff on ward rounds; Allow hands-free access to the controls of medical devices during examinations; Present process-related data to the physician

A number of alternative positioning technologies were explored as the requirements and constraints for the various scenarios vary greatly. In terms of positioning requirements, the last scenario is relatively unchallenging in its requirements and can make effective use of existing positioning techniques and systems. The Maintenance and Production scenarios are of intermediate difficulty. For these, the chosen positioning technology, particularly if it is RF-based, will have to operate in difficult propagation conditions. These are relatively non-standard environments that are quite different from the lab or office-cubicle environments where most positioning systems are evaluated and used. All things considered, however, the Emergency Response scenario is by far the most demanding and is a significant challenge to the state of the art. The positioning requirements for this scenario are the focus of this thesis.

1.2 Challenges

In many indoor application contexts, it is reasonable to assume that a pre-existing positioning infrastructure will be available. However, this will very likely not be the case during a building fire or other similar emergencies such as earthquakes and explosions. Also, one cannot assume that prior spatial knowledge, in the form of maps or building plans, will always be available or accurate. Consequently, various probabilistic position estimating techniques, such as particle filters, cannot be applied in the usual fashion. Finally, the operation of most sensors, such as visible light cameras, LASER, RADAR and SONAR, can be severely perturbed by smoke, vapour, open flames and heat [199]. While long-wave infrared cameras are used in some rescue operations, they are still expensive, specialized devices and are not likely to become available to the average firefighter in the near future. These facts would preclude the application of Simultaneous Localization And Mapping (SLAM) approaches, at least in the worst environmental conditions. A list of requirements for Emergency Rescue positioning systems can be found in [182]. Further analysis and discussion with WearIT@Work end users and partners (the Paris fire brigade, Rosenbauer) generated the following operating conditions, constraints and requirements:

- Operation in unknown and possibly damaged, irregular environments
- No access to pre-existing communication infrastructure, such as WiFi networks
- Possibly zero visibility (in visible spectrum)
- Bad RF propagation due to fire, humidity and NLOS propagation
- Bad Radar and Sonar propagation due to smoke, fire and humidity
- Very high availability and reliability
- Autonomy, that is no dependence on permanent communication links to external servers
- Accuracy requirement: <1 - 2 m position error
- Real-time calculation and fast update at >1 Hz
- Maximum distance from last absolute reference point: 50 - 500 m
- Low cost, that is under $\sim$1000 Euro per firefighter

Based on the results of an extensive literature review, it would appear that creating an infrastructure-less pedestrian positioning system satisfying these requirements is still an open engineering problem, see sections 2.4 and 2.5 in the next chapter. From the scientific perspective, only a few research groups are actively investigating this

domain and this particular formulation of the pedestrian positioning problem, see Section 2.3.

Accurate first responders position information would have additional benefits to the overall use case. It would simplify the derivation of additional, high-level "context" features such as escape routes, relative partner location, hazard areas (flames, collapsed floors, staircases), and victim positions. Locomotion capture and classification could support high-level activity recognition, for example distinguishing between moving, stationary, walking, running, climbing, and searching behaviours. This could be useful for firefighter health monitoring as well as for overall incident management. These are also interesting topics in the general area of wearable research. However, this thesis will be concerned with "context" only in terms of *position*.

1.3 Objectives and Definitions

For the purpose of this work, *infrastructure* is defined as pre-installed systems, such as cellular, WiFi and sensor-node networks, that can be used for used for positioning. It is assumed that such systems may not be available to first responder or public safety organizations during emergency incidents and cannot be counted upon. The only exceptions are GNSSs (Global Navigation Satellite Systems) such as GPS and Galileo which are assumed to be available outdoors, a reasonable assumption in peacetime, civilian (i.e., non-jammed) contexts. It is also assumed that map and building plan information, which could be used in map filtering algorithms, is not available at all or only partially available. Consequently, "infrastrutureless" is defined as making use of GNSSs when available outdoors plus other sourceless sensors for indoor use. In the present case, the latter are inertial sensors.

The goal then of the research presented herein is to enable infrastructureless indoor positioning with an accuracy better than room scale, a performance requirement for many emergency and "tactical" scenarios. Since most first responders and other workers wear some sort of uniform and possibly standard accessories like safety helmets and footwear, this thesis also investigates how inertial and other sensors could be incorporated into this clothing and thereby be made "wearable".

For those who not familiar with navigation terminology, Dead Reckoning (DR)[1] is a *relative* positioning technique. Starting from a known *absolute* location, successive displacements are added up. The displacement estimates can be in the form of changes in Cartesian coordinates (i.e., x and y coordinates) or more typically, in the form of heading and speed estimates. With sufficiently frequent absolute position updates (e.g., from GPS), dead reckoning's linearly growing position errors can be contained within pre-defined bounds.

[1]The term is the source of some minor etymological controversy. See `http://www.straightdope.com/columns/read/2053/is-dead-reckoning-short-for-deduced-reckoning` (link last visited 3/03/2009).

1.4 Thesis Outline

This document is structured as follows:

- An extensive literature review is provided in Chapter 2. As will become apparent, infrastructureless pedestrian positioning has been an active research domain since the early '80, when compact and low-power sensors and computers made man-portable systems possible. The domain is rapidly maturing, and working deployable system for first responders should appear commercially in the next few years, at the latest.

- Chapter 3 presents some results using "occurrential" Pedestrian Dead Reckoning (PDR) techniques with novel headwear-mounted sensors. This class of techniques is called "occurrential" since the inertial sensor measurements are used to *indirectly* detect the "occurrence" of steps as well as to estimate step lengths.

- In Chapter 4, an alternative to the occurrential PDR approach is presented. The "foot-inertial" approach involves attaching an Inertial Measurement Unit (IMU) to the foot and estimating the length of each step *directly* through strapdown inertial navigation algorithms. To limit the otherwise rapid position error growth, a so-called Zero Velocity Update (ZUPT) of the inertial system is done at each foot standstill. Step headings are estimated by a combination of inertial and magnetic measurements.

- In order to overcome the problem of inaccurate PDR headings indoors, map aiding with particle filters was investigated. The results, given in Chapter 5, show that minimal building plan information, easily obtained from aerial photographs, cadastres, escape plans, or other sources can be used with PDR step length and heading data to provide very useable position estimates in many cases.

- Chapter 6 concludes with a review of the thesis contributions and a list of directions in which these results could be extended in the immediate future.

- An extensive list of over 250 references consulted during the preparation of this thesis is provided in the Bibliography.

Chapter 2

Background and Related Work

Before describing the core experimental part of this thesis, it is important to provide a comprehensive context for this work. With the advent of GPS and of compact computer and inertial sensor systems in the 1980's, it started to become possible to envision man-carried systems for accurate positioning and near-real-time situational awareness. Since then, many techniques have been proposed to solve the ubiquitous pedestrian positioning problem. As will be seen, many of the approaches have significant fundamental or practical pitfalls. At the time of this writing, it cannot be said that this very difficult technical problem has been definitely solved. Therefore, in this chapter, an extensive bibliography and review of technologies and techniques related to personal and pedestrian positioning is presented.

2.1 RF-based Localization

In this section, an overview of relevant RF-based localization technologies is given. The ordering of the following sections is from the largest coverage (in the case of GNSSs, it is global) to the smallest coverage (RFID waypoint aiding at arm's length). As will be seen, the fundamental problems of multipath and attenuation are major stumbling blocks to good indoor and outdoor positioning using radio-frequency waves. Figure 2.1 gives an overview of the coverage of a wide range of RF positioning technologies and techniques.

2.1.1 GNSS

Global Navigation Satellite Systems (GNSSs) are made up of not only the well-known U.S. NAVSTAR Global Positioning System (GPS), but also the GLONASS (Russia), Galileo (Europe), Beidou/Compass (China), QZSS (Japan) and IRNSS (India) systems. When GNSS signals are available, absolute position fixes to within a few meters of ground truth can be attained using commodity, stand-alone, single-frequency receivers. Advanced post-processing techniques combining raw dual-frequency GNSS measurements from multiple reference stations can attain accuracies in the millimeter range for long, static dwell times [93], and in the decimeter range with in-

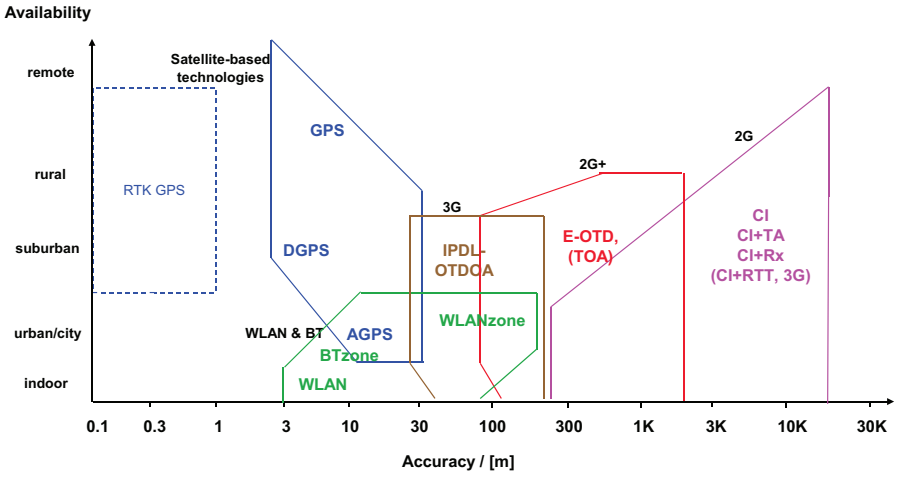

Figure 2.1: Comparison of RF Positioning Technologies (adapted from [215])

expensive, single-frequency commercial receivers [32, 73]. For moving rover receivers, differential corrections (obtained using the NTRIP protocol over any Internet connection [135], using the RASANT service over FM Radio Data Service in Germany [140], or using dedicated radio modem links) can be used for real-time kinematic (RTK) positioning in the decimeter range. This performance can be improved by sophisticated post-processing incorporating IMU measurements and forward-backward smoothing in time. Such techniques have been applied to air and ground vehicle tracking, to downhill skiing and motorcycle dynamics studies [226] as well as to pedestrian positioning [16].

Despite the astonishing accuracy often attained using GNSS outdoors, it is generally agreed that reception of GNSS signals in urban canyons and indoors is difficult and error prone [123]. Assisted-GPS (A-GPS) techniques can dramatically reduce satellite acquisition times via the use of aiding information supplied by cellular network operators. However, this does not help in the acquisition of extremely weak signals typically found indoors. High-sensitivity GPS (HSGPS) techniques can often provide position estimates indoors but these are generally poor [121] (with errors often greater than 50 m) and the required long integration times only work well if the receiver is stationary [122, 247]. The fundamental difficulties are due to receiver sensitivity and clock stability issues as well as due to harsh multipath environments [125, 124, 233, 171]. Encouraging recent results using tightly-integrated GPS/INS software receivers [234] demonstrate reception with 35-40 dB attenuation relative to the nominal, outdoor signal strength values. This is sufficient for reception quite deep indoors and in the future this level of performance might become possible for moving GPS/INS receivers. Nonetheless, at a recent workshop on precision personnel positioning [109], experts were of the opinion that neither existing nor planned GNSS systems would totally solve the indoor positioning problem. According to Lachapelle [123], even with new GNSS satellites (Galileo) and signals (L2C and L5) as well as future low-cost MEMS sensors and their ultra-tight integration with

HSGPS, it will still be very difficult to get consistent accuracy indoors better than 10 m. Additional position aiding, such as from in-building instrumentation, short-range RF/acoustic ranging devices, and 3D maps of buildings will likely be required. Despite these limitations, the existing GNSS infrastructure and proven accuracy will continue to make GNSSs an attractive component of indoor positioning system and particularly for the short outdoor sections that are likely to be part of most rescue missions.

Pseudolites and Reradiators

For short-range aiding of GNSS receivers, it is in principle possible to use so-called Pseudolites, or pseudo-satellites (PLs). PLs are non-orbiting transmitters of GPS signals that were originally developed for ground tests [48]. An excellent review of pseudolite technology can be found in Wang [228]. The basic idea of PLs is that a range of satellite IDs (33 to 37) and the associated pseudo-random number (PRN) spreading codes were reserved for initial GPS tests and this information can be used in GPS receivers with only minor changes to firmware. PLs transmit dummy orbital parameters so that the receiver can correctly incorporate the pseudorange measurements into standard navigation algorithms. Close and tight coupling of GPS, INS, and PLs [229, 245, 134, 26] are possible. Unfortunately, there are several major issues with PLs that prevent their widespread adoption [103]. The electronics required to generate the signal are quite complicated. The "near/far problem", where a strong "near" transmitter completely overwhelms weaker "far" one, has to be addressed. It can be solved by pulsing the pseudolite with a low duty cycle or by special cancellation algorithms in the receiver [141, 91] (which are non-standard at this time). Great care must be taken in order to satisfy national and international standards for RF emissions in the protected GNSS bands and special permits are often required. In another variant of pseudolites, the Japanese QZSS GNSS will provide the Indoor MEssaging System (IMES) for seamless indoor and outdoor positioning in difficult environments [53]. The IMES signals will be transmitted by geolocated L1 band transmitters spaced at separations of 20-30 m. Unfortunately, the IMES messages will only provide the transmitter ID and their own position and will not offer any ranging capability so the positioning accuracy will be quite limited. The IMES system is still in its infancy and issues of infrastructure cost, interference with weak GNSS, jamming of adjacent IMES transmitters and security (e.g., tampering and spoofing) have yet to be addressed .

There have been a few commercial ventures in this area. The Naviva NAVIndoor [155] is one commercial offering, but at 30-40k Euro for 6-8 pseudolites and a control station, it is not likely to sell well. The use of pseudolites indoors has been described in [107, 157, 227]. Unfortunately, the C/A (coarse/acquisition) code chipping rate used in GPS is not sufficiently high to resolve closely-spaced multipath components and so non-standard correlation and multipath mitigation algorithms are required. PL carrier-phase information could in principle also be exploited [172] but this is "beating a dead horse". Consequently, pseudolites in their present form are unlikely to be a viable solution for indoor navigation applications.

PLs are not to be confused with repeaters and "Reradiators", which simply receive, amplify and relay the entire GPS L1 band to a remote transmitting antenna. For example, signals captured above ground can be reradiated in a tunnel. The typical application is time and frequency transfer and it is not clear if accurate positioning can really be made to work [97]. The use of reradiators and repeaters is prohibited in the EU.

2.1.2 Communication Network Positioning

If signals from existing outdoor communication infrastructure (i.e., GSM and/or UMTS networks) can be detected, they could be used opportunistically for indoor positioning [32]. Technically, it has proven to be very difficult to do so. For example, positioning errors in cellular systems can be on the order of the cell radius, even outdoors. For many envisioned indoor positioning applications, a maximal positioning error of 5-10 m (i.e., room scale) is required. Unfortunately, performance is ultimately limited by a single phenomenon: RF multipath. Positioning relies on the ability to determine a direct path range from a number of reference points to a mobile user. Within indoor environments, the received signal strength of indirect paths is often larger than that of direct paths, often resulting in undetected direct paths and detected indirect paths [167]. As can be seen in Figure 2.1, if one discounts the infrastructure-based wireless LAN and Bluetooth technologies, the estimated indoor accuracy is 30-50 m using IPDL-OTDOA (Observed time difference of arrival with Idle Period on the Downlink) in 3G networks. Therefore, improvement to the left boundary of the 3G zone will be needed. Higher accuracy is of course desirable but it is technically very difficult to attain using the existing outdoor RF communication infrastructure.

Public broadcast signals can also be used for positioning. The US firm Rosum holds a number of key patents on using analog and digital TV signals for positioning purposes [180]. The advantage of these signals is their high power, low frequency (for good penetration into buildings) and large bandwidth (range measurements from multiple 6 MHz channels could be combined). The European DVB-T system has the added advantage that a timing pulse synchronized to the GPS second pulse is transmitted several times per second. Presumably the upcoming US digital TV broadcast standard will also include such a time pulse. Both of these can be in principle be used for range estimation. Unfortunately, signals from these systems suffer from exactly the same indoor performance limitations as outlined above and so will likely result in ranging errors on the order of tens of meters or more.

The disadvantage of using broadcast and cellular communication systems for positioning (whether indoor or outdoors) is that the horizontal positioning accuracy is very much dependent on the number and geometrical layout of the transmission towers. Operators of such systems place their towers so as to optimize coverage and minimize costs, which is exactly the opposite of what one would want for positioning. In conclusion then, outdoor communication systems can be used in an opportunistic way to provide general purpose, low-accuracy (i.e., mass market and consumer) posi-

tioning services, particularly in combination with GPS *outdoors* (for example, using the patented eGPS technology [194]). However, none of the published approaches are likely to be sufficiently accurate for *indoor* emergency / rescue scenarios.

With regards to indoor wireless communication networks, such as WLANs, WSNs and Bluetooth, there is an extensive body of research on using RF signal measurements, pattern matching, map filtering techniques and motion modeling for positioning purposes [167, 240, 239]. Most often, the RSSI (less often range values [179] or the channel impulse responses [147]) are compared to a "fingerprint" or "signature" database of these values, collected during a measurement campaign and/or estimated with RF propagation models [166, 88, 113]. State-of-the-art systems give better than room-level accuracy or on the order of 2-3 m positioning error. Unfortunately, at typical transmission wavelengths, the RSSI and other channel measurements are very sensitive to changes in the propagation environment, for example if furniture is rearranged or if there are people or vehicles moving around. Also, for the target application of first responder positioning, it is quite unrealistic to suppose that local wireless communication infrastructures will be operational during emergencies and that building RF signature databases would be accessible.

2.1.3 Local Positioning Systems

Local positioning systems (LPSs) are those systems that could be used temporarily around emergency sites. LPSs transceivers could be installed permanently on fire/emergency vehicles, set up by emergency crews on the ground, or they could be part of a wider, ad hoc emergency/tactical communication network.

An example of such a system is the commercial Locata technology. This is basically a network of pseudolites but operating in the 2.4 GHz ISM band [29, 190]. This choice of frequency circumvents the regulatory issues involved with pseudolite operation in the L1 GPS band. Much higher transmission power than GPS plus special signal structures allow for better penetration into buildings and for mitigation of multipath effects. Locata receivers use commodity GPS chipsets in combination with a modified RF front-end to tune into the ISM band rather than the L1 band. Note that good GPS reception at one or more transceivers is required to self-survey and synchronize the network. A similar approach geared purely toward indoor geolocation has been proposed by Progri et al. [175, 176, 178]. Other local positioning system include the Novariant Terralite XPS, which combines the classic L1/L2 PL approach with additional proprietary transmissions on non-GPS bands; the ENSCO Ranger, which uses 2.4 and 5.9 GHz band Direct-Sequence Spread Spectrum (DSSS) signals; and the WITRAK system from Fraunhofer IIS. While these approaches are interesting, they have not yet taken off commercially, likely because of high system costs.

Some US military tactical radios use special modulation and synchronization schemes and can provide peer-to-peer range measurement capability even indoors [181, 145]. Maximal indoor positioning error is reported to be 4 m but no details on the test conditions are available. It would be interesting for civil defense, emergency

and fire organization to have access to this technology. However, this is problematic given the national security issues involved with using protected military technology.

2.1.4 UWB

There has been much hype in the last decade about Ultra-wideband (UWB) radio for communication as well as for positioning. Initial reports on using so-called impulse UWB for asset tracking showed that it does not really work all that well [69, 68, 70], particularly in indoor environments where there is a lot of multipath and NLOS conditions (e.g., in a ship's gangways or in container storage areas). An alternative more recent approach to impulse UWB modulation is to split a very wide band (> 80 MHz) into subbands and to use a multicarrier scheme like OFDM [175], frequency hopping plus DSSS [86], or even chirped waveforms in each band individually. By careful management of the subband use, one can avoid interfering with other communication systems. While positioning performance of some research systems is quite good in static, controlled conditions [86, 46], it is not clear that these results will transfer well to real indoor emergency conditions. One operational constraint is that UWB beacons would have to be deployed around the emergency site with good geometry and then left some time to synchronize and self-survey. It is not clear if rescue organizations would be willing to adapt their intervention procedures to this end. Consequently, it may be more practical to use a smaller number of UWB transceivers mounted on emergency vehicles and to augment the UWB position estimates with other information rather than try to get good position estimates from UWB ranges alone in all circumstances. This would be particularly true for mixed outdoor/indoor scenarios. For example, the multicarrier UWB positioning system from WPI [51] has been fused with IMU measurements [21] for improved accuracy while EPFL researchers have fused UWB range estimates with PDR displacement estimates [185].

2.1.5 Sensor Node Aiding

RF/ultrasonic ranging nodes, dropped or thrown some distance into the smoke and fire, have been proposed as navigation aids and in some cases as position aiding devices to be used in conjunction with PDR [67, 8]. However, there are a number of practical issues that have not been examined in any real detail in the literature on first responder systems (for example, in [112]). First of all, in many research prototypes up to now, a combination of RF and ultrasound signals have been used for ranging, like in the Cricket system [174]. Ultrasound signalling is not appropriate for emergency scenarios due to distortions from temperature gradients, air currents and ambient noise. Also, in typical indoor environments, range and direction of arrival estimates can be very poor due to multipath and reverberation effects. The location of the ultrasonic transducer on the first responder will probably have a critical influence on ranging performance: placing it on the boot [67] is probably the worst possible option. Second, most studies on sensor node-based positioning

assume a relatively uniform and dense distribution of nodes over a wide space (for a discussion of the algorithmic challenges, see [198]). Unfortunately, many rescue scenarios involve long corridors or other narrow spaces. In these situations, the sensor nodes will be deployed mostly in a line, with a resultant high horizontal dilution of precision (HDOP). Third, it is often assumed that the nodes can be deployed "on the fly" and autocalibrate their positions. Unfortunately, 2D autocalibration algorithms work properly only if sufficiently dense and accurate mutual ranges between nodes are available. These conditions will rarely be satisfied given the difficult RF and ultrasound propagation condition likely to be found in fires. And finally, very little consideration has been given to cost (how many nodes), maintenance (batteries), deployment (fireman cognitive overload), safety (walking hazard, explosion), and recovery/recycling/disposal issues. All these issues were ignored in an early study on deployable pseudolites for emergency and rescue operations [177]. Consequently, the author does not feel that deployable sensor nodes will be viable for positioning purposes in first responder scenarios, and certainly not with the current low-cost RF/ultrasound technology. A small number long-range radar transponder nodes [225] deployed by the firefighter might make more sense, but these devices have yet to be tested under realistic fire conditions.

2.1.6 RFID Waypoint Aiding

Radio-frequency identification (RFID) is an automatic identification method, relying on storing and remotely retrieving data using devices called RFID tags or transponders. RFID tags are small electronic devices that can be attached to or embedded in documents, cards, animals, or other assets. Originally, this was done for the purpose of identification, tracking or inventory keeping, but the technology has spread to various access control functions, such as electronic door keys. The tags can be used to store information related to the tracked item and the tags typically have very little or no processing capacity. The data can be read out and possibly modified by a RFID reader. The tags are divided into two basics types: the active type, which contains a battery, and the passive type, which has no battery. Active tags can be read at a range of a few meters. (It was reported that 433MHz tags can be read at distance of up to 30 m [150]). Passive tags must be close to the reader's transmitting antenna in order to capture enough energy to power the tags' on-board electronics. Passive tags are typically interrogated while in the near field of the reader's antenna, that is well below one wavelength of the RF link. Ranges of up to 20 m are possible by using longer wavelengths, large antenna arrays and higher transmission power. However, useful ranges with handheld readers without these features is quite short [111]. With regards to location, a very approximate tag distance could in principle be estimated via round trip time-of-flight measurements but positions estimation would in addition require angle-of-arrival estimate using, for example an antenna array. The author knows of no compact handheld RFID reader that can provide angle-of-arrival estimates, let alone position estimates. As an example of the state of the art in this domain, the method described in [241] matches tag detection pat-

terns under different signal attenuation levels to a database of detection patterns, attenuation's and distances from a base station reader. This approach is impractical for firefighting since the "fingerprint" database would have to be established ahead of time via a measurement campaign.

The "philosophy" of most RFID-assisted positioning systems involves reducing the dependence on unreliable RF links to external data sources by exploiting the capability of RFID tags to store critical building information for retrieval. This philosophy can also involve the use of tags as fixed, geolocated waypoints for navigation purposes. For example, in the SARHA project [236], short-range RFID-like transponders provided ID and absolute position information [183]. While RFID tags may be useful in less demanding scenarios, like tracking nightwatchmen as they do their rounds, this author does not feel they are a practical solution for the firefighting scenario for the following reasons. If passive tags are used, the fireman would have come close enough to place a reader directly on the tags. If the pre-stored geolocation information (read from the tag using a fireman-carried reader) is correct, then it could used to update an icon on the commander's map and be fed into a position estimating filter (if there is one) as position update. However, if the stored information is actually wrong, then the situational coherence is actually diminished and filter position estimates could become even more unreliable. Otherwise, if the fireman can recognize that the tags are not properly geolocated, then he has to uniquely identify the waypoint by interacting with a detailed map (for example, on a heads-up-display). In practice, this would amount to a manual position update triggered by the user and may be operationally untenable.

To be of use, the tags have to be geolocated to quite high precision, possibly to within 1 m of the true geographical coordinates. However, this is a tall order. As a case in point, in [42, 151, 150], RFID tags are assumed to be deployed ahead of time in a building at known locations and properly geolocated. As an example of notoriously time-consuming and error-prone geolocation can be, in [151], the test building corner coordinates were determined from the Google Earth interface. Due to parallax, landmarks on Google Earth aerial and satellite images can be off by many meters relative to their true coordinates. These coordinates (in WGS84, degrees latitude and longitude) were then converted to a local level Cartesian coordinate frame (UTM, meters). This step is also error prone, especially when insufficient significant figures in the latitude/longitude values or the wrong grid conversion parameters are used. The interior waypoints and candidate positions for RFID tags were then determined as offsets from the building corners. It was later discovered that the calculated coordinates of the building corners were in fact wrong. The authors had to resort to the detailed CAD drawing of their building to manually determine the interior waypoint locations (but only in the drawing coordinate frame). Based on this example, it is difficult to imagine a large number of buildings ever being surveyed and equipped with geolocated RFID tags, not least because of the installation costs and of the difficulties in agreeing on a standardized data format for the tags.

In [187], the use of RFID tags was more like the idea of a deployable waypoints.

The first leading fireman, equipped with a MEMS-based positioning system, deploys the RFID tags while he is progressing indoors to reach the fire or victims. When the RFID tags are deployed, their positions have to be known and which therefore implies the existence of a database providing the geographical coordinates. The fireman (or someone else) has to match up the MEMS/fireman estimated position with a landmark on a map and associate it the newly deployed tag. This is no simple matter in the "heat" of a fire. If the tags cannot be correctly geolocated, then one could alternatively view these deployed RFID tags as "breadcrumbs" to follow to get back out of the building. It does however assume that the RFID tags, and especially the passive ones, can actually be found again in the presence of smoke and under stress.

2.2 Commercial Products

There are a number of patents and commercial products using various sensors for speed/distance estimation for walkers and runners. It is not clear how or even whether the described methods could be extended to suit fire fighting positioning needs. They are nonetheless reviewed here not least because the price points of these consumer items are well within the cost envelope of public safety organizations.

The Nike/Apple in-shoe 1D accelerometer is a step/stride time interval detector, see Figure 2.2(a). With a user-specific look-up table, step/stride length can be estimated. The shoe sensor communicates wirelessly with the iPod, where pace, distance and workout information is stored and optionally provided to the user via the iPod's user interfaces. In the near future, the GPS-equipped iPhones may also be able to decode the information from the foot pod and fuse it with the measurements from the phone's internal 3D accelerometers and magnetometers. In this case, much more sophisticated tracking and navigation applications will become possible (at least outdoors).

The firms Polar, Suunto and Garmin all market products based on a foot pod that attaches to the shoe laces. The Dynastream SpeedMax technology[1] is based on a pod with two parallel offset 2D accelerometers that measure accelerations in the sagittal plane [1]. A DSP computes the foot angle and the resultant acceleration in the direction of travel at high frequency over the stride, see figures 2.2(b) and 2.2(c). These data are integrated for every stride to provide the running speed and distance in real time to the user (see [210] and [72] for detailed descriptions of the estimation principle). Without calibration, the approach is 97% accurate in terms of distance travelled for a wide population of users and over a large range of gait velocities, from slow walk to full run. Since the exact trajectory of the foot is somewhat user dependent, calibration can be done to increase the accuracy to around 99% [2]. Only in a research prototype was magnetic heading and thus navigation available [211, 212]. Consequently, for the standard foot pod systems, course information can only be provided by a GPS receiver, integrated into a wristwatch or carried in an

[1]Note that the firm is now owned by Garmin, a leading GPS receiver manufacturer.

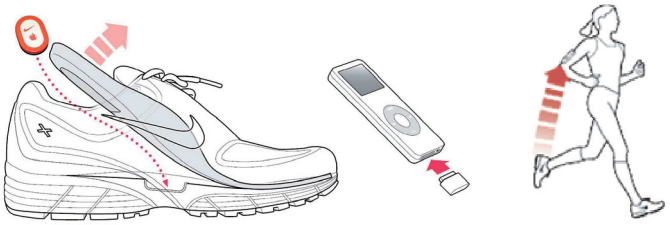

(a) Nike+ sensor and Apple iPod

(b) Suunto foot pod and Garmin GPS watch

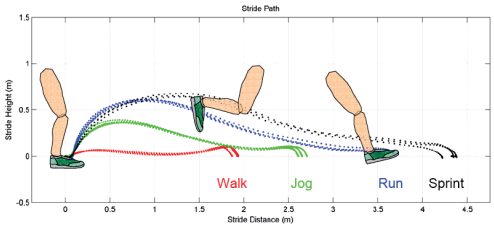

(c) SpeedMax stride length estimation principle

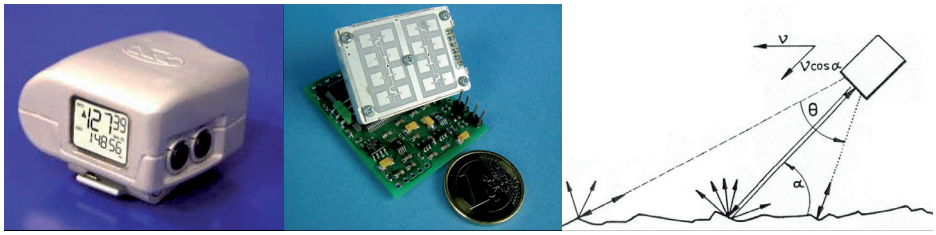

(d) CycloSport RDS (Radar Distance Speed) product

Figure 2.2: Examples of commercial speed and distance sensors and accessories for running and walking. See text for detailed description. (Sources: a) adapted from [3]; b) adapted from [6] and [75]; c) [1], p. 4; d) [235], p. 3 and p. 1)

armband case, for example. All products also have heart rate measurement chest straps.

Figure 2.2(d) depicts the CycloSport Radar Speed Distance (or RDS) product, developed under contract by Fraunhofer IIS [235]. It works using the Doppler frequency shift principle as measured via a low-cost continuous wave radar module. In the author's evaluations, the device works quite well for walking, yielding an error of about 1-2% of the distance travelled. Unfortunately, this approach has problems. The device needs to be calibrated to compensate for sensor height above ground. It is also sensitive to changes in the angle between the radar beam and the ground. It does not work very well for running since these values can change depending on speed[2]. Despite these obvious problems, radar velocimeters have nonetheless been used in several military integrated systems (see Section 2.5 below).

Multicomponent devices are difficult to sell to consumers. Consequently the trend in the near future will be towards more highly integrated devices. For example, for sports, a wristwatch with inertial, barometric, 3D compass and GPS sensors could very well become the norm in a few years. Handsets will likely follow the same integration path. In both cases, sensor fusion algorithms and other a priori (e.g., map) information will likely be required for good positioning performance, particularly indoors.

2.3 Research Platforms

There are have been several attempts to use multi-sensor fusion techniques in research project addressing indoor pedestrian localization needs. The NavMote system [63] used relatively standard occurrential PDR algorithms and a magnetic compass for heading as well as wireless telemetry and map matching procedures. As a result of the low-power design, very little computational power was available on the worn sensors. Preprocessed displacement data (i.e., step length and direction) were sent over a multi-hop wireless sensor node network to a server for further processing. When the tracked person was out of range of the network, displacement data was buffered locally. Positions estimates were calculated in a delayed fashion when the tracked person came back into range of the (dense) Berkely Mote wireless sensor node network. Good distance over ground accuracy is reported ($\sim$3% error) but indoor trajectories were affected by magnetic heading perturbations.

The NAVIO project (Pedestrian *Navi*gation Systems in Combined *I*ndoor / *O*utdoor Environments) [188] used WLAN RF fingerprinting plus a pedestrian dead reckoning module (a DRM III from Honeywell) attached to the small of the back, a digital compass, and pressure sensor, see Figure 2.3(a). Knowledge-based preprocessing (i.e., a rule base and an inference engine) selected the most useful sensor outputs at each moment. Outliers, such as GPS position fixes with high GDOP (Geometrical Dilution of Precision), were rejected. The selected measurements were then fused in a Kalman filter, providing position, speed and heading in three di-

[2]It is therefore not surprising that the product is no longer on the market.

mensions. Interestingly, the motion model included linear and radial acceleration states, useful for following pedestrian stop/go and turning behaviours. Standard deviations in the range of a few meters in 3D were achieved in urban areas, including urban canyons, and height estimates from the barometer measurements had errors around 1 m. It was found that 150-200 m GPS outages could be effectively bridged by the DR sensors. The ESA[3] project SHADE[4] [15, 232] used the same kind of PDR sensors and approach, and demonstrated roughly the same level of positioning accuracy. Part of the project used a portable LORAN receiver. In urban canyons and in almost all indoors setting, the LORAN signals could be tracked but these often resulted in invalid position solutions, with errors up to several hundred meters [165]. The SARHA system [236] is another example of such an occurrential PDR system, using commodity IMU and GPS units plus a barometer (Fig. 2.3(b)). Drifty DR positions were corrected via absolute position fixes retrieved from preinstalled transponders (with capabilities similar to active RFID tags). In the Pena project [195], step length estimates from ultrasonic foot-to-foot range measurements were fused with 2D laser scanner measurements using SLAM techniques, see Figure 2.3(c).

In an project sponsored by Vectronics and carried out by the TOPO laboratory at the *École Polytechnique Fédérale de Lausanne*, a pedestrian tracking system using multiple IMUs was developed [187], see Figure 2.4. The research goal of the Enhanced Dead Reckoning Device (EDRD) was to get around the limitations of basic occurrential systems like the DRM (Honeywell) and the CNM (Vectronics). In particular, personal calibration was to be avoided and a wider range of walking behaviours as well as postures were to be recognized. The chosen approach used *a priori* biomechanical models [52] and fuzzy logic classification of preprocessed inertial measurements [222]. Step lengths were calculated by a simple inverse segment model during a specific phase of the gait cycle. Walking direction was inferred from the 3D magnetic field sensor and the yaw-axis gyro on the upper body. Vertical displacements, i.e., steps up stairs, were recognized via the patterns in shank rotation and acceleration rates. Measurements from this multi-IMU set up were fused with GPS for seamless indoor/outdoor positioning. Tests [46] showed very good positioning performance but the heading estimate was susceptible to local magnetic disturbances from building metallic structural components, piping, electrical equipment, etc. (however much less so than the foot-mounted IMU, see Chapter 4). Given the complexity of this particular multi-component system, it is not at all clear whether it would be accepted by the targeted end users (i.e., first responders or soldiers).

The "man-motion" system designed by QinetiQ of the UK, described in [144], is a combination of a proprietary military GPS receiver, a BAE SiIMU MEMS IMU, a 3D magnetometer, a barometer and a manual ZUPT indicator, see Figure 2.3(d). Classic GPS/INS algorithms and altitude matching were used. Initially, occurrential PDR methods were exploited by detecting steps from the body-mounted IMU. How-

[3]European Space Agency

[4]SHADE is an acronym for "Special Handheld Applications in Difficult Environments".

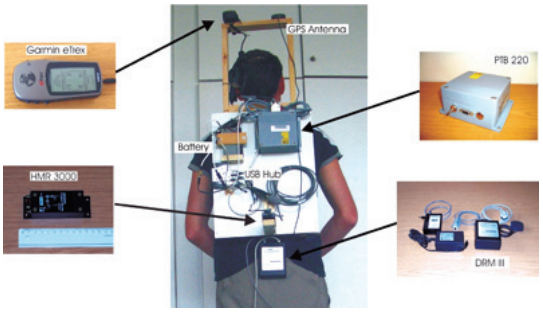

(a) NAVIO

(b) SARHA

(c) PENA

(d) QinetiQ

Figure 2.3: Integrated Pedestrian Positioning Research Platforms. See text for descriptions. (Sources: a) [188], p. 552; b) [236], p. 2; c) [4]; d) [81], p. 6)

ever, a fixed step length was assumed. In a later publication [81], the system was extended to use the step interval time, the variance of the magnitude of the specific forces and slope value (estimated from barometrically-corrected INS solutions) in the step-length estimator. This set-up was compared to an approach using a foot-mounted IMU. While distance over ground results were good, trajectories using the foot-mounted IMU showed some anomalies due to the fact that the magnetometer was body mounted and not aligned with the foot.

2.4 First Responder Systems

At the time of this writing, there were very few working integrated positioning and situational awareness systems for first responders. One American company, ENSCO, is developing the Mobile Response Command System (MRCS)[5][217]. The first-responder-carried sensor suite is very similar to the one proposed in the WearIT@Work Emergency/Rescue scenario, with a foot-mounted PDR subsystem, a heads-up display and a helmet-mounted camera, see Figure 2.5(a). Deployable external ranging beacons (called "smart cones") are presumably geolocated using GPS. "Wireless Network Extenders" can be distributed around the incident site for data relay and for augmenting PDR estimates via range estimates. An Incident Commander Sys-

[5]Developed in collaboration with Rex Systems Inc.

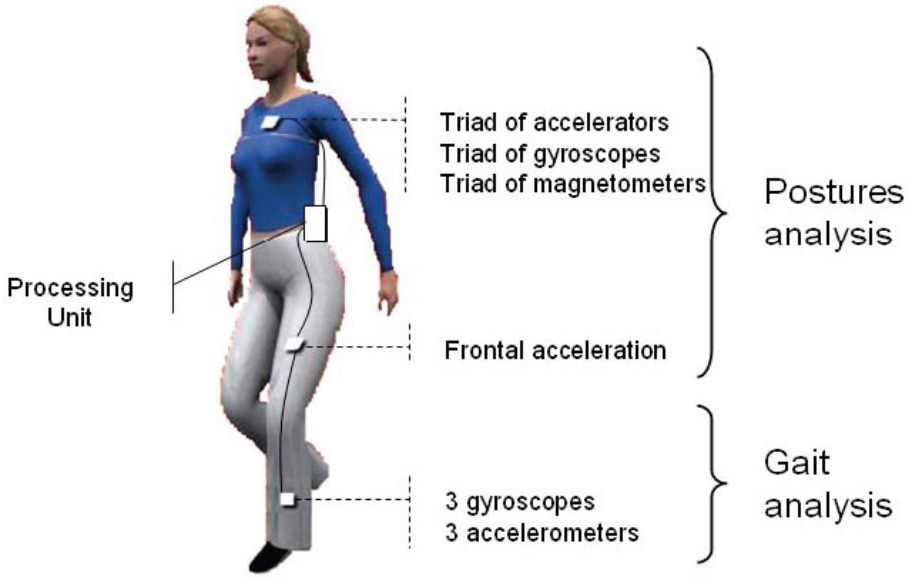

Figure 2.4: Enhanced Dead Reckoning Device. ([186], p. 36)

tem has also been designed and tested, see Figure 2.5(b). Another American firm, TRX Systems, recently described its "Sentinel" firefighter tracking system [218]. The devices carried by the firefighter includes GPS, inertial, barometric sensors plus a RF sensor node (Zigbee) interface. Judging from system diagrams, the author speculates that occurrential PDR techniques are being used with the belt-mounted "inertial navigation unit" along with RF ranging or fingerprinting techniques. Map filtering, on-the-fly map building based on historical path data, and GIS overlay features have been presented. Impressive full system test results were reported, with less than 3 m position error after 25 minutes of displacement in a deep indoor scenario. As the software and GUI interfaces for both these systems seem quite far along in their development cycles, commercial deployment in the next year or two seems likely.

In the research domain, only partial first-responder systems or individual subsystems have been presented or demonstrated. A group at DLR (*Deutsches Zentrum für Luft- und Raumfahrt*) has presented papers on foot-mounted IMUs, map filtering and rescue team coordination [23, 115, 116] but these results seem to be quite far from actual deployment. The LoCoSS project [50] used an occurrential PDR approach plus grid-based map filtering. In both projects, only single test runs were shown, so it is not possible to say if the performance on these tests was representative. A standard for electronic search and rescue maps was proposed in the context of the Pelote project [11]. The proposal was very close to current ISO, EU and German standards and the data was structured in such a way (i.e. using Extensible Markup Language, or XML) that it could be imported directly into map-aided positioning systems. Interestingly, the proposal included provisions for localization beacon icons and a beacon layer.

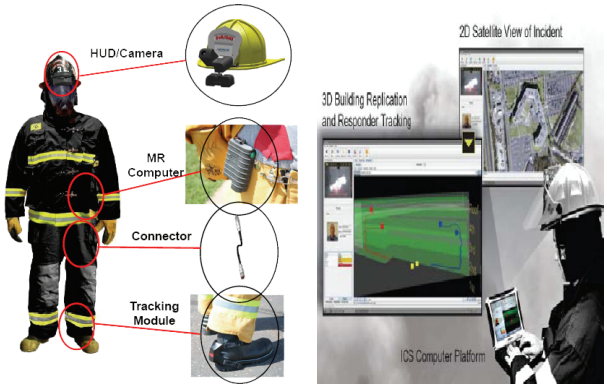

(a) Fireman System (b) Commander System

Figure 2.5: ENSCO Mobile Response Command System. ([217], p. 2-3).

The NIST[6] Building Tactical Information project [92] aims to develop technology and standards for making real-time building information accessible to emergency responders to enable safer and more efficient interventions. The project addresses both the information needs of the fire, police and emergency medical services and the technology needed for moving building data out to emergency responders. An offshoot of the project looked at how existing building information infrastructure could be used for storing static building plans as well as for gathering sensor information such as temperature and presence via HVAC[7], security, access control subsystems [223]. The Precision Rescue Personnel Location and Tracking research project [151, 150], also at NIST, used a Honeywell DRM and geolocated RFID tags for waypoint-assisted navigation indoors. Without using the waypoints, performance in the indoor tests is as one would expect, with local magnetic perturbations causing heading errors and the lack of GPS preventing good step length model calibration. Using waypoint information about every 15 m (!) along the ∼200 m test tracks, the stride length and heading were corrected using a simple position update algorithm for much better performance. The obvious practical difficulties of installing and geolocating such a dense collection of RFID waypoint tags ahead of time and of locating them in a smoky fire were ignored, however.

2.5 Military Systems

Because there is a large overlap with the requirements for first responder applications, and consequently also in the possible technical solutions, military personnel positioning systems are reviewed here. There are, of course, some differences between first responder and military positioning systems:

- For military systems, a larger fraction of the total missions time is likely to be

[6]National Institute of Science and Technology
[7]Heating, Ventilation, and Air Conditioning

spent outdoors

- Because there is more outdoor time, more emphasis can be put on using GNSSs, and in particular on advanced signal processing techniques for multipath mitigation and anti-jam functions

- Smart military tactical radios (i.e., "cognitive radios") can be leveraged to give peer-to-peer range information, which is difficult to do with current standardized police radios (e.g., Tetra)

- R&D budgets for the military are likely higher

- The targeted unit costs for military users are very likely higher than those for public safety users.

DARPA SNIPER

One of the earliest examples of a system designed for urban and indoor military use is the DARPA-funded SNIPER project [95]. The goal was to demonstrate a tightly-coupled GPS/INS/Loran system with a 5 m accuracy in mountainous areas and forested terrain, and a 10 m accuracy in an urban environment. The sensor suite consisted of a tactical-grade IMU, a digital LORAN sensor, and a state-of-the-art Microprocessor-Controlled Crystal Oscillator (MCXO) frequency reference and a commercial avionics GPS receiver (with analog correlators!). Differential GPS corrections as well as navigation data were transferred to and from a commander station via a VHF radio modem link. All these systems as well as hefty batteries giving 2 hours of autonomy were mounted in a relatively large backpack. Particular attention was paid to synchronizing the Loran and GPS subsystems to the nanosecond level. All measurements were used in a closely-coupled configuration. The system was demonstrated in 1998 in a series of Small Unit Operation scenarios at a government MOUT (Military Operations in Urban Terrain) test facility. Weakness and distortion of LORAN signals in urban canyons and indoors[8] as well as the slow response of the receiver to rapid changes in orientation severely limited the usefulness of the Time-of-Arrival measurements from this subsystem[9]. It was not possible to use the MEMS IMU-only mode for indoor sections due to the immaturity of MEMS technology at the time. Consequently, only the 2.5 kg and 15 W tactical-grade IMU with fiber-optic gyros was used. Overall, the test results showed that the 5 m goal outdoors could be achieved but that the 10 m urban/indoor goal was problematic.

[8] For a detailed explanation of the phenomena, see [169].

[9] These conclusions were later echoed in a follow-on 2004 Request for Proposals for a handheld, Loran-C capable positioning system [9].

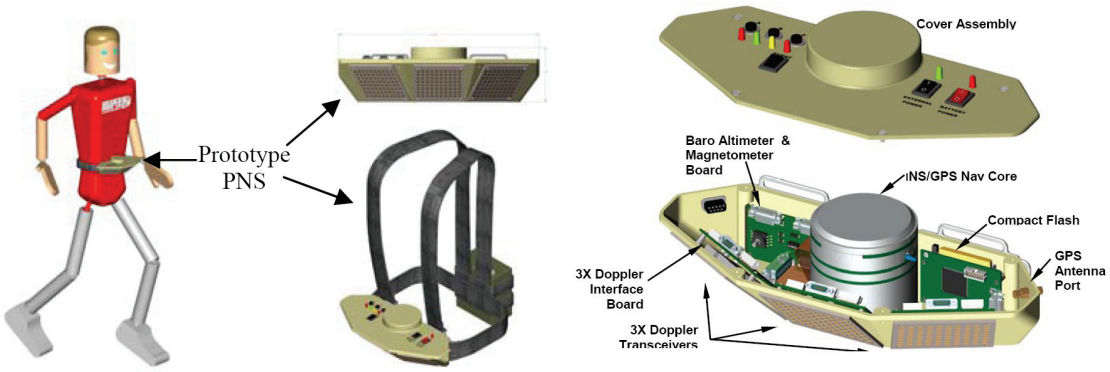

Figure 2.6: Draper Lab Personal Navigator System (PNS) ([203], p. 39-40)

Draper Lab PNS

The Draper Laboratory Personal Navigator System, or PNS, was a small package containing a tactical-grade MEMS IMU, a GPS receiver, a triad of Doppler radar velocity sensors, a barometric altimeter, a PDA for human interface and a processor running real-time, sensor-fusion navigation algorithms including occurrential PDR [203]. The package, worn by the foot soldier in the front at waist level (Fig. 2.6), had the objective of providing long-term accurate coordinates in both outdoor and indoor environments, including significant periods of GPS signal blockage. The software comprised strapdown navigation algorithms, deep GPS/INS integration for tracking loop control plus special nonlinear GPS measurement functions for line-of-sight error estimation [132]. Both IMU and the deep integration algorithms were based on previous Draper work on smart munitions (i.e., artillery shells with inertial and GPS sensors [231]) with modifications to quickly reacquire satellites after blockages. Accurate urban canyon performance under sparse GPS availability was demonstrated [201]. The Doppler radar sensors provided a three-dimensional velocity vector using short-range, low-power transceivers. These were arranged orthogonally so that in normal walking motion, each reflected a signal off the ground. The Doppler measurements were crucial to the PNS when GPS was unavailable since it was the primary means of reducing position, velocity and orientation drift inherent to the IMU-based navigation system. Tests demonstrated excellent performance indoors for extended periods, with a 3-4 m average error over 15 minute test, which was close to the stated goal of geolocation to a hallway and a room. Since position errors were bounded, GPS satellite reacquisition was also very quick on return to outdoors. RF ranging, A-GPS and PDR techniques were planned for later inclusion in the system. The technological roadmap called for power and size reductions in the short term.

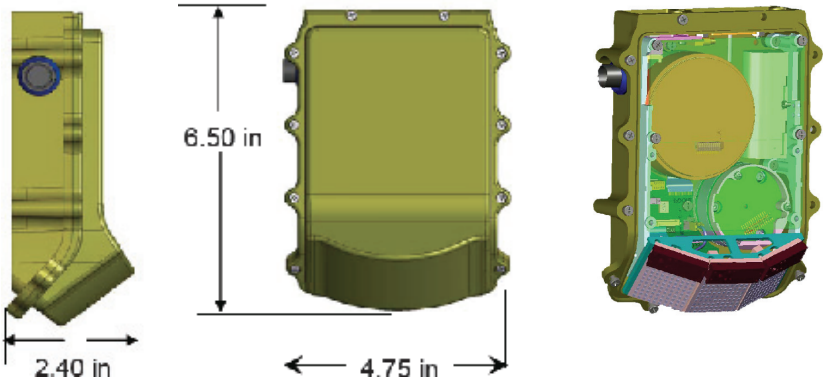

(a) Side view (b) Front view (c) Cut-away view

Figure 2.7: Draper Lab Precision Positioning System (PPS) ([202], p. 6)

Draper Lab PPS

In April 2008, Draper Laboratory successfully demonstrated a second-generation prototype called the Precision Positioning System (PPS) with a compact, ergonomic form factor, see Figure 2.7. It showed extremely good accuracy in mixed urban canyon and indoor tests [202]. The small belt-mounted PPS unit contained a tactical-grade MEMS IMU, a P(Y)-code L1 GPS receiver, a 3-axis magnetometer, a baro-altimeter, and three W-band (77 GHz) Doppler velocimeter radars. All sensor data was deeply integrated into the GPS receiver's tracking loops. Gait information was also exploited. Interestingly, the dominant source of error was identified as heading and position errors at building entry.

DARPA iPINS

DARPA also funded the iPINS, or individual Personal Inertial Navigation System [206]. The main contractor in this project, Honeywell, combined its strengths in INS, GPS and magnetometer technologies with PDR expertise acquired from Point Research. The sensor fusion filter was simpler than the ones in the PNS and PPS projects. More emphasis was put on the modeling walking and running motions than on GPS/INS deep integration [207]. The project objective of <1% error in distance travelled was demonstrated conclusively in outdoor tests while for indoor tests the errors were in the 1-5% range. The project also tried to determine whether "terrain correlation positioning", a kind of map matching in the vertical dimension, could be successfully used outdoors. Simulations showed that the barometric altitude sensor used in the iPINS system would enable accurate correlation in a low slope variation scenario and that it would be a useful method for bounding navigation error under a broad range of conditions.

ONR NAVGPSDE

In 2006, the U.S. Office of Naval Research (ONR) launched the "Navigation in a GPS Denied Environment", or NAVGPSDE, program [13, 242]. The purpose of the proposed system was to provide situational awareness (SA) and dismounted resource tracking capabilities to system users when they are located in GPS-limited or -denied areas such as caves, urban canyons, buildings, heavily forested or jungle environments. Interestingly, the system was called to provide for operation of 100 m into underground or cave-like environments with the use of up to three RF relays. Nominally, each soldier would carry a lightweight device capable of reporting its own location as well as reporting the location of other members of a clique[10]. Often knowledge of the relative position of the other members of the clique is more important than their absolute positions, for example in the case of a SWAT or fire team surrounding a building to be stormed from several sides simultaneously. Previous work undertaken by Mercury Data Systems on an earlier tactical navigation system was extended in the NAVGPSDE project by fusing PDR, GPS, and Doppler radar velocimetry measurements with RF ranging measurements from tactical radios, pseudolites and LORAN. The goal was to maintain a 25 m Spherical Error Probable (SEP) and over a range of 10 km and over an 8 hour period, during which there might not be any GPS reception. Consequently, critical to the whole system was the peer-to-peer tactical radio system[11] which provided ranging estimates from specially-structured packets and a patented signal modulation and processing scheme [145]. Horizontal ranging accuracy indoors was reported to be 0.5-4 m Circular Error Probable (CEP). (Due to improved signal processing, this is a factor of two improvement over results reported in [181]). Also implemented was a distributed and extended version of the Leapfrog Navigation System [164] called eLNS. This allowed for the dynamic establishment of virtual anchor reference nodes (i.e. clique members with good GPS position fixes) and thereby reducing the overall position drift of the clique over time.

In the NAVGPSDE project, a 6-DoF (Degree-of-Freedom) motion sensor board combined triaxial accelerometers, rate gyros and magnetometers; a barometer; a Doppler radar velocimeter; and a programmable commercial GPS receiver. Due to the challenge of writing a complete sensor fusion algorithm, not all these sensors were fully integrated in the time span of the project and a PDR unit from a previous project was reused. The Vectronics DRC, or Dead Reckoning Compass, consists of triaxial accelerometers, triaxial magnetometers and a microcontroller capable of outputting NMEA-0183 position messages. This device, which can be belt or torso mounted, uses a fixed step length for displacement calculations (see Chapter 3). Forward and backward walking as well as side-stepping can be recognized but vertical motions are not. The barometer on the new sensor board provided estimates of vertical displacement and its gyro provided some heading stabilization in the presence of magnetic disturbances. The sensor board was meant to eventually take

[10] A clique is a group of devices/soldiers operating together, usually in close proximity.
[11] ITT Clique Member Radio (CMR)

over all the functions of the DRC and to eventually support more types of mobility such as running, crawling and jogging. The PDR component of the system had to be calibrated for user step length and mounting position, i.e., alignment of the sensor relative to the forward walking direction. The velocimeter sensor component was used to overcome the limitation of the step length estimation algorithms by providing an alternative odometry signal accurate to within 1%. Velocimeter measurements were used during the step length calibration procedure as well ([13], p. 9).

Rockwell Collins DNSM

The Denied Navigation Sensor Module (DNSM) from Rockwell Collins was described recently in trade magazines [12, 108]. The DNSM is to be used in combination with the Defense Advanced GPS Receiver (DAGR, a dual frequency L1/L2 device) and a tactical radio system for urban and indoor positioning and situational awareness. While very few details are available, it would appear that the DNSM consists of two components, a belt/torso mounted box and a foot sensor, see Figure 2.8. It is not clear if there is a sensor on each foot. Presumably the larger unit contains a 6-DoF IMU, a barometer, and a computer running sensor fusion algorithms that also make use of raw GPS measurements (pseudorange, Doppler frequency, and carrier phase) from the DAGR and possibly range measurements from the tactical radio, as described above. The foot sensor may be a simple switch for triggering zero-velocity updates in the belt-mounted IMU. Alternatively, the foot sensor may be a mini-IMU, where step length and direction estimates could be made using the foot-inertial technique (see Chapter 4) and then sent to the belt-mounted main unit for fusion with the other measurements. If two foot units are present, foot-to-foot ranging might also be used for increased accuracy [41] but it might be difficult to make the ranging signals covert, a requirement for military applications.

Other

In a publication by a Canadian Defence R&D Center [120], requirements for military geolocation and situational awareness similar to those for the above systems are given. A passing reference is made to boot-mounted IMUs for localization in GPS-denied areas, but no further details are given.

2.6 Summary

As is clear from this review, many systems and techniques have already been explored in order to address the positioning requirements of pedestrians in general, and of technical users, in particular first responders and military personnel. The main conclusion that can be drawn from this review is that the military and at least one US commercial firm appear to be very close to fielding practical positioning systems which might satisfy the technical requirements for first responders. However,

Figure 2.8: Rockwell Collins Denied Navigation Sensor Module ([12], p. 3)

it remains to be seen whether any of these systems will actually perform as expected when used by real end users in realistic, non-controlled test conditions.

Chapter 3

Occurrential PDR

It is well known that the key to solving the generic ubiquitous localization problem is a combination of different positioning techniques and sensor modalities. Since GPS is basically useless indoors and is unreliable in urban canyons, alternative systems and techniques are essential for urban and "tactical" personnel positioning. Occurrential Pedestrian Dead Reckoning is one such technique. The term "occurrential" comes from the fact that inertial sensor measurements are used to detect the "occurrence" of steps as well as to indirectly estimate step lengths [131]. In this chapter, a combination of occurrential PDR and GPS positioning is explored. An novel combination of neural-network step length predictions and helmet-mounted sensors is presented. The experimental system shows low accumulated error over an extended walk and indoor/outdoor positioning is demonstrated.

In a nutshell, PDR is simply the estimation of a step length (or walking speed) and a course over ground (or direction of walking). GPS/Galileo position fixes (or fixes from some other local positioning system) are used to calibrate the step length estimation algorithm to the walking patterns of a particular user. In this respect, a configured system is not transferable to another user. The biggest advantage of PDR is that the error in position is propagated linearly as a function of the number of step taken, and is independent of time. This is a different from traditional strapdown inertial navigation systems which calculate displacement over time, resulting in a quadratic growth in position error over time. The PDR approach was shown to yield positioning performance thought to be adequate for many end applications in many previous projects. These are summarized in the next section.

3.1 Related Work

There is an extensive body of research on the occurrential PDR technique. One of the earliest public descriptions is the 1996 patent by Levi & Judd [138]. The patent's step detection and length estimation algorithms, described in detail in [100], appear quite rudimentary. Steps are simply counted by filtering the vertical acceleration detected with a sensor unit mounted, preferably, on the small of the back (though other mounting positions are possible). A threshold on this acceleration eliminates

false step detections from normal body movements while standing still. The step size is initialized to an approximate value. The step direction is determined by assuming the module is attached to the user in an orientation that is fixed relative to the body and by measuring the horizontal component of the earth's magnetic field. Once the user starts moving and has good GPS position fixes, a Kalman filter blends dead reckoning and GPS to obtain optimal estimates of position, module angular offset relative to the body, and step size. Accelerometer and magnetometer signal processing includes a Fast Fourier Transform. This requires a large number of raw sensor samples to be stored and thus steps cannot be analyzed separately [224]. Consequently, a steady gait should be maintained to minimize the estimation error. When GPS is lost, the most recently estimated step size is used for dead reckoning.

In [62], there is reference to work at the Draper Laboratory on "Bio-Kinematic Navigation" (BKN) systems [82] which use a combination of pedometry with an individual gait look-up driven by accelerometer measurements at the waist, magnetic compassing, and baro-altimetry. It is not clear if this report[1] dealt with novel in-house R&D or simply evaluated of existing pedestrian navigation systems, i.e., Judd's.

In the earliest versions of the Dead Reckoning Module (DRM) from Point Research Corporation [101] which included a MEMS gyro-compensated magnetic compass and MEMS accelerometers, it is claimed that with a calibrated unit the error would be about 2% of the distance traveled for level sidewalks and 5% for grassy hills. More recent versions of the DRM are able to discriminate between forward, backward, and side stepping gaits as well as crawling and running. The backward walking model was the same as the forward model except that step lengths were scaled back by 0.75 - 0.85, depending on the user. The running model was based on the step period. During treadmill tests, this approach was found to be accurate for slow to moderate running speeds but inaccurate for sprinting [206]. This is not surprising because with increasing running speed, stride length increases but then plateaus out while stride frequency increases non-linearly [158]. This effect does not appear to have been modeled in the DRM.

Another thread of research revolves around the work of Q. Ladetto and his collaborators at *École Polytechnique Féderale de Lausanne* (EPFL) in Switzerland. Their patented algorithms are more sophisticated than Judd's in that every individual step length is estimated based on the variance and frequency of accelerations [129] with GPS position fixes used as algorithm training data. Step direction (forward/backward, lateral) can be determined from the relative phases of the 3D accelerations while gyro heading is stabilized with magnetic measurements [128, 131]. Baro-altimetry augmentation experiments were described in [170, 127, 49]. These PDR algorithms plus the Vectronix DRC (Dead Reckoning Compass), used during EPFL's experimentation, eventually found their way into the U.S. Land Warrior Program. Later, a more integrated device called the CNM (Core Navigation Module, also from Vectronix) was combined with a military GPS receiver (the DAGR) and briefly marketed by Rockwell Collins as the DRAGN (Dead Reckoning Augmented

[1]The report is not publicly available.

(a) Camera, light and HUD (b) Heat camera (c) Conformal antenna

Figure 3.1: Examples of helmet-mounted sensors and accessories. (Sources: a) [10], p. 2; b) [7]; c) [89])

GPS Navigation System)[2].

In the same time frame as Ladetto's work, similar PDR studies were done using a belt-mounted HSGPS / IMU / baro-altimeter unit [149, 148]. Collin [49] considered handheld and torso-mounted devices with similar sensors. More recently, a group at the UK firm QinetiQ have explored the use of body-mounted IMUs for occurrential PDR tightly-coupled with GPS and baro-altimeter measurements [144, 81].

3.2 Wearable Helmet-mounted Sensors

Since most persons in public safety, emergency or military service wear some sort of protective headgear, an interesting question is whether basic PDR navigation sensors could be incorporated into the otherwise unused head mount point. See Figure 3.1 for previous examples of helmet-mounted sensors. Figure 3.1(a) shows some of the U.S. Land Warrior project's helmet-mounted electronic components, including an antenna for the tactical radio, a daylight video scope, a thermal weapon scope, and an HUD (heads-up display) [12]. A concept for a heat camera with external viewer mated to a commercial firefighting helmet is shown in Figure 3.1(b). This attachment point was explored for use with other sensors in the WearIT@Work project.

A very important motivation is that the top of the head is an especially good location for a GPS antenna since placing it anywhere else can cause reception problems, in particular multipath effects from ground reflections plus attenuation and frequency shifts from the body [131]. The military positioning systems described in Section 2.5 gloss over the fact that an antenna (usually a patch type) and cable have to installed somewhere high on the body, affecting the overall system's ergonomics. Since professional users will be carrying other RF communication devices, it seems reasonable to incorporate the radio antennae into the helmet as well. It has been shown to be possible to use the helmet as an wideband omnidirectional antenna

[2]Personal communication with Q. Ladetto in December 2008.

by applying specially-designed patterns of conductive paint onto a standard Kevlar helmet [89], see Figure 3.1(c). Alternatively, a liner of conductive, flexible fabrics forming an antenna[3] can be fitted under a helmet's camouflage cover [133]. Hopefully solutions of this type will help to reduce the "Christmas tree" wiring problems so frequently encountered in complex wearable systems.

In this chapter, the head was chosen as a mounting point for both the GPS antenna and an IMU, see Figure 3.6. As far as the author knows, this combination is original. This colocation presents some distinct advantages for GPS / PDR coupling. The information about walking speed derived from the PDR algorithms to be described below could certainly be used as part of a motion model in a loosely-coupled GPS/INS configuration for outdoor and light indoor use. At the very least, the presented PDR technique could provide good zero-velocity detection, which is of great aid in (re-)acquiring very weak GPS signals deep indoors. Also, the combination of GPS and INS sensors could improve positioning indoors and in so-called "urban canyons". With a helmet-mounted GPS antenna and an IMU, tight coupling between the two systems would be possible. Another possibility is an ultra-tight (or deep) configuration, where accelerometer aiding can allow for the reduction of GPS tracking loop bandwidths [17]. This can result in better performance in very weak signal conditions [74], robustness against carrier cycle slips and and less noisy Doppler shift estimates [25]. It also permits novel algorithms for dealing with severe multipath conditions (e.g., outdoors close to buildings), by using high-resolution Doppler shift measurements to separate direct from reflected signals [208]. The reflected path signals can then be used constructively in velocity and position calculations. An important benefit of these approaches would be better vehicle-to-door positioning performance, essential for providing accurate position fixes for calibration and initialization of the algorithm described in this chapter. (These fixes are also essential for the alignment of the foot-mounted IMU to be described in the next chapter).

3.3 Algorithm Details

The PDR technique is naturally decomposed into the step detection and estimation part and the heading estimation part. Each of these is discussed in turn.

Step Model

Many papers on PDR simply rely on a fixed average step length for each specific user. This naïve approach gives relatively good navigation results for typical speeds but performs less well with walking patterns far outside of normal range. The step length estimation algorithm used here is based on the method described in [104] and [136]. Other authors have proposed somewhat simpler variations to this same basic idea [224, 127, 149, 81, 204]. First an acceleration magnitude signal is calculated from the three orthogonal accelerometer signals obtained from the helmet-mounted IMU.

[3] See for example products from Pharad `www.pharad.com`.

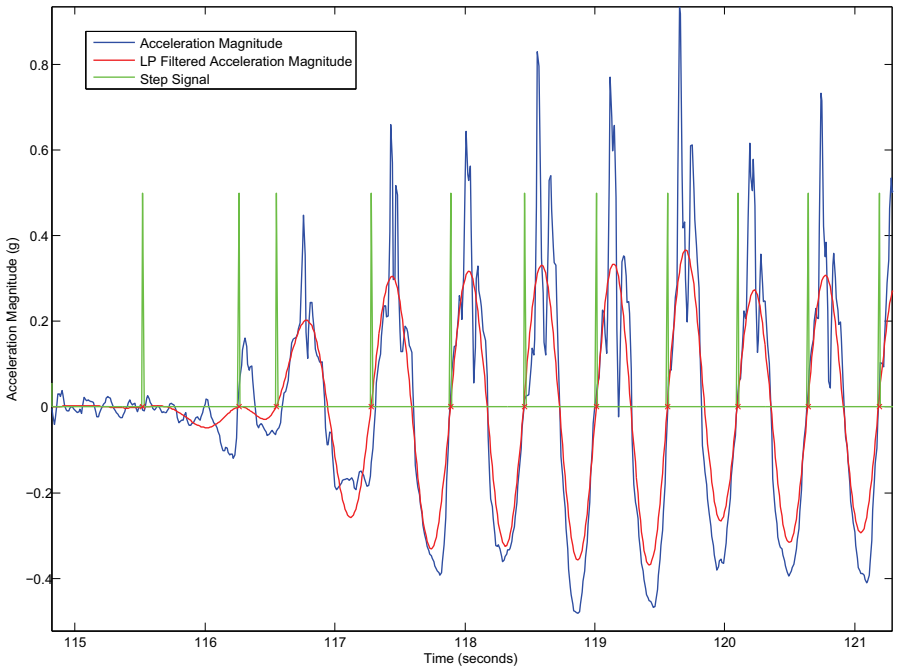

Figure 3.2: Step acceleration during start from standstill.

Step boundaries are defined by the positive-going zero crossings of a low-pass filtered version of this signal, see Fig. 3.2 for details. Next, numerical step features are created. The acceleration magnitude's maximum value, minimum value and variance are determined for each step (i.e., each time interval between zero crossings). These are depicted in Fig. 3.3. Notice that at standstill, both the acceleration maxima and minima are 1 g and the variance is zero. The integral of the acceleration magnitude between footfalls is also calculated. Hand-tuned thresholding rules, based on the distributions of step frequency and of step acceleration features, are created to reject false step detections.

The numerical features calculated above are then used in a feed-forward neural network [154] as input training patterns. The output training patterns are the step lengths estimated from GPS position fixes, interpolated to footfall occurrences. The neural network (NN) was configured with a hyperbolic tangent activation function in the hidden layer units and a linear activation function in the single output unit. Direct (bypass) connections between the input and output layers were used in addition to the usual (non-linear) links through the single hidden layer, see Figure 3.4. The values of the nodes x_0 and z_0 are fixed to one and this is done to add biases to the network via their accompanying weights. The complete explicit expression for the function represented in the diagram is

$$y(x;w) = \sum_{j=1}^{M} w_j^{(2)} g(\sum_{i=0}^{d} w_{ji}^{(1)} x_i) + w_0^{(2)} z_0 + \sum_{l=1}^{d} w_l^{(direct)} x_l \tag{3.1}$$

Here $w_{ji}^{(1)}$ denotes a weight in the first layer, going from input unit i to hidden

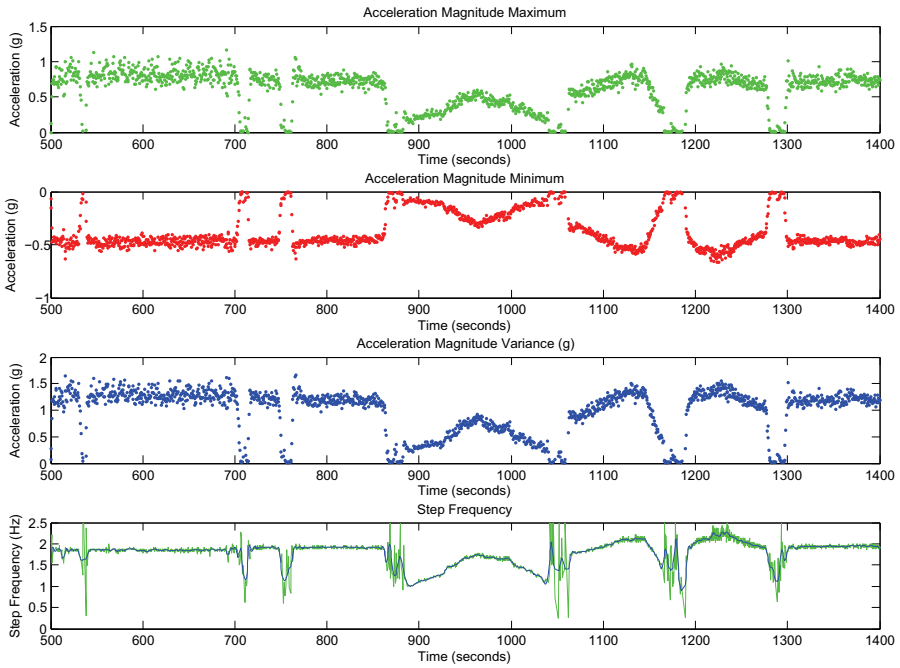

Figure 3.3: Step Features

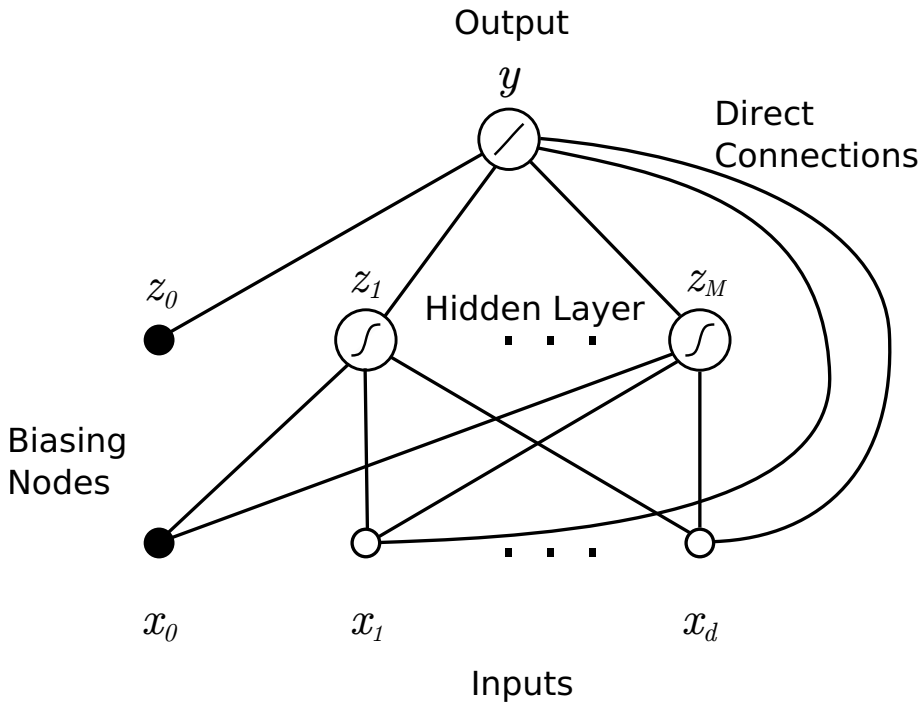

Figure 3.4: Neural Network Structure for Step Length Estimation

unit j and $w_{j0}^{(1)}$ denotes the bias for hidden unit j. Similarly, $w_j^{(2)}$ denotes a weight in the second layer, going from hidden unit j to the output unit, and $w_l^{(direct)}$ denotes a weight for a direct connection between input unit l and the output unit. $w_0^{(2)}$ denotes the bias for output unit. The activation function g of the hidden layer units is the hyperbolic tangent. The network parameters, i.e., the set of weights $w = \{w^{(1)}; w^{(2)}; w^{(direct)}\}$, were adjusted using a standard non-linear technique (e.g., scaled conjugated gradients) to minimize the sum-of-squares error

$$E = \sum_{n=1}^{N} \{y(x_n; w) - t_n\}^2$$

between the network step length estimates $y(x_n; w)$ (from inputs x_n (i.e., the step feature values) and the set of weights w) and the target outputs t_n (i.e., the step length obtained from GPS fixes) for N training examples.

It is well-known in the machine learning literature that such an NN can approximate arbitrarily well any smooth, continuous mapping (one-to-one or many-to-one) from one finite-dimensional space to another, provided the number of hidden units is sufficiently large (see [39] on p. 130). However, the use of additional direct links allow for much more efficient learning from data with significant linear dependencies in the mapping between input and output (see [154] p. 184 for details). Because of this, only a few nodes in the hidden layer are required to capture the mild non-linearities in our application's training data. As far as the author knows, direct connections were not used in previous research on NN-based occurrential PDR.

As is standard practice, in evaluating this approach and in tuning the neural network, one portion of the recorded experimental data was used for training the network and a different, independent held-out portion of data for verifying the neural network predictions. In the present case, a period at the beginning of the experiments was used for training and the rest of the experiments was used for evaluation. The optimal network set-up was established by looking at the tests error while varying the number of hidden nodes. The results in Table 3.1 show that 5 nodes gives good performance, with a step length estimation error of 3.9 cm (RMS). The variance on the GPS based step lengths (used for training the network) is around 4 cm under optimal reception conditions. Note that the exact number of nodes is not critical as long as there is enough training data. Between 200 and 500 training examples (approximately 100-250 seconds of walking) are sufficient to train this small network. Figure 3.5 shows a typical fit of the model to training data. For the time window between 900 and 1050 seconds (experiment time), a test subject walked in a very wide range of speeds, from barely advancing (0.5 m/s) to an Olympic race walk clip (2.0 m/s). The model handles the resulting wide range of step lengths very well. Note that for the period around 900 seconds, the GPS position and speed fixes were erroneous. This did not adversely effect the fit of the neural network to the data.

# of Hidden Nodes	Train Error (cm (RMS))	Test Error (cm (RMS))
0	4.0	4.4
1	3.6	4.1
2	3.7	4.0
5	3.7	3.9
10	3.5	4.2

Table 3.1: Neural Network Hidden Layer Sizing. Using 500 training examples and 2371 test examples and 50 iterations of the numerical parameter optimization routine, the Root-Mean-Squared test error is minimized using 5 hidden layer nodes.

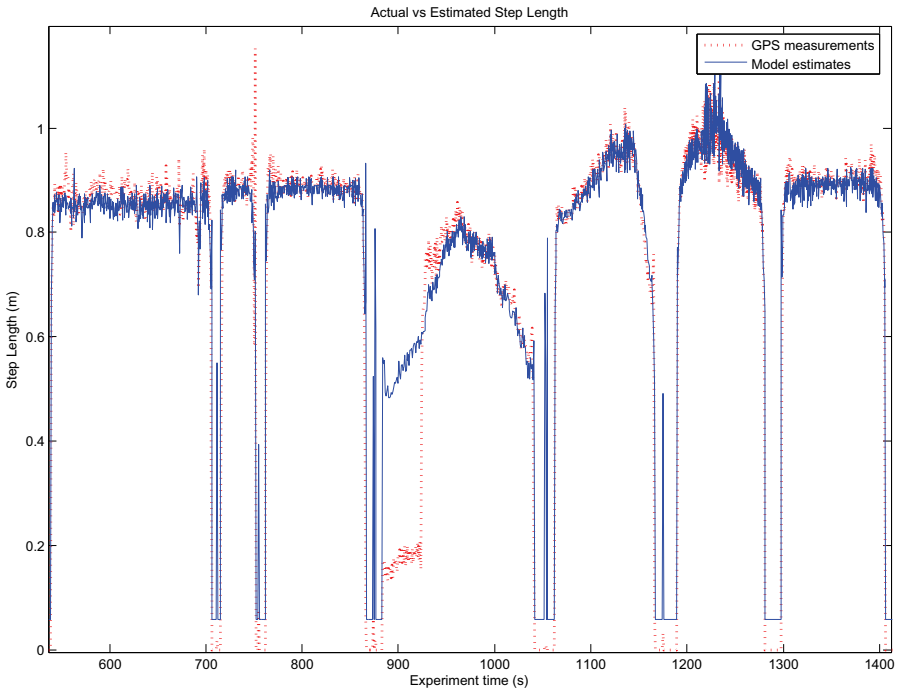

Figure 3.5: Step Length Model Results

Heading Estimation

The motion sensor's yaw angle estimate (rotated from the sensor-fixed frame to the local-level navigation frame) was used for deriving an azimuth and hence the step headings. A fixed bias was added to the sensor's raw yaw angle value so that the orientation of initial estimated outdoor segments were aligned to the true paths on the ground. The bias effectively removed any azimuth misalignment due to the local magnetic declination and small mounting offsets. This was done for the sake of simplicity. This bias could alternatively been estimated using a Kalman filter and successive GPS fixes. More generally, a full 3D alignment of the motion sensor with respect to the local-level frame could have been done using successive GPS fixes in a procedure called kinematic alignment (see 4.6 in next chapter). However, both these Kalman-filter-based estimation methods were deemed to be overkill for the

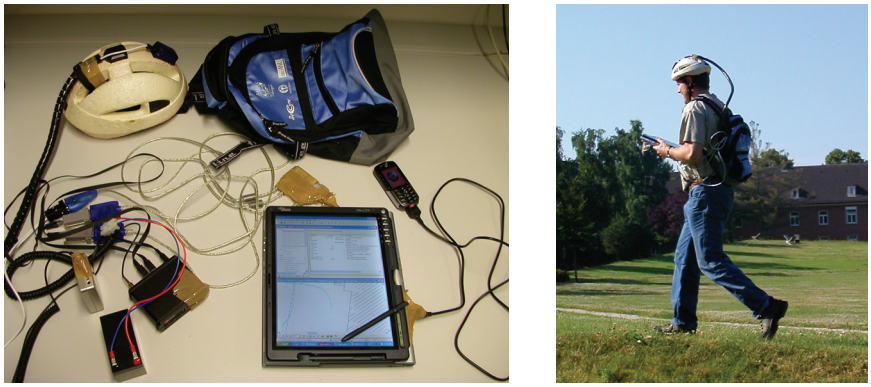

Figure 3.6: Experimental Set-up. (Photos by the author.)

immediate purposes of these experiments (e.g., determining if the step length and step heading estimates were accurate and reliable).

For the experiments, the motion sensors were mounted in a fixed orientation relative to the user's body, i.e., the helmet was worn tightly. Also, the test subject kept the helmet pointed in the direction of motion at all times. Future research will aim at eliminating this restriction. Estimating a direction of motion from a body-mounted sensor is fairly straightforward and can be done by comparing accelerations along horizontal axes to magnetometer and gyroscope heading measurements [130, 114]. However, applying such a technique with arbitrary gaze orientation and walking style, e.g., side-stepping, is not at all simple with a head-mounted IMU. Very accurate rotation matrices and non-trivial inertial calculations are required to derive a direction of travel under these circumstances. A helmet-mounted camera (low-light or IR) combined with some very simple optical flow algorithms could provide additional attitude change measurements that could be fused with the IMU rate gyro measurements. This, however, is beyond the scope of this thesis.

3.4 Tools

The main instrument for these experiments was the Xsens MT9 IMU and the UBlox GPS receiver. The IMU sensor head and GPS patch antenna were attached to a helmet with double-sided tape. Data was logged using a laptop computer and the USB cabling and GPS receiver were carried in a small backpack, see Fig. 3.6. The Xsens and UBlox application software was used for data logging. Measurements were reprocessed off-line to convert the raw binary log files to ASCII. These were then reformatted and cleaned-up (for record corruption from communication glitches) using Perl before import to the analysis package. Matlab and a Machine Learning package [154] were used in the analysis and plotting of results. The MTx magnetometers were recalibrated periodically, typically every few experiments as the drift on these sensors is normally quite low. Using the Xsens "Magnetic Field Mapping" software utility and carefully following the procedure given in the user's guide, the magnetometer offsets and gains compensating for hard- and soft-iron distortions

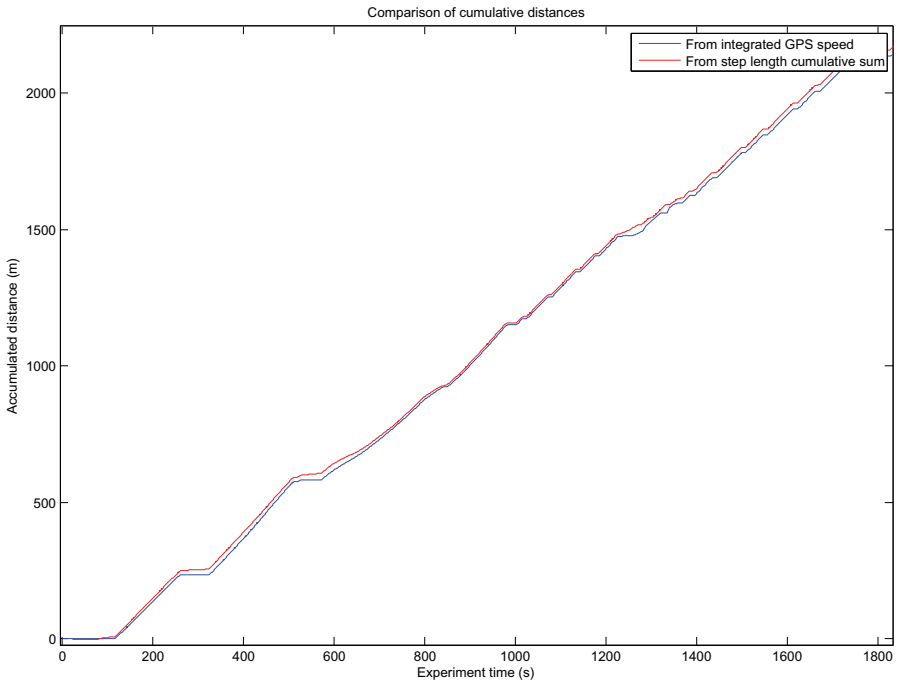

Figure 3.7: Accumulated Step Lengths vs GPS Distance over Ground

were established. For a detailed description of the algorithm, see [144]. Note that this procedure must be done in an unperturbed Earth magnetic field. Once calibrated, the angular error in magnetic field vector measurements was expected to be less than 1 degree (according to the manufacturer's utility)[4].

3.5 Results

The results of the neural network prediction for one typical outdoor-only experiment are shown in Fig. 3.7. The difference between the accumulated model step lengths and the true surveyed distance is only a few percent. These step length estimation results are similar to those reported elsewhere [126, 42] and compare very favorably with [136][5], where errors were as large as 5.4% of the total distance travelled[6]. The results also confirm those found in earlier work by the author [32, 31]. (Note that there was not much to be gained by doing extensive repeated tests or statistical analysis of the results since the occurential PDR technique has severe practical limitations, as will be discussed below).

[4]Some smaller GPS antennas contain magnets for quick mounting to car roofs, for example. It is imperative that these magnets be removed if the GPS antenna is placed close to the MTx, as it was on the helmet.

[5]In a non-public document from Draper Lab on a "Bio-Kinetic Navigator" [83], a distance-travelled error of 1% is reported but no details on the test protocol are given.

[6]The relatively large errors in these experiments were mostly caused by unmodeled step length changes while going up and down slopes.

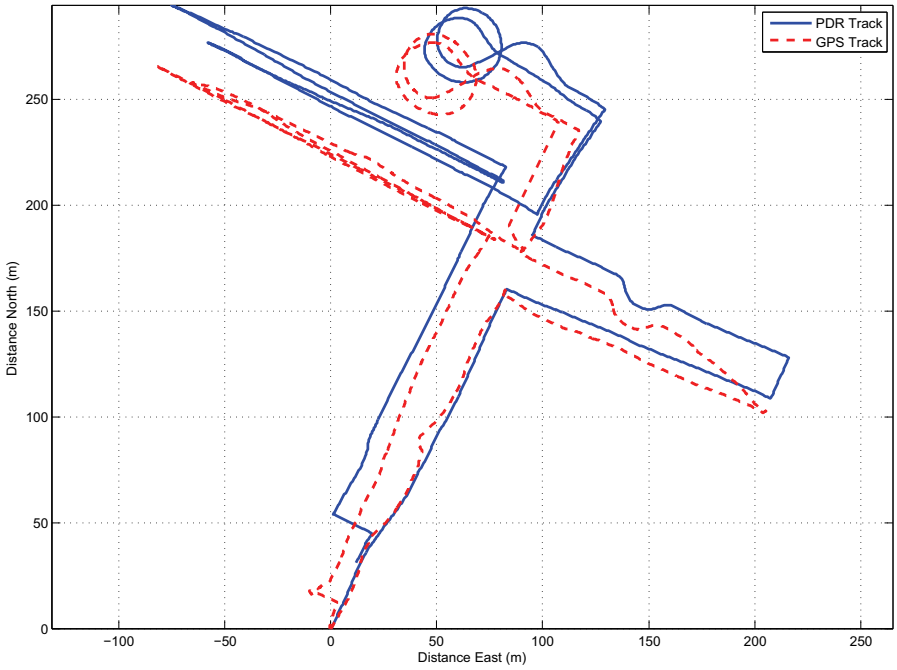

Figure 3.8: Outdoor GPS and PDR-estimated Tracks

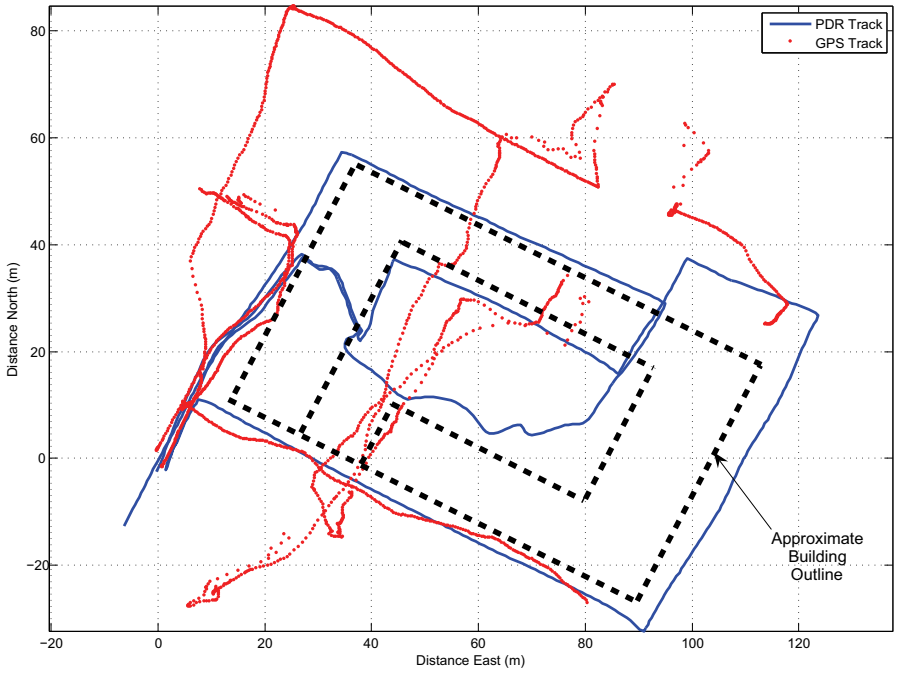

Figure 3.9: Indoor / Outdoor Test Course

Using the magnetic heading information available from the motion sensor, it is possible to calculate an estimated track on the ground. Figure 3.8 shows this estimated track in comparison to the GPS track ground truth for an outdoor test. The track segment lengths are comparable and the position offset after the approximately 20 minute walk is only about 40 m. The discrepancies between the GPS and PDR tracks can be attributed to heading errors and to GPS blunders due to nearby buildings. In Figure 3.9 showing an indoor/outdoor test, the GPS position fixes were clearly very poor. Frequent position fix blunders, on the order of 20-30 m, due to satellite signal masking and multipath from nearby buildings, distort the path. Along the entire south-eastern side of the building, there is no fix at all. Our receiver features a HSGPS mode that is advertised to work in certain indoor environments but in the glass-covered inner courtyard, it is giving very poor results. The PDR estimated path, on the other hand, shows very good behavior and performance indoors and outdoors.

3.6 Discussion

As shown above, the neural-network based estimation of step length using step features is very accurate. This begs the question, "Why?".

In Astrand's classic on work physiology [24], the relationship between animal size and locomotion speed is discussed. Very generally, the frequency of limb motion is inversely proportional to limb length. While an important relation between preferred step length and frequency of individuals is suggested, no information is given about the exact functional relationship. The energy cost of various activities is also discussed. With regards to walking, the energy cost varies widely depending on the individual and circumstances. However, the freely chosen step rate is said to be the one that requires the least energy expenditure (i.e., oxygen uptake) at any given speed.

It is known from many decades of biomechanical research that many parameters such as

- the effective value of the vertical body accelerations
- the step length
- the forward velocity change in each step, and
- the stride time

are all correlated to walking speed [45, 191, 44]. In Kuo's work [118, 119], several biomechanical models for bipedal walking are discussed and a relationship between speed and step length is proposed. A surprisingly simple "inverted pendulum" model is shown to be very accurate in terms of energy expenditure at different walking speeds [58], see Figure 3.10. In [36], it is shown that the preferred speed to step length relationship arises because humans are trying to minimize the total metabolic

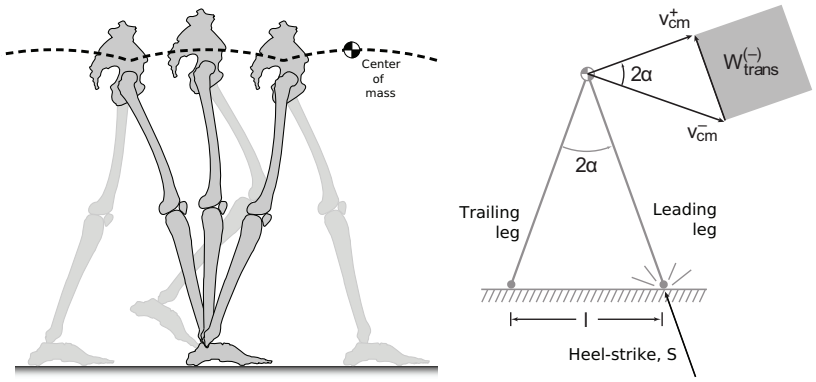

(a) Skeletal view (b) Work at foot strike

Figure 3.10: Inverted Pendulum Walking Model, adapted from [58] and [119]

cost at a given walking speed. Using data gathered from treadmill experiments, it was demonstrated that the relationship between walking speed v and step length d proposed by Kuo

$$d = Cv^{1-b}$$

or in terms of step frequency f,

$$f = Cv^{b}$$

fits very accurately to the empirical data. The scalar constant C was confirmed to depend mostly on body size and can be determined for each individual through testing. The optimal value of the exponent, $b = 0.58$ or $1 - b = 0.42$, was found to be valid over a wide range of walking speeds and across individuals. Taking data gathered during walking tests with a belt-mounted sensor and doing a manual adjustment to C, a very good fit to the empirical data was obtained[7], see Figure 3.11. The fit using noisier data from head-mounted sensors would also likely be very good. In a practical system, a linear fit using the log-transformed data could easily be automated and made to run in real time. For outlier rejection, the RANdom SAmple Consensus, or RANSAC method could be used. This would likely give superior results to those reported in [57], where an unconstrained step length/frequency look-up table was used.

Looking at the recorded data from our experiments, one can make the following observations. In Figure 3.12, a clear increase in the acceleration magnitude variance with walking speed can be seen. This is not surprising as the hips, and hence the head-mounted IMU, follow an approximate circular arc during each stride, as shown in Figure 3.10(a). For a given stride length, the acceleration minimum measured near the center of gravity or at the head will decrease with increasing speed since the circular arc will be traversed faster, resulting in a higher "centrifugal" force which is

[7]This work was part of a Master's student project done under the supervision of the author [54].

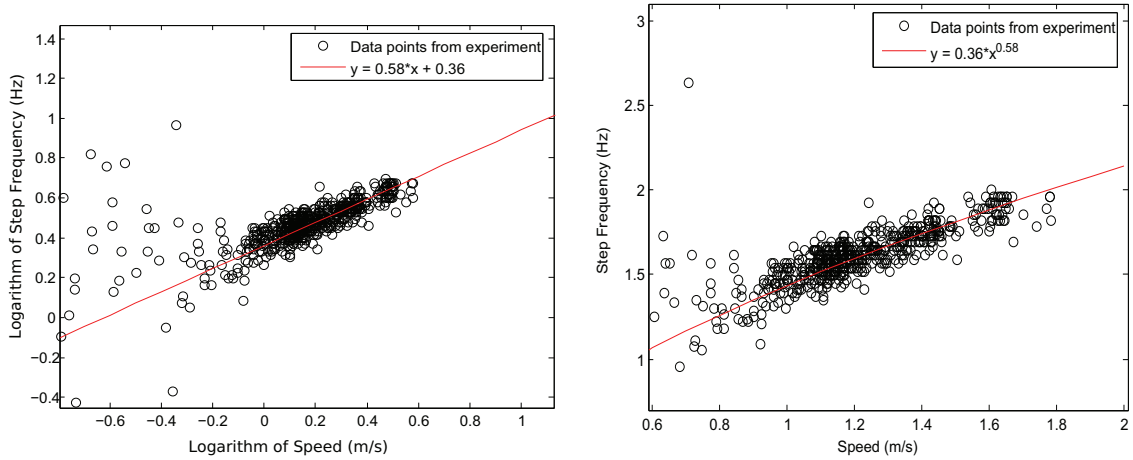

(a) (b)

Figure 3.11: Fit of Empirical Speed/Step Length Model for Belt-mounted IMU (adapted from [54]).

measured by the accelerometers[8]. At the center of the stance phase, this centrifugal force is aligned with the vertical as is gravity but is working in the opposite direction. Consequently, there is a maximum cancelation, or "unweighting", in the middle of the stance phase. Due to the velocity change at heel strike (depicted in Figure 3.10(b)), the acceleration maximum, which is in fact experienced at the heel stike, will increase with increasing speed. The net effect is that the acceleration magnitude variance increases as walking speed is increased, which is what was observed in the experiments.

It is worth noting that, contrary to measurements made at the pelvis, head accelerations are not affected by the quality (i.e., hardness and irregularity) of the walking surface [146]. This is likely because the human locomotor system is trying to optimize the stability of the head. Consequently, the head-mounted sensors might actually yield more reliable step length estimates than their body-mounted counterparts.

It would be possible to extend the neural-network prediction model by looking at the variation of the detected features with changes in slope. The author observed over many experiments that the step features from the helmet-mounted sensor definitely change with the angle of walked inclines. Extensive analysis on this data was not carried out as the expected phenomena have already been thoroughly studied by other researchers [129, 170, 22, 81].

Finally, Alvarez et al. [20] showed that there are several simple closed-form step feature to step length relationships that can be derived from the inverted pendulum

[8]Accelerometers sense are specific force sensors and as such detect the sum of all forces acting upon them. In force rebalance accelerometers, a small servo loop maintains a small proof mass at a null point by supplying a restoring force. The value of this restoring force is directly proportional to acceleration. In the present case, the accelerometer measures the sum of a "centrifugal" force and the gravitational force.

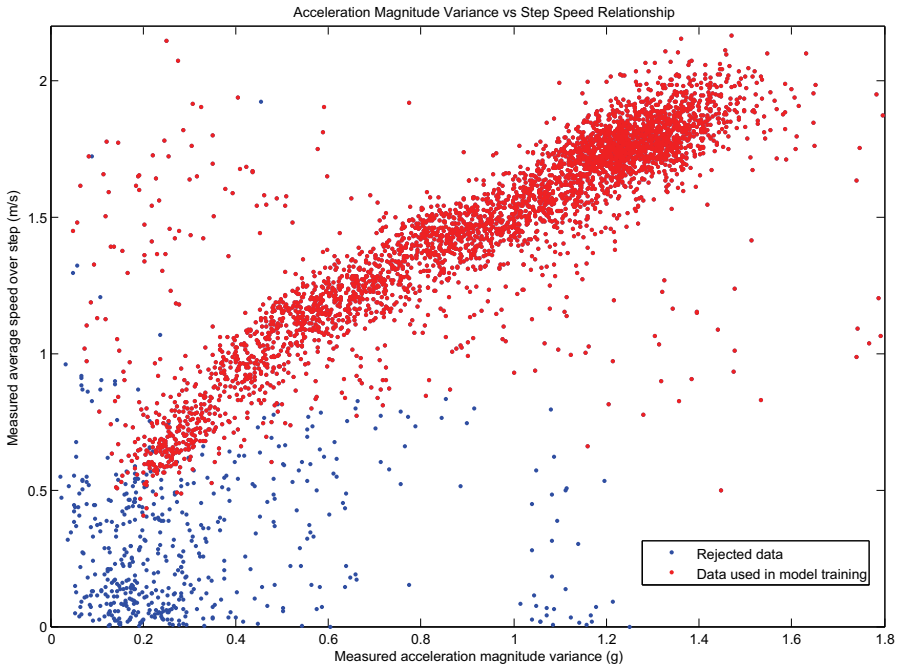

Figure 3.12: Step Acceleration Magnitude Variance vs Speed

model and that these have different predictive power. Kuo has also derived more complex relationships for walking energetics and dynamics with the addition of toe-off mechanics to the simple inverted pendulum model [119]. In effect, the neural-network configuration described above is simply finding a mapping between the input and output features in the training data that is very similar to the closed-form, theoritical ones. The expected smooth, continuous functional relationship (which has a large extent linear component) between stride features and walking speed is simply being learnt by the NN from the training data.

At first glance, the technique would appear to address the target application domain requirements. However, from extensive experiments carried out by the author [34, 33], it was determined that this and similar occurrential PDR approaches are likely to provide good results only if the user's locomotion is *regular* and *essentially rectilinear*. Step dynamics (i.e, the step time interval and the acceleration profile) change during manoeuvres, see Figure 3.14. In the author's opinion, occurrential PDR techniques are likely to break down when the user walks an irregular, curved or halting trajectory. It is exactly this type of locomotion that will predominate when rescue personnel are "sweeping" buildings or manoeuvring through a fire, for example. A possible solution to this problem would be to build an explicit model for every possible locomotor pattern. However, this would rapidly become unwieldy and likely be prone to error. Consequently, occurrential PDR based positioning will likely perform poorly during real world tests. How to overcome this major pitfall is the subject of the next chapter.

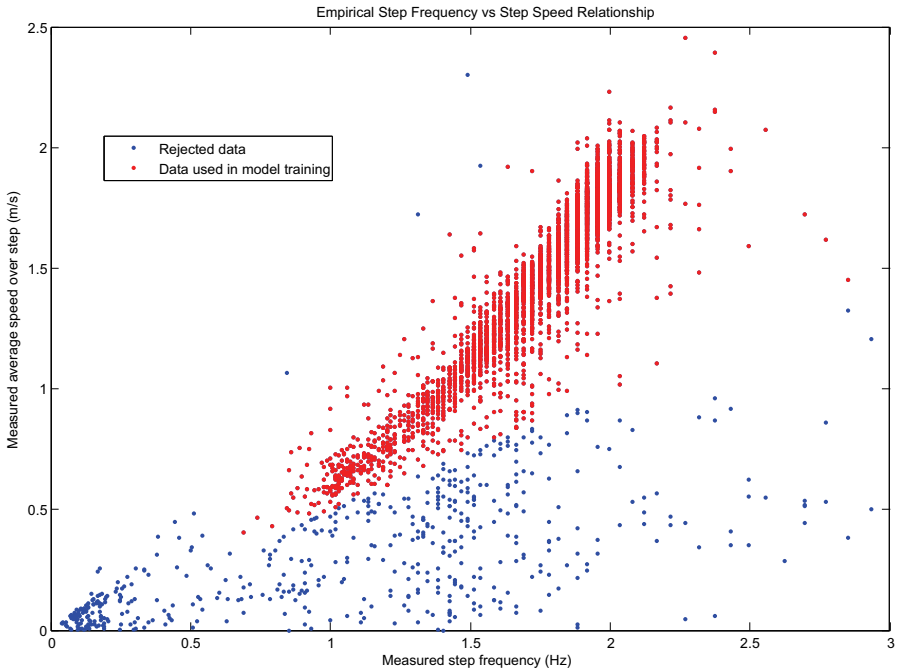

Figure 3.13: Step Frequency vs Speed

3.7 Summary

The mounting of the PDR motion sensors on a helmet in our experimental set up is novel and performs quite well. This configuration, as well as the waist and torso mounts, may be appropriate for some end users (e.g., firemen and police officers). Moreover, the helmet has an advantage in that it can be used as a mounting platform for other useful sensors.

The step length estimation results are comparable, if not superior, to those published elsewhere. This can be attributed to the developed neural-network-based step-length estimation technique. The NN is in effect learning, from the training data, a non-linear mapping from step features to step length that is similar to those deriveable from well-established biomechanical walking models and having similar predictive power. Since a practical heading estimator was not used, only walking speed estimation has been conclusively shown to work. Heading, and thus trajectory, accuracy is very much dependent on the head orientation, which was carefully controlled in these experiments. The problem of separating the gaze orientation from the direction of travel remains a major challenge. Helmet-mounted video cameras could be combined with computer vision algorithms and IMU measurements for this purpose [64]. Many avenues to occurrential head-mounted PDR performance improvements, such as the detailed modeling of loitering, steering and stair climbing behaviours, are still open for future research. Running behaviours would be very useful too, and fortunately step length estimation algorithms for this class of motion patterns seem relatively easy to implement [206]. However, it is not clear that occurrential PDR based positioning will perform well during real world tests with

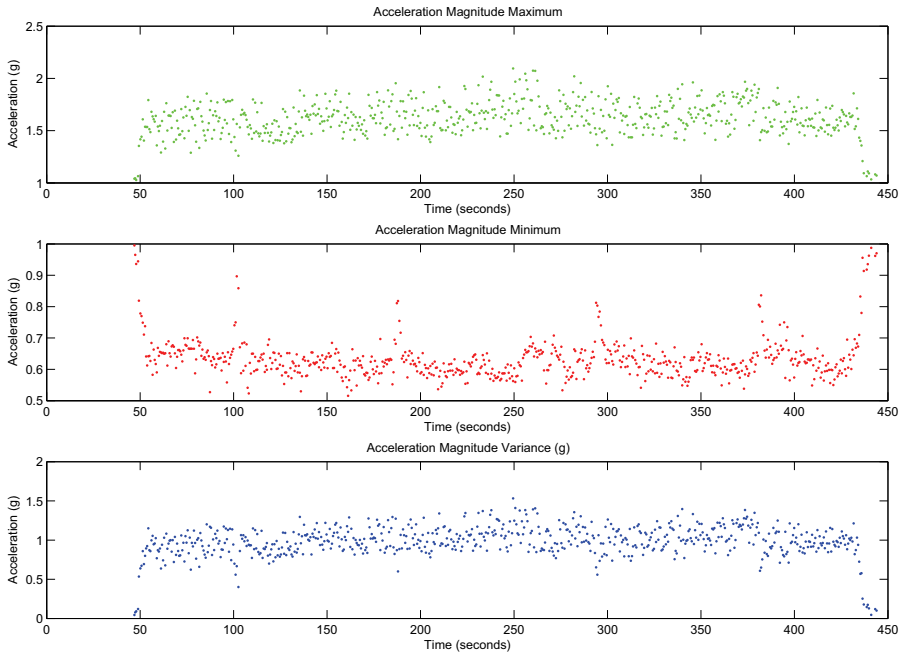

Figure 3.14: Step acceleration features during sharp right-angle turns while walking around a square course. The spikes in the acceleration magnitude minima are caused by additional radial accelerations during turn manoeuvre at 102, 188, 294 and 382 seconds. (Adapted from [34]).

users who may have very varied and even erratic locomotion patterns (see discussion in [65]).

Chapter 4

Foot-inertial PDR

There exists an alternative to the occurrential PDR approach described in the previous chapter. It involves attaching an Inertial Measurement Unit (IMU) to the foot and *directly* estimating the length of each step through inertial calculations. To limit the otherwise rapid position error growth of unaided inertial navigation, a so-called Zero Velocity Update (ZUPT) of the inertial system is done at each foot standstill. Step heading is estimated by a combination of rate gyro and magnetic measurements. Undesirable gyro behavior can be controlled via a Zero Attitude Rate Update (ZARU), also done at foot standstill. The main advantage of this technique relative to the occurrential one is that no biomechanical or locomotor modeling has to be done and there is complete freedom to move the feet in any direction. Another benefit is that in principle only a single IMU is required for good performance (in contrast to the EDRD shown in Figure 2.4, for example).

The author at first thought that this technique was fairly novel. An initial, brief literature search uncovered a number of publications describing some aspects of the approach, but they were not particularly convincing. Later, a more extensive search revealed that the approach dates from at least 1994 and that a number of patents have been filed. A review of previous work is provided in Section 4.1. Nonetheless, at the time this research was begun, there was still very little in terms of performance evaluations even for straight-ahead walking. As far as the author knows, there were no tests whatsoever done for non-regular movements, such as sharp turns, side-stepping, crisscross motions, etc. For first responders and other professional users, it is imperative that any pedestrian positioning system work for these types of locomotion.

4.1 Related work

When this work was initially undertaken, the author thought the foot-inertial technique quite novel. However, a more extensive literature search, undertaken after initial tests were completed, revealed that the technique is hardly new and that many individuals and groups have tried to develop it. The high level of recent activity, both scientific and commercial, indicates that the technique may ultimately

be successfully deployed in real-world scenarios.

The earliest reference to foot-mounted motion sensors for pedestrian navigation is in a non-public document by Elwell [61], cited in [62]. Leveraging Draper Laboratory's expertise in MEMS-based inertial navigation (gained from smart munitions programs), the Personal Inertial Navigation System (PINS) used zero-velocity updates (ZUPTs) at each footfall and zero-attitude rate updates (ZARUs) when stopped longer as a means of aiding the inertial navigation system, based on an Extended Kalman Filter tightly coupled with GPS measurements. In order to isolate the sensors as much as possible from human motion during the ZUPTs and ZARUs, the IMU was mounted in the heel of the soldier's boot, see Figure 4.1(a). Contact switches along the sole detected ground impact, duration and lift-off of the boot during gait. A barometer was employed to stabilize the vertical channel which would deviate if it weren't for the presence of an independent altitude sensor. Navigation computations were stopped when both the linear and angular motions fell below threshold values. Magnetic field sensor values were used in conjunction with the rate gyros to detect near-zero angular motion. GPS position fixes were used to initially locate and align the INS. In simulation studies, the mission profile included a 15 minute section with GPS reception and the balance of the 120 minutes was indoors. Position errors at the end of the simulation were approximately 3.5m in both the East and North directions. It is not clear from publicly-available information whether the PINS was ever actually built and tested with end users.

A 2001 US patent award[1] from L. Hutchings [94] describes what is effectively a shoe-mounted IMU and algorithms for running and walking speed estimation. With the use of a 3D magnetic compass, navigation capability was also said to be possible. The descriptions of the initial alignment and step displacement algorithms present nothing new relative to standard strapdown navigation methods and gloss over the need to accurately estimate gyro and accelerometer biases as well as the need to compensate for local magnetic disturbances. A Neural Network is proposed to improve accuracy, but no further details are given on how this was to work. In a later publication [105] based on this patent, the position error behavior clearly shows that the authors had not properly addressed the alignment issue and had not implemented the required application-specific sensor-fusion algorithm (e.g. a Kalman Filter). Compared to the thorough analysis done by Elwell at Draper Lab, the technical sophistication of this patent can be described as rudimentary.

Before foot-inertial PDR systems using full 6-DoF IMUs became prevalent, a number of researchers successfully demonstrated reduced-IMU implementations. Sagawa et al [197] used a 3D accelerometer plus one rate gyro. The latter was used to measure the pitch angle of the foot. When this was combined with the accelerometer readings, the stride lengths were estimated. A baro-altimeter was used to detect vertical excursions. This sensor cluster was sufficient for the project's stated goal of activity monitoring but was clearly insufficient for dead reckoning as no heading information was available. In the same vein, Stirling's pod (see Figure 4.1(b)) had only 2 parallel offset 2D accelerometers measuring in the sagittal

[1]Filed in 1999 and based on an earlier 1995 filing.

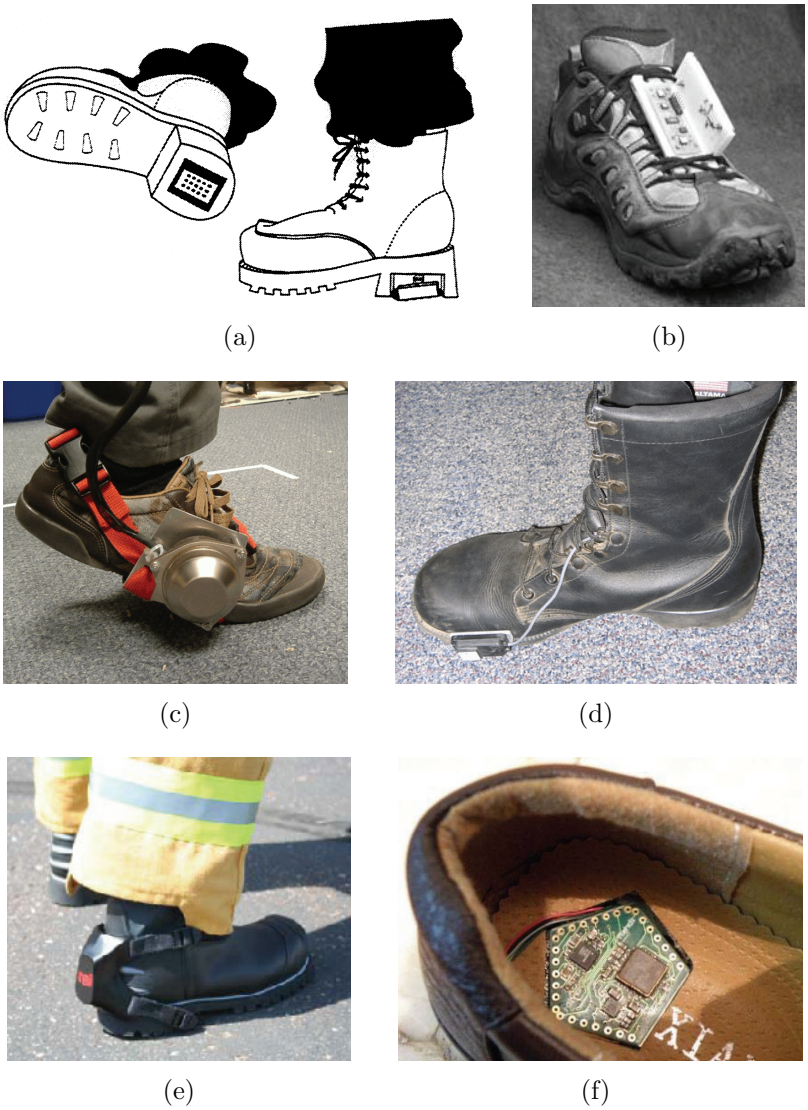

Figure 4.1: Evolution of Shoe-mounted IMUs: a) Draper Labs concept, circa 1994 [62]; b) University of Calgary Prototype Foot Pod, circa 2002 [211]; University of Michigan c) BAE SiIMU, circa 2005 [163] and d) Memsense nIMU, circa 2006 [160]; e) ENSCO nIMU in housing, circa 2007 [217]; f) 6-DoF IMU PCB, circa 2008 [98]

plane and a 3D magnetometer [211, 210, 212]. Differences in the offset accelerometer readings were used to estimate rotation rates in the sagittal plane and then by integration, the pitch angle of the foot. This angle was then used with the average of the offset accelerometer readings to estimate the acceleration of the foot in the forward direction, parallel to the ground. This was then integrated twice to yield a step length. During outdoor tests in a magnetically-benign forest environment, distance over ground estimates were encouraging but trajectory accuracy was not that good when compared to the GPS and waypoint ground truths. The approach relied heavily on the stance phase of walking for sensor attitude estimation and step heading determination. The assumption made during heading calibration was that the orientation of the foot during the stance phase remained fixed with respect to the user's direction of travel. Of course, this does not hold if the user is negotiating turns and/or ascending/descending slopes. As there were no gyros in the sensor cluster, it would have been impossible to correct for (indoor) magnetic perturbations and no indoor tests seem to have been performed. With both these reduced IMU set-ups, it was not possible to handle irregular walking motions, such as side-stepping and no Kalman filtering techniques were used.

At around the same time, Foxlin presented an implementation of an error-state Extended Kalman Filter for positioning with a low-quality but reasonably small foot-mounted IMU [71]. Considerable detail is given on the set up of the error-state filter's transition matrix, on methods for kinematic alignment using GPS, and on magnetometer calibration. He proposed an original method for handling magnetic disturbances in the environment by estimating a "magnetic deviation" in the horizontal plane but only once per footfall. A few outdoor tests as well as a single indoor 3D test through a house are given, both showing very promising positioning performance.

In contrast, Ojeda and Borenstein [162, 160, 163] used a high-quality, 6-DoF IMU (a BAESiIMU01). Unfortunately, the set up was far from practical due to the very large IMU, see Figure 4.1(c). The system used only the raw measurements (quartz accelerometer and silicon resonating ring gyro readings) and there were no magnetometers. They did not implement a Kalman filter so there was no on-line inertial sensor calibration. No initial IMU alignment (in particular, leveling) was performed, presumably because the IMU accelerometers had such small switch-on biases that this was not necessary. Also, the gyros were calibrated to high accuracy on a rate table [161] beforehand, so that scale factors were very well compensated while the device was in use. Unfortunately, the whole experiment was completely unrealistic: real foot-mounted sensors will not be high quality (at least not simultaneously with low cost), will be subject to extreme temperature changes and will have difficult-to-characterize non-linearities (such as gyro cross-axis and acceleration sensitivity). In later publications by this group [160], a smaller and more practical IMU was used (see Figure 4.1(d)) and they encountered precisely these kinds of difficulties. A Kalman filter for estimating the system's random errors was not implemented and was left for future work.

Godha et al. used a hybridization of the occurrential and foot-inertial PDR

techniques in combination with GPS for navigation in signal-degraded environments [78]. A Kalman filter was used to fuse raw HSGPS pseudorange measurements with PDR step length and direction estimates obtained via a 6-DoF, foot-mounted IMU. During GPS outages, the occurrential step length was fixed to the last estimated value, and no attempt was made to estimate it from acceleration variances or stride frequencies. This hybrid approach showed very good step length estimation results, with distance over ground errors of $0.1 - 2.5\%$. However, the low-cost IMU did not contain a magnetometer so it was not possible to limit gyro drift via compass measurements. ZARUs do not appear to have been used either. Consequently, heading drifts indoors were very large. In one test, they reached 58.1° after a 30 minute GPS outage.

REX Systems recently fielded a system with a 6-DoF commercial IMU attached to the back of a firefighter's boot [217], see Figure 4.1(e). The IMU is housed in an insulated, rugged box that can be adapted to the end user's footwear and is connected via a cable to another processing unit worn on the belt. An Extended Kalman Filter using ZUPTs and heading updates runs on the processing unit. This *external* heel mounting may not be a very good long-term solution, given the extreme heat and other abuse the IMU will very likely experience. ENSCO staff themselves have identified rapid temperature changes as a problem for the targeted end application, first responder tracking [66]. Nonetheless, very recently[2], ENSCO and REX systems presented results that were very impressive in terms of position error over long USAR exercises [217, 218].

At about the time the present thesis was undertaken, the Navigation group at DLR in Wessling, Germany also began working on the foot-mounted IMU approach. Their publications [23, 115, 116] address exactly the same emergency / rescue scenario requirements as outlined in this thesis. A cascaded, two-level approach was taken, with an Extended Kalman Filter estimating foot displacements as well as sensor biases and a Particle Filter system doing map filtering over building maps. As depicted in Figure 4.1(f), Jadaliha et al. [98] have made a significant step by mounting a 6-DoF IMU printed circuit board in the sole of a shoe. It is not known if this component contains a DSP or if it is dependent on other devices (e.g., a belt-mounted processing unit). Preliminary PDR positioning results using this device have been reported and it is clear that further work is required, particular with regards to the estimation algorithms which appear somewhat *ad hoc*. Very recent work on the fusion of the data from the two foot-mounted IMUs using a centralized Extended Kalman Filter was reported by Brancroft et al. [28]. By using physiological constraints on step length (and thus the relative position between the IMUs) plus a unified EKF and tight coupling to GPS (for alignment), significant positioning performance improvements over the single foot-mounted IMU case were obtained. Magnetometers were not used, however, and so indoor paths showed some heading jumps plus some slow drift.

[2] A test campaign was completed in mid-2008. Commercial release is expected in 2009.

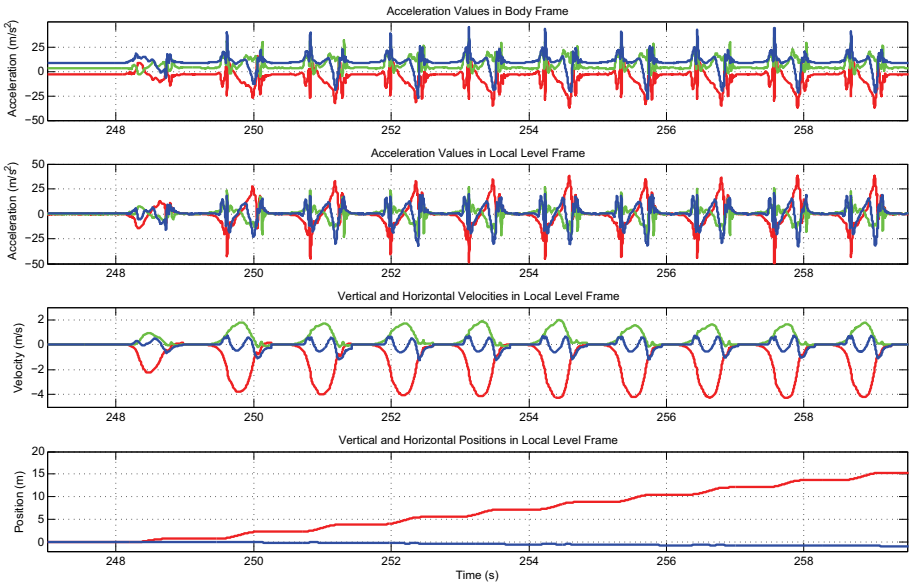

Figure 4.2: Mechanization and Step features

4.2 Algorithm

The foot-inertial PDR technique is actually quite complicated if implemented from first principles using only the raw inertial (accelerometer and rate gyro) sensor data. The difficulty lies in the estimation of the orientation, or attitude, of the IMU relative to the navigation (in present case, local-level) frame. However, the technique is quite straightforward if the attitude of the IMU is already available from some other source. In our case, the software supplied by the IMU manufacturer can provide quite good orientation estimates in the form of a rotation matrix.

At algorithm initialization, the foot is assumed to be stopped, so the initial velocity $\dot{\mathbf{x}}(t_0)$ and position $\mathbf{x}(t_0)$ variables are both set to $[0,0,0]^T$. The algorithm then consists of essentially only two parts, both of which are performed for every time step:

1. The motion state of the foot, either stopped or moving, is established by the values of the acceleration and rate gyro magnitudes, that is

$$|\mathbf{f}| = \sqrt{f_x^2 + f_y^2 + f_z^2} \tag{4.1}$$

and

$$|\boldsymbol{\omega}| = \sqrt{\omega_x^2 + \omega_y^2 + \omega_z^2} \tag{4.2}$$

where the f_i's are the specific forces measured by the accelerometers and the ω_i's are rotation rates measured by the gyros, both in the body frame. When both $|\mathbf{f}|$ and $|\boldsymbol{\omega}|$ drop below empirically-established threshold values, the foot is deemed to be in the stopped state. Otherwise, it is deemed to be moving.

2. If the foot is in the stopped state, the velocity $\dot{\mathbf{x}}(t_n)$ is reset to $[0,0,0]^T$ m/s and the position is held constant $\mathbf{x}(t_n) = \mathbf{x}(t_{n-1})$, where n is the time step index.

Otherwise, the foot is in the moving state and simplified, strap-down inertial navigation equations are used [221, 80]. First, the specific-force measurements in the body frame are transformed to the local-level frame and gravity is subtracted to yield the net acceleration in the local-level frame

$$\ddot{\mathbf{x}}(t_n) = \mathbf{R}_b^l(t_n)\mathbf{f}^b(t_n) - [0, 0, g]^T \tag{4.3}$$

where $\mathbf{R}_b^l(t_n)$ is the so-called "attitude matrix" that does a coordinate transformation (a rotation) from the body frame to the local-level frame. The accelerations are integrated once to yield the velocity

$$\dot{\mathbf{x}}(t_n) = \int_{t_{n-1}}^{t_n} \ddot{\mathbf{x}}(\tau)d\tau + \dot{\mathbf{x}}(t_{n-1}) \tag{4.4}$$

and a second time to yield the position

$$\mathbf{x}(t_n) = \int_{t_{n-1}}^{t_n} \dot{\mathbf{x}}(\tau)d\tau + \mathbf{x}(t_{n-1}) \tag{4.5}$$

both in the local-level frame.

The integration is done numerically at every time step using the attitude matrix and compensated specific force measurements, both calculated by the Xsens XKF filter. The specific force measurements in the body frame are compensated for internal misalignment and for temperature by this same software. (The implications of using these pre-processed values are elaborated below in Section 4.6). Example intermediate and final results for a short straight-ahead walk from a zero-velocity start are shown in Figure 4.2.

A few comments about this simple navigation algorithm are in order. The threshold on the gyro magnitude in combination with the acceleration magnitude threshold is required to prevent false stop detection during some motions, for example slow walking up or down stairs. It was found that using only the acceleration magnitude for these situations was not reliable. In the mechanization given above, local variations in gravity (from the distance to the center of the Earth, latitude dependence, or geological effects) as well as Coriolis forces due to the Earth's rotation have been ignored [221, 80]. These effects will be much smaller than the those due to uncompensated sensor bias variations and sensor noise for the low-grade IMU that is used in these experiments. At the sampling rates used here (at least 100 Hz) and with foot dynamics that are slow relative to this, a simple trapezoidal numerical integration method was found to be as accurate as more complicated, higher-order schemes. The horizontal coordinates generated by the algorithm are rotated and translated to map coordinates such that the initial starting point and the initial heading match to the values surveyed at the beginning of each experiment.

4.3 Experimental Set Up

For conducting the experiments, an Xsens MTi motion sensor was solidly attached to the shoe by passing the laces in crossed pattern through the MTi's baseplate holes

(a) Shoe-mounted IMU (b) Accessories

Figure 4.3: Experimental Set-up

and over the plastic housing. Once the laces were tightened, this ensured that the unit would not jiggle relative to the foot. This is especially important for the period from the heel strike to the beginning of the stance phase of walking, where there can be high acceleration and rotation rates. The IMU had to be mounted at a ∼45° angle relative to the shoe / foot axis because otherwise the 3 cm long connector for the data and power cable would have rubbed against the shoe tongue, see Figure 4.3(a). The cable was run inside the pant leg and came out at the waist and then anchored in place on the lower leg and on the belt with adhesive tape. A backpack was worn to carry the GPS receiver (a uBlox AEK-4H with the raw data output option), whose patch antenna was mounted on a construction helmet. See Figure 4.3(b). Note that the MTi used for the experiments was a non-standard version with a 1200 deg/s full scale range for the rate gyros. It was found in preliminary experiments that the standard MTi ratings of 300 deg/s resulted in signal clipping in the period between heel strike and the beginning of the stance phase. Also note that while data from two IMUs was often collected, this was done primarily for redundancy purposes. Data from only one of the IMUs will be analyzed here.

The IMU sampling rate was set to at least 100 Hz for all experiments. There was little change in the results with sampling rates above this value up to the 512 Hz maximum of the MTi. Raw IMU and GPS data were collected using a tablet PC during walks along predefined routes. The raw IMU data were post-processed with the Xsens MT Manager application to generate compensated accelerometer and gyro measurements as well as a rotation matrix for every time step. This inertial data was then post-processed using custom Matlab code implementing the algorithm described above. The starting position for each experiment was established by manual survey and was usually the same point in many experiments. As the algorithm does not have the ability to estimate the magnetic declination nor the orientation of the IMU relative to foot, the initial azimuth was set manually to give a correct heading (direction of travel) over the first few steps.

In the MT Manager application, the Kalman filter settings for “human - high accelerations” were used. In initial experiments with the MTi, the results were

considerably worse than the ones shown in this document. Partway through the experimental phase of this thesis, the author participated in a beta testing program with Xsens and supplied experimental data from walking experiments as well as considerable feedback to the firm's R&D group. The current MTi firmware and algorithms in the MT Manager application, branded as the "XKF", are the outcome of the beta program and work very much better than the previous filter versions for this application.

The following protocol was followed for all experiments. After powering up the MTi sensor (via the USB connector), the MEMS sensors and electronics were given 5-10 minutes to reach a stable operating temperature (as per the manufacturer's recommendations). After starting IMU recording, the test subject stood still for about 30 seconds to allow the XKF filter to converge to reasonable initial values. Again, this was simply following the manufacturer's recommendation as the author had no visibility into the XKF filter's internal behavior, and more specifically the covariance matrix. The foot was then repositioned and held static for 10-15 seconds in various orientations to help the filter to converge further. After another motionless 30 second period, the main parts of the experiments were performed. At the end of the experiment, the sequence of still and foot orientations were repeated. (These calibration sequences will hopefully be useful in the future if an application-specific sensor fusion filter is developed).

The MTi magnetometers were re-calibrated periodically, typically every few experiments as the drift on these sensors is normally quite low. Using the Xsens "Magnetic Field Mapping" software utility and carefully following the procedure given in the user's guide, the magnetometer offsets and gains compensating for hard- and soft-iron distortions were established. For a detailed description of the algorithm, see [144]. Note that this procedure must be done in an unperturbed Earth magnetic field. Once calibrated, the angular error in magnetic field vector measurements was expected to be less than 1 degree (according to the manufacturer's utility).

4.4 Test Results

The results presented in the following sections are representative trials drawn from ~50 test runs that were performed in various indoor and outdoor environments. A significant portion of these runs were unsuccessful, due to either technical issues (e.g., serial communication problems) or due a very inaccurate or diverging behaviour in the XKF filter output. For the sake of clarity, only results for tests done in Bremen are shown, and in particular in and around the author's building where overhead photos and construction plans are available. Quantitatively and qualitatively similar results were obtained from successful test runs done at other locations.

Only a small number of tests were performed with multiple users. It was found that there was very little variation in the results between different individuals. This is not surprising as the only important user-dependent factor in the foot-inertial technique is the time that the foot stays still during the stance phase. As long as the standstill detection thresholds are not too strict (i.e. low), individual variations

in gait will not have any effect on the estimated positions.

For the following plots, the red dots indicate the estimated position of footfalls. The blue lines between the red dots give the estimated trajectory of the foot given by the inertial calculations.

4.4.1 Distance over Ground

Over many experiments, the Distance over Ground (DoG) , that is the sum of the distance between successive footfalls, has proven to be very accurate. Examples of some of the DoG tests done are shown in Figure 4.4. The individual segment statistics are summarized in Table 4.1, where each row gives the DoG error for a single test run relative to an accurate path on the ground (and not relative to GPS positiion fixes which would not be accurate and repeatable enough for these fine-grained tests). The test shown in Figure 4.4(a) was performed down the center line of a road between two points exactly 50 m apart. The data for the back and forth test was split into individual 50 m segments by looking for the long stop periods at the end of every length. (Note that the slight bend in the path is not a heading anomaly but a deliberate manoeuvre to avoid a truck that suddenly pulled into the test area). The next two tests were both performed on a standard athletic track. The one shown in Figures 4.4(b) was back and forth four times between the 100 m start and finish lines following a land separation line. Again, the back and forth experiment was split into individual 100 m segments by looking for long pauses in movement at the end points. The test shown in Figure 4.4(c) covered a complete lap of the track. The lap was walked exactly on the line separating the fourth and fifth lanes in order to have a precise reference trajectory to follow. Starting at the fifth lane's 400 m start mark and ending at the starting line, the ground truth distance along this lane separating line is slightly less than 400 m[3]. The continuation of this path beyond the finish line back to the 400 m starting mark for the fifth lane was not used. As can be seen from the table, the DoG error is consistently better than 1.8%, superior to results reported elsewhere for this technique [163]. The discrepancies in error rate between the different tests is partly due to the adaptive behaviour of the XKF filter and hence its varying performace from test to test. Also environmental factors, such as temperature changes that may not be fully compensated and magnetic perturbations that are not estimated perfectly by the XKF filter, can explain some of these discrepancies. As shall be shown below, the DoG error has a far smaller impact on overall positioning performance than the

[3]This was due to the fact that distances around the track are set not at the lane edges, but by a line offset outward 10 cm (in the first lane, 20 cm) from the lanes' inner border. The curve radius in the first lane's reference line is 36.50 m and the lane width is 1.22 m. Consequently, the distance around the track along the described trajectory is one arc plus one straightaway plus one half circle plus one straightaway, or 100.11 + 84.39 + π * (36.50 + 4*1.22) + 84.39 = 397.89 m. The first term in this sum is the distance around the first bend calculated knowing the angular position of the start mark for the fifth lane. The dimensions used for this distance calculation are based on the IAAF track standard [96] and are shown in the figure. The test track conformed to this standard.

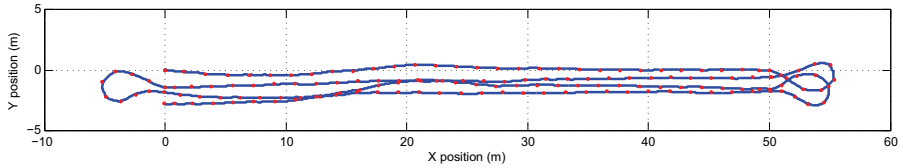

(a) Road center test

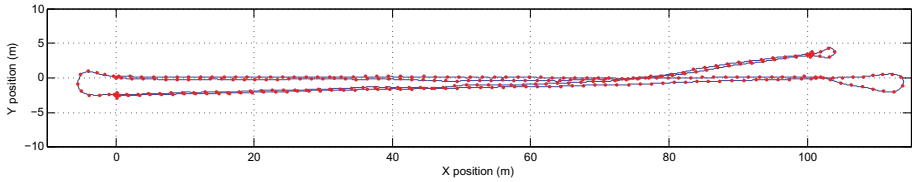

(b) Track straight test

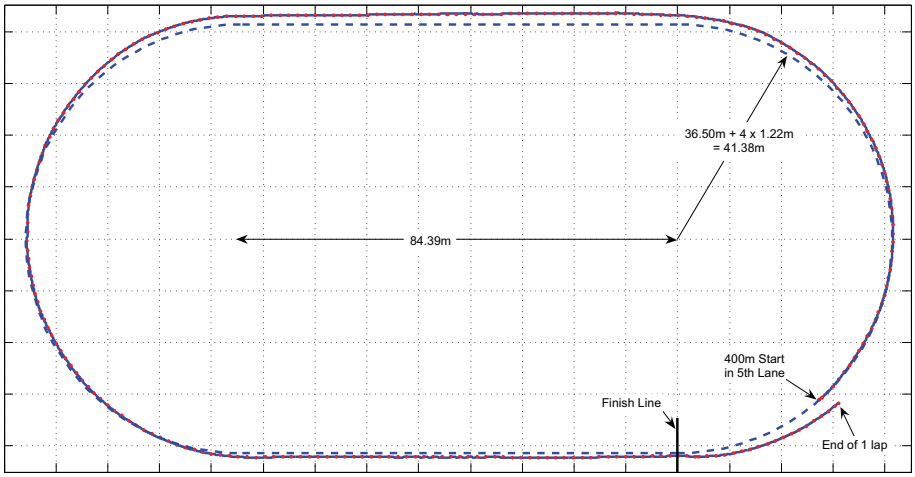

(c) Track lap test

Figure 4.4: Distance over Ground Tests. For the third plot, the ground truth path along a running lane divider is shown as a dashed line.

heading error. Consequently, more extensive DoG tests and statistical analysis were not done as these would likely have not have revealed much more than what has been show here.

4.4.2 Heading

There are some noteworthy heading anomalies in the tests shown in the previous section. For the 100 m tests, there is a systematic heading change at the 80 m mark on two of the four stretches. The experimenter noticed that there was a high lamp post on the edge of the track at this location. It was matched to a magnetic disturbance which may have caused the heading jump on the first two stretches. Why the heading jump did not occur on the other stretches is unknown. Also, the looping back to the zero mark does not close as it should and yet there was not obvious magnetic artifact at this location. For the 400 m lap test, there

Test name	True distance (m)	Est. distance (m)	% error
Road #1	50	50.1	+0.2
Road #2	50	50.3	+0.6
Road #3	50	50.3	+0.6
Road #4	50	50.2	+0.4
Track #1	100	100.7	+0.7
Track #2	100	98.3	-1.7
Track #3	100	100.8	+0.8
Track #4	100	98.9	-1.1
Lap	397.89	405.0	+1.8

Table 4.1: Distance over Ground Performance

is a cross-track error on the order of 1.5 m and no significant heading anomalies. However, there appears to be a slight heading jump after stopping at the finish line and before continuing to complete a full lap (428.78 m). On top of small magnetic perturbations, there are additional, more subtle effects at work on the heading, see Section 4.6 below.

4.4.3 Vertical displacements

Three-dimensional positions are available with the mechanization method presented. The positioning in the horizontal plane is quite good, as has been shown. With regards to the vertical axis, however, the raw results are very poor. There is a systematic trend in the vertical position in all experiments, see Figures 4.5(a) and 4.6(a). This is likely due to a combination of misalignment (or more accurately, non-alignment) of the IMU, to the use of uncalibrated accelerometer values as well as to a time delay in the orientation output relative to the accelerometer values. As there is no *principled* way of augmenting XKF filter to deal with these issues, an *ad hoc* correction method was developed for fixing the vertical channel. The relatively constant downward (and occasionally upward) drift over an entire experiment is nulled out by adding a small bias to the vertical acceleration channel (not the sensor Y acceleration channel). The value of the detrending bias can be established by graphically matching the starting and ending vertical positions in a closed loop course. Alternatively, it could have been estimated in real-time using a baro-altimeter. This simple detrending makes the small-scale vertical excursions of the foot very visible, see figures 4.5(b). Figure 4.7 depicts another such a detrended path through an office building stairwell. The actual vertical climb, as determined from manual measurement, is around 11 m (∼60 cm from sidewalk to door, followed by 6 flights of 10 steps at 17 cm / step). The estimated altitude gain is about 13 m. While not perfect, this level of accuracy is more than sufficient for determining which floor one is on, particularly if used in conjunction with a 3D building plan and by counting steps and flights.

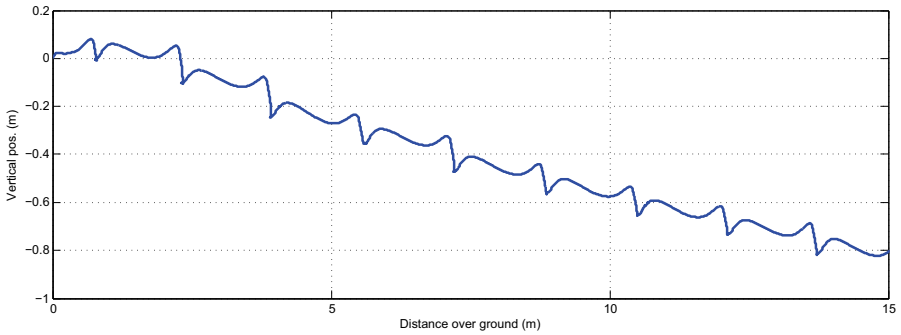

(a) Raw

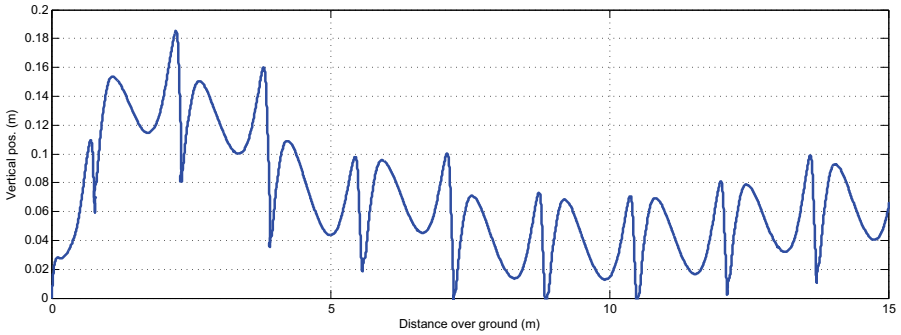

(b) Detrended

Figure 4.5: Vertical Position Drift and Detrending for one of the 100 m tests shown previously.

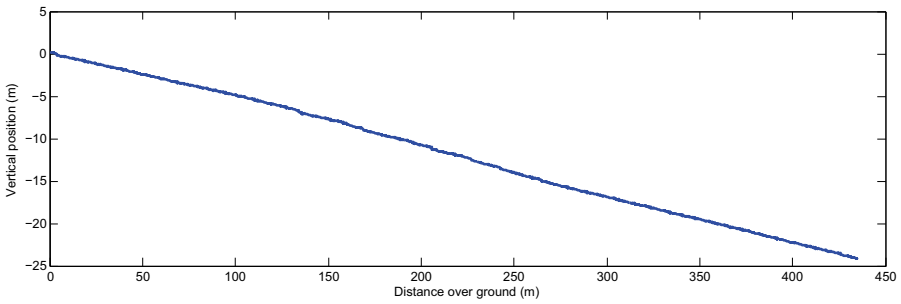

(a) Raw

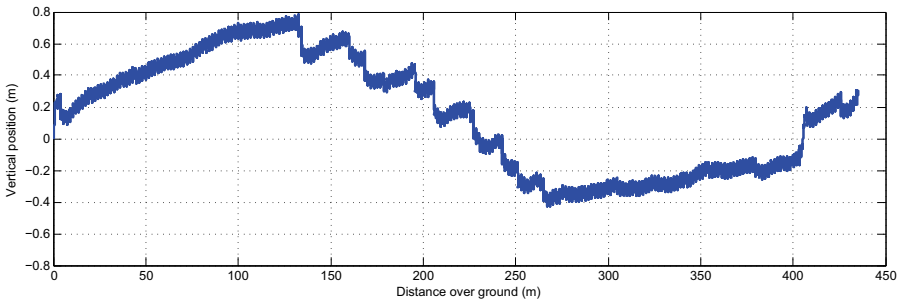

(b) Detrended

Figure 4.6: Vertical Position Drift and Detrending for the lap test shown previously.

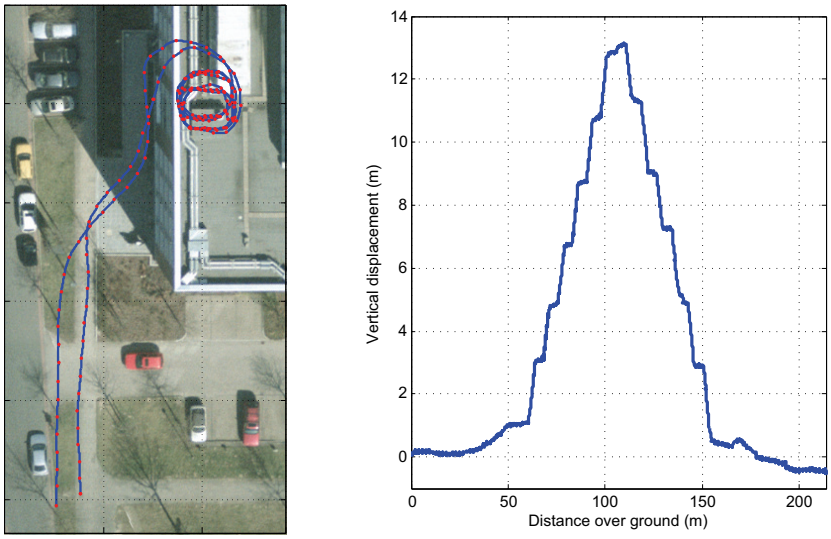

(a) Top view (b) Side view

Figure 4.7: Vertical Displacement

4.4.4 Omni-directional movement

In order to be useful for emergency and rescue scenarios, it is essential that the selected PDR method correctly handle not just straight-ahead walking, but also non-regular, turning, and halting motions, or in other words, omni-directional movement. First responders travel much larger distances (up to 500 m, to the limit of their air supply) using upright locomotion than they do crawling, shuffling or duck walking since these latter modes are very demanding physically. Consequently, a set of upright walking patterns that would likely constitute a large percentage of the distance travelled during emergencies were selected for testing. The outcome of typical experimental runs are shown in Figure 4.8. This particular test was performed outdoors so that GPS position fix data could be collected, see Figure 4.8(a). Note that this was only used for qualitative positioning performance analysis. The GPS fixes have at least 1-5 m time-varying errors which are due to mild multipath, to the inherent noise in the GPS pseudorange measurements, and to the motion model implemented in the receiver software. Since the latter is designed for normal pedestrian movements with modest dynamics, it does not correctly track all the very tight turns or stop/start behavior. The GPS antenna is mounted on the helmet, so there is, at a minimum, a varying horizontal position offset of around half a step length between the GPS position and the position of the foot. Consequently, it does not make much sense to calculate position error statistics based on the GPS position fixes. Therefore, only a qualitative positioning performance analysis is provided here.

The first segment of the test began at position (0,0) and proceeded to the right around a counter-clockwise loop and returned to the starting position, see Figure 4.8(b). Note that the longer, straight sections were on sidewalks exactly 10 m on

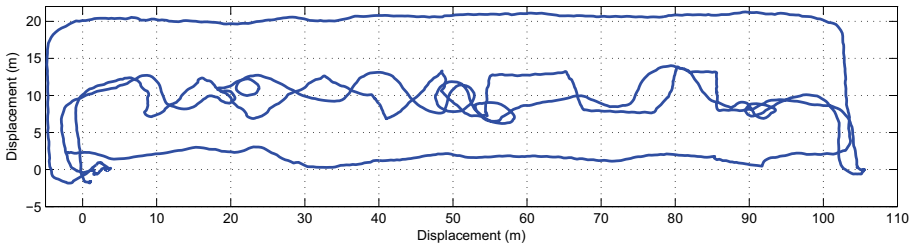

(a) GPS ground truth path

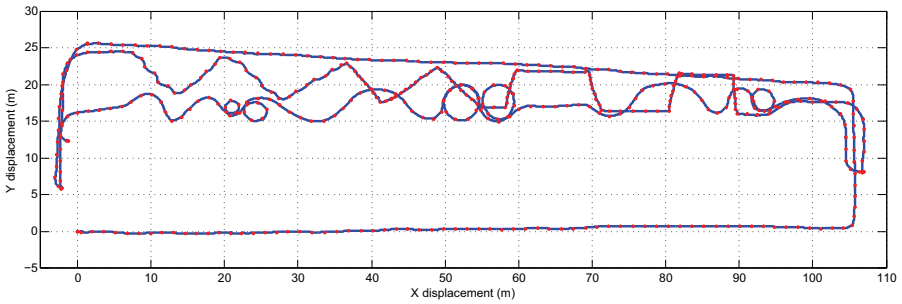

(b) PDR-estimated path

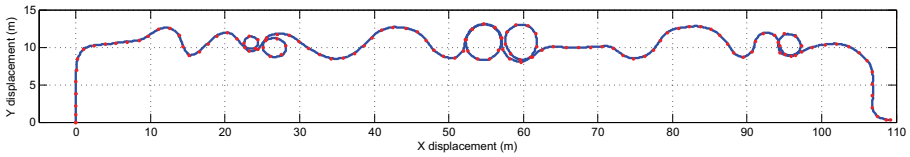

(c) Looping path detail

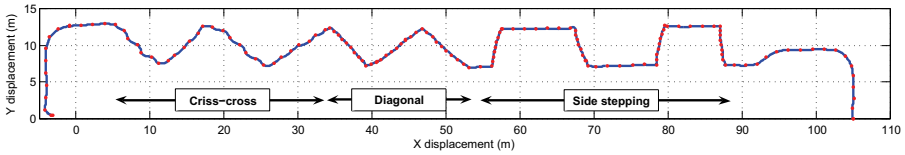

(d) Non-linear path detail

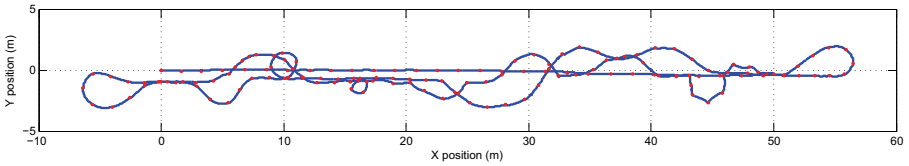

(e) Pirouette path

Figure 4.8: Omnidirectional Movement Tests

either side of the center line of the road. As evident in the figure, most of the ∼6 m PDR position offset at the end of the outer loop is due to the slight heading error at the second turn. This may be due to an XKF filter effect or to a very slight residual error in the magnetometer calibration. The next two segments, running down the center of road, faithfully reproduce the motion performed and mirror the noisy GPS path, save for a slight offset of final position. The tight turning and non-linear manoeuvres are detailed in figures 4.8(c) and 4.8(d), with the position offset from the outer loop segment removed to show that the center line of the road was followed (along the 10 m Y coordinate). The tight turns were performed while walking in the forward direction only while the side-stepping and crisscross motions were done half forward and half backwards.

The last plot (Figure 4.8(e)) shows the result of a different experiment where an exact 50 m stretch down the center line of a road was walked, first with a regular forward pattern and then with looping turns and pirouettes every few steps. Except for a slight heading error and a maximum 1 m cross-track error, the path does not show any noticeable anomalies. While not shown here, the author also performed very exaggerated "silly walks"[4] back and forth over the same 50 m stretch with no significant position errors. Stepping up and down slopes or small obstacles (e.g., walls) was also tested. In summary, as long as footfalls are detected reliably and as long as the interval between them does not exceed ∼2-3 seconds, any arbitrary motion between footfalls can be correctly reproduced with the foot-inertial PDR method. These results are repeatable and reliable outdoors, but as will be explained below, are not so in deep indoor scenarios.

4.4.5 Indoor / Outdoor

For light indoor conditions, the PDR-estimated paths do not suffer too much from magnetic disturbances. For the case shown in Figure 4.9(a), they have only a small effect on the heading and the position offset at the end of the 600 m path, which is only a few meters. This path was covered at a normal walking speed with no stops indoors except at doors. There were therefore few moments where local magnetic perturbations could have affected the heading. For comparison, a plot of the GPS position fixes for this experiment is shown in Figure 4.9(b). As expected, the GPS fixes are often very poor, with large position biases due to multipath across the parking lot at the back of the building and no fixes at all to the right of the building. Also, the few "High-Sensitivity GPS" fixes in the inner courtyard are off by tens of meters. This highlights the fundamental advantage of PDR techniques over GPS for this kind of scenario.

For the deep indoor scenarios, the results are unfortunately not nearly as good. See Figure 4.10 for a typical test which included many stops, direction reversals, and on-the-spot turns. This was done to mimic firefighter "room sweep" behavior. While individual, short-range manoeuvres can be recognized (e.g. turns into rooms), frequent and sudden heading anomalies ruin the overall shape of the path relative to

[4]Inspired by a Monty Python's Flying Circus skit.

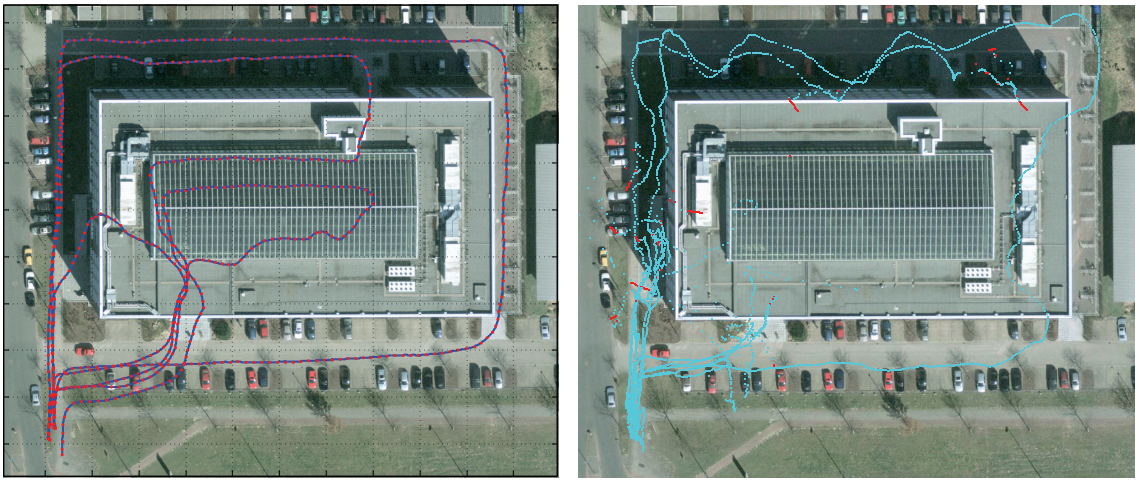

(a) PDR-only position estimates (b) Corresponding GPS position fixes

Figure 4.9: Outdoor and Light Indoor Test

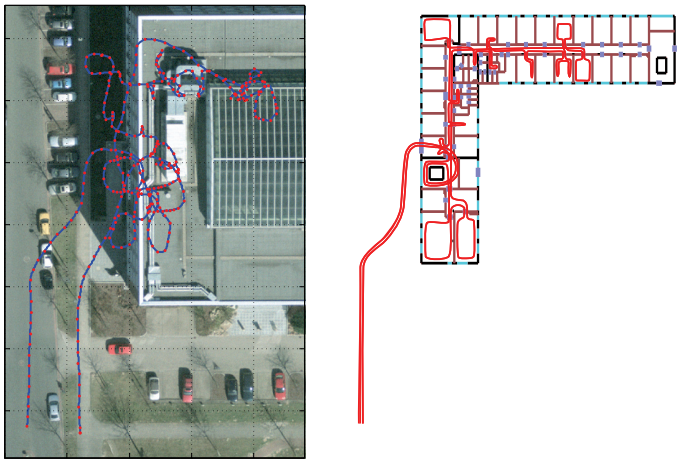

(a) Estimated path (b) Ground truth path

Figure 4.10: Deep Indoor Test

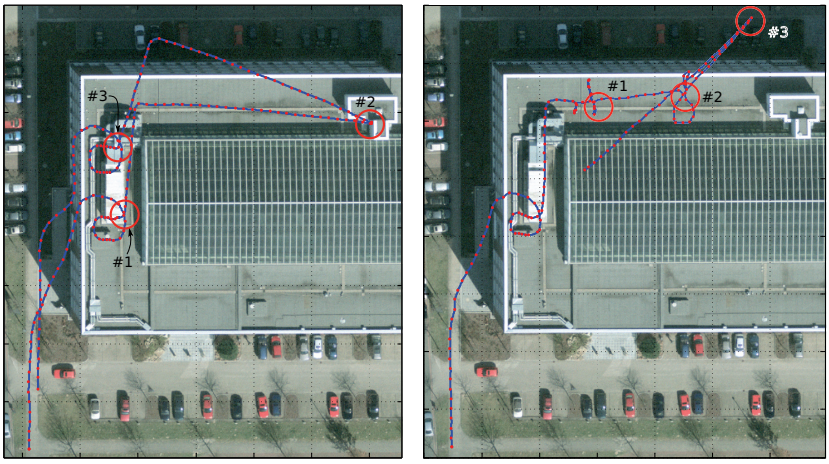

(a) (b)

Figure 4.11: Indoor Heading Jumps

the ground truth. The explanation is that there is a high density of magnetic disturbances caused by metallic and electrical objects such as automatic door actuators, door frames, in-floor concrete "rebar", electrical conduits and vertical structural elements. The magnetic fields from these objects are superimposed on the Earth's magnetic field and can cause heading "jumps" during longer stops. A more detailed discussion of the magnetic disturbances seen in these tests is given below.

4.5 Magnetic Disturbance Mapping

In order to gain insight into the heading problem in indoor environments, the peaks in the magnetic field magnitude were identified. It was initially thought that heading jumps corresponded to high magnetic field strength points along the walked trajectory. This turned out not to be the case. For example, in the tests shown in figures 4.11 and 4.12, there was no correspondence between the magnitude of the ambient magnetic field and heading errors over the straight non-stop segments. The heading was generally very steady even in the presence of very large magnetic perturbations while moving. However, during some stops longer than a normal footfall, the orientation estimate rotated (in roll, pitch and yaw) slowly over 2-4 seconds. The points where this occurred are circled in red in Figure 4.11. The exact time course of this fictitious rotation at stops depends on the relative weighting of the accelerometer, gyro and magnetometer measurements inside the XKF filter as well as on other the values of other adaptive parameters that may be present in the filter. This time course is impossible to predict. The final value that the heading settles to is dependent on the attitude error from gyro drift accumulated over the non-stop segments as well as on the horizontal component of the magnetic field. As there is no way to obtain the covariance matrix from the XSens API, there does not appear to be a principled way of doing a *post hoc* correction to the heading by leveraging

the relative uncertainties of these measurements[5].

Interestingly however, it turned out that the peaks in the magnetic field intensity corresponded very well with "cultural objects" in many instances. Outdoors, where there is a low density of metallic, man-made objects, it is quite easy to spot the artifact corresponding to a particular magnetic intensity spike, see Figure 4.12. Because the magnetic field intensity of a dipole drops off at least as the third power of the distance to the dipole, the magnetic effect of individual objects can often be isolated and identified. In addition to manhole covers, lamp and fence posts, transformers, and door frames produced very noticeable magnetic features (also reported in [144] for a body-mounted magnetometer). The perturbations can be caused by an object's intrinsic magnetization. For example, the magnetic field of a manhole cover is established when it is cast in an ambient magnetic field, i.e., the Earth's. Also, the perturbations can be the result of the object distorting the Earth's magnetic field. Judd recently showed how magnetic intensity profiles can be used to match points on repeated (outdoor) loops and thereby reduce positioning error by cancelling long range drift [101]. This is a potentially interesting approach for outdoor and light indoor applications, and particularly if areas and paths can be magnetically surveyed ahead of time. For the light indoor case shown in Figure 4.12(d), it would certainly possible to detect passage through some doors and potentially other features in the inner courtyard. In fact, a simple "magnetic signature" approach was tried in conjunction with laser scanning of indoor environments for robot localization some years ago [14].

The strength and density of the spikes varies greatly depending on the building type. For example, they can be almost non-existent in structures with wooden frames (for example, American homes) but completely mask the Earth's magnetic field in heavily reinforced structures (e.g., train station underground passages). Unfortunately, in many common indoor environments, local magnetic disturbances are dense and can overlap completely[6], making the identification of meaningful peaks very difficult. Even in the case of a standard office environment, isolated magnetic peaks and cultural features can be difficult to identify or used for position aiding. For example in Figure 4.13, corresponding to the deep indoor path shown in Figure 4.10, it is easy to pick out the magnetic disturbances due to the door on both entry to and exit from the building, but in the hallway, magnetic spikes that might correspond to some physical features cannot be readily isolated. Similar dense magnetic features from a walk through a steel-framed building were discussed in [66].

Another approach was investigated for dealing with the heading problem discussed above. It was inspired methods used for finding unexploded ordnance, or "UXO", in military and post-conflict activities [244, 37, 153]. In normal UXO oper-

[5]In the experiments described here, "human - high accelerations" XKF filter tuning parameter set was used. Alternative filter tuning parameter sets, which are fixed and defined by Xsens, can be selected by the user for other applications. For example, with the "machinery" settings, the magnetometer readings are ignored by the XKF, which is a sensible thing to do when operating close to electric actuators or metal structures, for example. Unfortunately, these "machinery" filter settings perform very poorly with the foot-mounted sensor in the PDR application.

[6]Private communication with E. Foxlin, President of InterSense Inc.

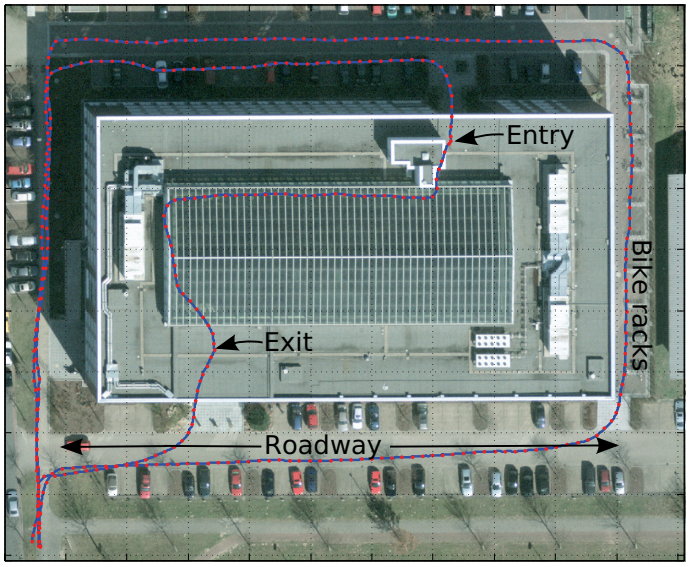

(a) Outer loops

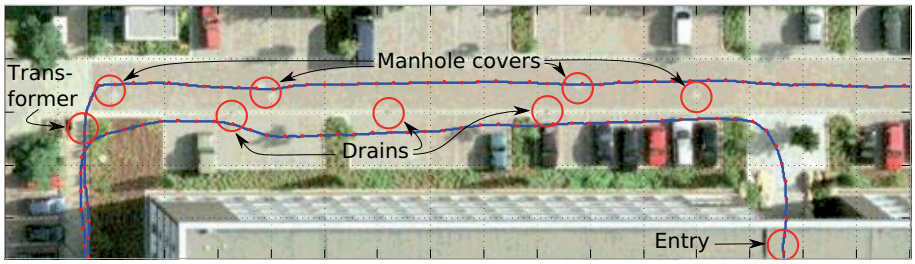

(b) Magnetic perturbation versus Cultural features

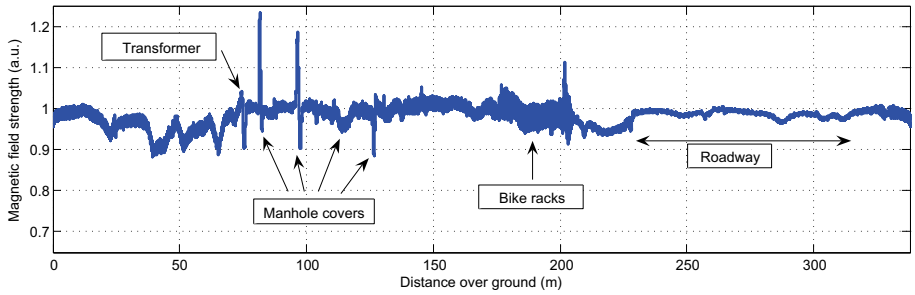

(c) Outer loop magnetic features

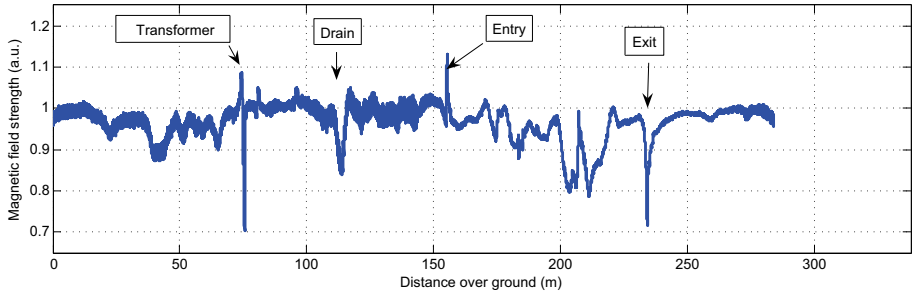

(d) Inner loop magnetic features

Figure 4.12: Magnetic Disturbance Matching

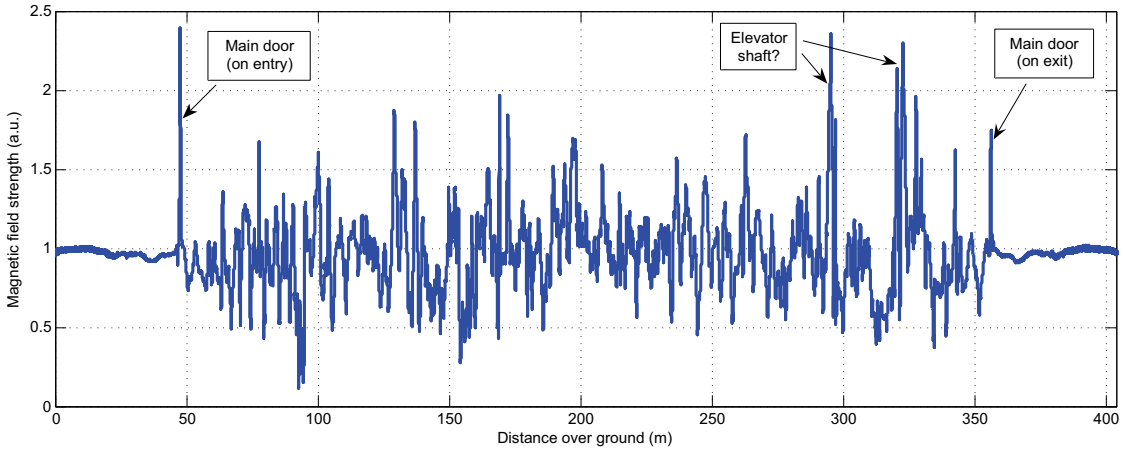

Figure 4.13: Deep Indoor Magnetic Field

ations, a systematic 2D magnetic survey of an environment is performed and then the spatial grid of measurements is fit to the magnetic field equations in order to locate metallic ordnance. Unfortunately, this kind of survey is impractical for the emergency scenario being addressed here. The new idea is first to estimate the position of "virtual dipoles" via "dipole inversion" from the vector magnetic measurements at each point along the foot's path. Then, one could compensate for the dipoles by a *post hoc* adjustment to the magnetic measurements and re-running them through the XKF. To do so, the measured magnetic field values and the short-term-accurate foot displacement data for short windows were fit to the magnetic field equation for dipoles

$$\hat{\mathbf{H}} = \frac{3(\mathbf{m}\cdot\mathbf{r})\mathbf{r}}{r^5} - \frac{\mathbf{m}}{r^3} \tag{4.6}$$

where $\hat{\mathbf{H}}$ is the magnetic field at the observation point, $\mathbf{r}$ is the vector between the observation point and the dipole, $r = |\mathbf{r}|$, and $\mathbf{m}$ is the dipole magnetic moment. The fit was performed by minimizing the squared difference between the measured and modeled magnetic fields $(\mathbf{H} - \hat{\mathbf{H}})^2$ by adjusting the dipole position $\mathbf{r}$ and magnetic moment $\mathbf{m}$ using a non-linear numerical optimization routine in Matlab. Unfortunately, as the paths ran generally in a straight line past the magnetic objects, the collected data was not spatially-diverse enough to stably solve the field equations. Very often, the minimization did not converge and inaccurate position and strength estimates for the virtual dipoles were obtained, even after constraining[7] the strength and location of the dipole or by reducing the problem to 2D. Essentially, this approach amounted to trying to solve an ill-posed inverse problem. If the paths had curved around the magnetic objects, there would have been more spatial diversity in the data and the fit might have been better behaved.

[7]Via "regularization", see for example [220].

4.6 Discussion

Since the Xsens XKF filter is proprietary software, it has effectively been used here as a "black box". The author did not have access to the filter's internal functions or data structures so "grey box" testing could not be performed. Systematic "black box" testing was not attempted either to determine more about the filter since this would likely have been unfruitful due to its adaptive nature. However, over the course of many experiments, many important aspects of the filter's behaviour were observed. Also, some details on the internal strucutre of the filter was obtained from discussions with the Xsens engineers during a beta testing program in which the author was a participant. Consequently, the following paragraphs summarize the author's incomplete view into the filter's internal structure and give a qualitative summary of the filter's resulting, external behaviour.

The XKF filter was designed primarily for limb orientation estimation in human motion capture applications. As an *orientation filter*, neither velocities nor positions were made part of the filter state since they are not needed. Obviously then, there are no API facilities for triggering ZUPTs (e.g. by detecting thresholds in sensor magnitudes or by a foot switch), for introducing velocity or position aiding information, or for doing azimuth estimation based on successive position fixes since neither position nor velocity information is contained in the filter. Consequently, the XKF filter's orientation cannot be kinematically aligned [205, 80, 18, 156, 230]. The presumption is that the XKF does do some coarse static alignment to the local horizontal using the accelerometers (a procedure called "leveling"). However, this is probably only to low accuracy as the accelerometers have unknown, random switch-on and time-varying biases which are very likely not fully observable (see Section 3.5 of [77]). Also, the XKF API does not give access to the filter's state covariance. Consequently, any state external to the filter, such as the magnetic declination or sensor biases and their uncertainties, cannot be combined with the filter's internal state in a principled fashion.

While moving, the XKF filter relies almost entirely on the gyros for orientation estimation, so passing through magnetic disturbances quickly has virtually no effect on the azimuth and thus on the heading. However, during low-acceleration periods lasting more than around 2-3 seconds, the adaptive Kalman filter starts weighting the accelerometers more highly than the gyros for estimating pitch and roll angles. It also starts using the horizontal component of the magnetic field for estimating the azimuth angle. Together, these measurements can correct for accumulated gyro drift. If the low-acceleration period occurs in even a slight magnetic disturbance, any bias in the horizontal magnetic field may turn the yaw axis in an incorrect direction. Consequently, the azimuth will be seen to suddenly jump when the foot comes to a stop. The XKF very likely changes the sensor relative weightings based on the acceleration magnitude but exactly where the switch over occurs is unknown. If a custom PDR Kalman filter were built, the switch over would clearly have to occur during the foot rest periods defined by accelerometer and gyro magnitude thresholds. Note that the heading jump effect on the heading is in addition to any

global heading distortions from residual magnetometer miscalibration.

It was noted in Section 4.2 that the attitude matrix is estimated by the XKF filter. Internally, this filter may be estimating the switch-on biases (as random constants) and time-correlated bias variations (as first-order Gauss-Markov processes) for each of the accelerometers and rate gyros. Oddly, however, the "compensated" sensor measurements (provided via another API call) are corrected for mounting misalignment and temperature effects only. Bias estimates are *not* applied, even if they are likely available internally to the filter. Consequently, when the accelerometer values without corrections for these biases are double integrated, one may get subtle heading changes that have nothing to do with the real trajectory. This may explain some of the small heading changes seen in the earlier figures for outdoor paths.

Detailed examination of the mechanization plots (e.g., Figure 4.2) showed that there is a systematic non-return to zero of the vertical channel velocity just before ZUPTs. As discussed in Section 4.4.3, adding a bias can remove almost all the downward vertical *position* trend, but it does not completely remove the vertical channel's *velocity* offset just before ZUPTs. After considerable investigation, it was determined that there is a very slight lag in the XKF orientation estimate relative to the inertial measurements. Note that the calibrated sensor readings do not go through extensive preprocessing and are thus delayed only a few microcontroller clock cycles relative to the A/D sample times. By applying 1-3 timestep backwards offset to the orientation estimates relative to the calibrated sensor readings, it was possible to make the velocities return much closer to their correct zero value. The overall positioning performance of the system improved, but only slightly. This makes sense since the response of a *causal* Kalman filter can lag the dynamics in the measurements by a few predict/update cycles. In contrast, *non-causal* filters use future and present values in addition to past values and their output can be made to have no lag with respect to the input data stream. In many cases, non-causal Kalman filters are just normal filters run forward and then backward in time over the same data and then the results from each pass are combined. One popular approach is the Rauch-Tung-Striebel (RTS) smoothing algorithm [184]. Of course, non-causal techniques can only be used with non-real-time data (recorded or held in a delay buffer). Besides the output having no lag relative to the input, non-causal filters and smoothers also generally perform better than their causal counterparts. As far as the author can determine, the XKF orientation filter is a causal filter and so has some lag.

Further analysis showed that the magnetometer output is quite lagged relative to the gyro and accelerometer outputs and this is particularly visible during the onset of the stance phase. The magnetometer outputs continue to rotate even after the gyros and accelerometers clearly show that the foot has come to a stop. The manufacturer's IMU specifications state that the accelerometer, rate gyro and magnetometer sensors are bandwidth limited to 30, 40, and 10 Hz respectively. These limits are fixed in hardware by simple RC filters. The RC filter time lags likely cause some loss of displacement and orientation accuracy during fast foot rotation (i.e., in

the time from heel strike to beginning of stance phase). Unfortunately, these effects are difficult to characterize via black-box testing or to circumvent without making modifications to the IMU hardware.

In the experimental procedure, the azimuth is established by hand by setting the estimated direction of motion of the first few steps to the desired direction on a map. Consequently, any azimuth errors caused by uncorrected accelerometer biases were invisible until significant heading changes were made, i.e., after turns or over back and forth paths, recall Figure 4.8(b). Depending on the relative sizes of the uncorrected biases and of the misalignment, square and back and forth paths can get systematically distorted. For closed paths, start and end position offsets tend to be small because bias errors are mostly cancelled out [149]. Therefore, positioning performance results reported using this start/end offset statistic, for example in [105], should be taken with a grain of salt. For similar reasons, distance over ground performance results tend to mask bias and alignment errors and particularly over closed paths.

In summary then, the XKF orientation filter's performance is surprisingly good but the filter's usefulness in high-precision pedestrian positioning applications will remain limited. It cannot be precisely aligned to the local-level navigation frame, either statically or kinematically. Its output cannot be combined in a principled fashion with other state external state information (e.g., in a cascaded Kalman filter set-up) since the filter's internal covariance information is not accessible.

4.7 Ongoing Filter Development

Given the shortcomings of the Xsens filter identified above, work on a custom sensor fusion filter implementation was begun during this thesis. Using Foxlin's description [71] as a starting point, an indirect (i.e., error-state) Unscented Kalman Filter (UKF) [102] was set up. A UKF was chosen over an EKF (Extended Kalman Filter) since the former is purported to be easier to work with (as analytical derivatives do not have to be specified) and can be more accurate for some non-linear problems. In the error-state configuration, the filter estimates *errors* in the inertial states (position, velocity and orientation) as opposed to the inertial states themselves. The major advantage is that this circumvents the need for modeling motion dynamics [193, 110], as task that would be next to impossible for unconstrained locomotion patterns. The entire sensor fusion algorithm was implemented in Matlab using a KF toolkit [87].

Considerable time was expended trying to get the implementation tuned and stable, and work is still ongoing. Several experts[8] have informed the author that tuning this kind of filter is extremely difficult, error prone and time consuming. While automatic KF tuning procedures exist [56], they have yet to become commonplace. For example, the uncertainty of the covariance parameters of the process noise and the observation errors has a significant impact on filter performance. These factors

[8]Personal communications with H. Luinge at Xsens, E. Foxlin at InterSense as well as P. Tomé and J. Skaloud at EPFL, all experts in Kalman filtering and inertial sensors.

influence the weight that the filter applies between past information and the latest measurements. Their values normally come from intensive empirical analysis and bench testing. Errors in them may result in suboptimal performance of the filter, or even divergence [56, 79]. For a foot-mounted IMU, the medium-term walking dynamics are low, which makes it difficult to initialize and maintain heading calibration using GNSS and inertial navigation alone [144]. Short-term levels of jerk (the first derivative of acceleration) and vibration of the foot can be high, making sensor bandwidth limitations, rate gyro acceleration sensitivity, scale factor accuracy, cross-axis sensitivity and orthogonality of the sense axes critical. It is not known how, or even if, these issues are handled in the XKF filter.

Despite these obvious challenges, a couple of basic points have been identified for future work on this filter. First, for the heading problem indoors, it is possible to estimate the bias to the magnetic azimuth based on the difference between the gyro-estimated azimuth and the magnetic azimuth at the stance phases. Large discrepancies between the values can be used to reject bad magnetometer measurements [144]. (The XKF filter does not appear to use any "outlier rejection" logic). The bias to the measured horizontal magnetic field could also be incorporated as a state in the Kalman filter, as was done by Foxlin [71]. Predictions of the evolution of this state variable might be done using the "virtual dipole" approach described above or using a more conventional Markov process modelling approach [144].

Second, in some classes of upright locomotion, the foot may stop in a non-flat orientation. For example, when a person is down on one knee, the front part of the read foot is on the ground but the heel could be oriented close to the vertical. In this attitude, an Euler angle parameterization of orientation has a singularity and consequently the filter could become unstable. For this reason, it may be better to use a quaternion parameterization for the orientation [117, 196, 173].

Finally and most importantly, practical methods must be devised for performing a "kinematic alignment" [80, 221, 205] of the foot-mounted IMU in the short time between fire vehicle egress and entry into nearby buildings. Alignment procedures permit an INS filter to establish the precise orientation of the IMU relative to a local-level navigation frame, usually with true North as a reference azimuth. Coarse alignment to the local horizontal is done with non-bias corrected accelerometers. This is also known as "leveling". Fine alignment refines this solution by determining the accelerometer biases very precisely. Multiple ZUPTs plus high-accuracy GPS position and/or velocity fixes are typically used to this end. Position and velocity changes are required to separate out heading errors from tilt errors and accelerometer biases as well as to estimate accelerometer scale factors. In a few cases of previous research on foot-mounted IMUs where kinematic alignment was performed, it was accomplished by some minutes of walking around outside with a clear view of the sky for GPS reception and far from any magnetic disturbances [71, 28]. This is clearly impractical for emergency scenarios. In previous research, little consideration has been given to the dynamic "lever arm" effect, caused by time-varying position difference between the foot-mounted IMU and the GPS antenna (which is typically mounted on or above the head). If uncorrected, the position errors introduced by

this effect may make rapid and fine alignment of the foot-mounted IMU unreliable. Also, innovative solutions for GPS positioning close to and around buildings as well as in urban canyons will have to be devised. Obtaining reliable GPS fixes under these extreme multipath conditions is very difficult and is the subject of current research. Given the fact that few satellites will be visible under such conditions, it may be necessary to actually *exploit* (rather than just mitigate) multipath phenomena in order obtain good positioning results [208, 84]. Alternatively, RF-based local positioning systems, such as UWB ranging systems deployed on parked fire vehicles, could be exploited for kinematic alignment purposes.

4.8 Conclusion

This chapter has shown that foot-mounted IMUs can be used for unaided pedestrian positioning in many situations. Outdoor and light indoor tests have shown that good distance-over-ground ($< 1.7\%$ error) and positioning accuracy with relatively low drift is possible using an unmodified, commercial sensor fusion filter designed for general motion tracking. Omni-directional, upright motions were also shown to be handled correctly, with relatively low drift over short test courses outdoors. This is an important result for the application of the technique to first responder scenarios, where "irregular" locomotion may be frequent. Significant problems remain with vertical position drift, but a simple detrending workaround was shown reduce this drift dramatically and provide at least qualitatively correct vertical displacement information, sufficient to determine the floor number, for example. Improving on these positioning results will definitely require the development of a sensor fusion filter specifically designed to use ZUPTs and ZARUs at footfalls and the development of supporting technologies for enabling the rapid kinematic alignment of the INS.

Significant challenges remain. With regards to positioning deep indoors, magnetic disturbances produce very obvious heading "jumps" during pauses in walking using the general purpose filter. There is no easy way of modeling the possibly dense and overlapping magnetic fields in many indoor environments. Some researchers claim to have filter implementations that compensate for these disturbances and these solutions are worth investigating further. Nonetheless, residual heading anomalies will likely remain and these must be mitigated somehow if positions estimates are to remain reliable and useful for first responder scenarios. How this might be done using map aiding is the topic of the next chapter.

Chapter 5

Map Aiding

The results of a recent location trial show that pedestrian oriented inertial technology achieves interesting performance (stand-alone positioning accuracy better than 3 m RMS after 4 minutes and less than 6 m RMS after 8 minutes of continuous pedestrian walk), but still lacks robustness against specific environmental conditions, in particular magnetic disturbances affecting orientation estimation and users' walking behavior [46].

It is well known that map matching can be used to improve the localization performance of both people and vehicles (see next section on related work). In many emergency / rescue scenarios, however, there may be only very limited building plan information available, such as an exterior wall outline obtained from aerial photographs or cadastres databases. Escape plans posted at the entrances to many building might be all that is available and might provide only approximate exit door and stairwell locations as well as hallway and room orientation. Also building plans might be inaccurate because they are simply out of date or more dramatically, the structures they represent may be partly demolished due to fire, earthquake or explosion. Moreover, there is currently no universally-accepted standard for printed, let alone electronic, search and rescue maps [11].

What is not known is how much map information is really required for an Urban Search and Rescue (USAR) mission and how much each level of map detail might improve positioning accuracy. A method for fusing building plans and PDR motion measurements was suggested by the authod and developed by the author and his collaborators [238, 30]. It was implemented using an existing Particle Filter and positioning code base developed at the Cork Institute of Technology for wireless positioning [239]. A novel implementation of Map Filtering (MF), called the Backtracking Particle Filter (BPF), was proposed by the author and was evaluated with real PDR displacement data and building plans as input. It was shown that the BPF can take advantage of long-range (geometrical) constraint information provided by various levels of building plan detail. It was clear from those studies that the geometry of the building and the course through it would have an effect on positioning performance. An indoor/outdoor binary measurement (based on GPS visibility) was also proposed by the author and was shown to prevent particle cloud

divergence. The contents of the two papers cited above are combined and expanded below.

There will undoubtedly be advances in MEMS sensors and the associated estimation/compensation algorithms that will allow for greatly improved positioning performance. However, it may be argued that real USAR scenarios will be remain technically very challenging, due to temperature variations [66] and completely unconstrained locomotion patterns. This chapter looks at how a priori building map information could be used to improve the performance of such MEMS-based PDR positioning systems. As will be shown, even minimal map information can help greatly in this regard.

5.1 Related work

Map matching, where a database of navigable paths/roads is available, was developed primarily in the field of probabilistic robotics. The principles are very well understood, see for example chapters 7 and 8 of [219]. It is well known that map matching can be used to improve the localization performance of ground motor vehicle navigation systems [214, 200, 47]. For pedestrians moving indoors, Elwell [62] suggested that building plans could be used in a map matching algorithm and thereby remove DR drift errors via position updates[1]. For outdoor pedestrian positioning, most research made some assumptions about how people move along sidewalks and at street crossings as depicted on detailed (usually 2D) urban plans [35, 192] or between buildings on coarser maps [159, 152, 142]. For the indoor case, *detailed* building plans were often assumed to be available. These were used unmodified [224, 243] or reduced to a node and edge representation and then combined with particle filters [209, 27, 43]. Consequently, map matching using *detailed* maps for indoor pedestrian localization cannot be considered novel.

A standard for search and rescue maps was developed in the context of the Pelote project [11] for the specific purpose of supporting map-aided localization of first responders. The proposed standard was very close to current international norms for this domain. The map data was to be structured in such a way (i.e., using Extensible Markup Language, or XML) that it could be imported directly into map-aided positioning systems. Interestingly, the proposal included provisions for localization beacon icons and a beacon layer.

A type of map aiding called terrain matching has been used for many years by cruise missiles [90] and more recently by lunar lander [99] and underwater vehicle [213] navigation systems and takes advantage of detailed digital terrain (i.e., altitude) models. Work by Soehren et al. [206] showed that digital terrain maps and altitude matching could be used in conjunction with sensitive barometers to reduce 3D position uncertainty for soldiers using a hybrid GPS/LORAN/occurrential PDR positioning system and moving through hilly, forested areas. For road vehicles, digital terrain models can be used in conjunction with GNSS pseudorange and

[1] However, it is not known the idea was subsequently implemented.

baro-altitude measurements to improve vertical and planar position estimates via map and altitude matching along road centerlines [139].

5.2 PDR Error Behavior

As discussed in Chapter 4, in the foot-inertial approach to pedestrian navigation, the distance between footfalls is estimated from 3D acceleration and orientation measurements sensed directly at the foot. Kalman Filtering (KF) and strap-down mechanization equations are applied to the raw IMU measurements for estimating foot displacements. To recapitulate, a rotation matrix that brings the body (i.e. sensor) coordinate frame to the local/level coordinate frame is estimated (in the present case, by the XKF orientation filter). Then the accelerations in the body frame are rotated to the local/level frame with this matrix and the resulting accelerations are double integrated to yield a displacement in the local/level frame. The velocity is reset to zero when the accelerations and rate gyro measurements drop below empirically determined thresholds. In a full KF implementation, sensor biases can be estimated and a coarse initial alignment can be performed using GPS position fixes obtained during short outdoor segments.

During near zero-velocity conditions at footfalls, it is usually possible to estimate the gravity vector from accelerometer readings and thereby determine roll and pitch angles. These facts can be exploited by the KF to correct for gyro drifts around these two axes. Gyro drift around the yaw axis is typically controlled via 3D magnetometer readings. Unfortunately, in indoor environments, magnetic disturbances can make magnetometer-based orientation estimates very problematic. Consequently, the adaptive KFs have to put more weight on the yaw gyro measurements versus the magnetometers. The result can be a slowly drifting heading. As discussed at the end of Chapter 4, an adaptive quaternion/ Kalman sensor fusion filter (similar to what was done in [71]) is currently under development. However, for the experiments presented in this chapter, the Xsens MTi sensor's software API was used to get the rotation matrix and compensated accelerometer readings. As explained in the previous chapter, the Xsens filter was designed for limb motion capture. It was not designed to handle the high dynamics at the foot and it cannot directly exploit any external information, such as velocity or position updates. When using the output from the Xsens filter software in the mechanization algorithm, the heading of the estimated path does not show the smooth drift pattern typical of dead reckoning systems. Over many experiments, sudden yaw/heading jumps were observed when stopping moving for a few seconds and/or when passing through an area with a high density of magnetic disturbances. See Figure 5.1 as well as Figure 5.8 later in this chapter. In addition, on-the-spot turns often produce greatly under- or overestimated heading/yaw changes, see Figure 4.10 in the previous chapter. It would appear that at these moments, the adaptive filter is modifying the magnetometer/gyro relative weighting and correcting for accumulated orientation errors due to gyro noise and bias drift. The net effect is that when the azimuth (heading) change between strides is small, one can assume that a heading jump artifact did

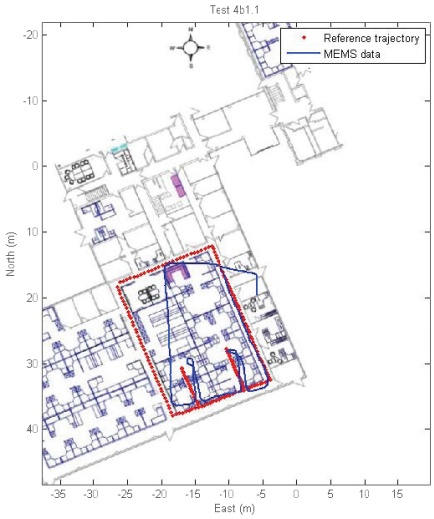

Figure 5.1: Typical Indoor Heading Errors for Foot-inertial PDR Technique [46].

not occur and can put a high confidence on the estimated heading. In other words, straight segments are mostly correct. On the other hand, when a large heading change is estimated, it may be due to a jump artifact or a real turn. Therefore, less confidence is put on measured turns. These observations were incorporated into the particle transition function described in the next section.

Once a custom foot-inertial filter is completed, different (and hopefully smaller) heading error behavior than the one described here will be observed. However, regardless of the sophistication of the filter or the quality of the sensors, the extreme operating conditions of USAR missions (high temperatures, in particular) will perturb IMU sensors [66]. MEMS gyros are quite sensitive to temperature changes and may also exhibit nonlinearities (due to the high, short-term dynamics at the foot) that cannot be easily modeled. The argument then is that significant heading errors will likely occur when this type of PDR system is deployed in the real world. Fortunately, these heading errors can be effectively mitigated with the techniques described below.

5.3 Particle Filters and PDR

Particle Filtering is a technique that implements a recursive Bayesian filter using the Sequential Monte-Carlo method [59, 189]. It is particularly good for dealing with non-linear and non-Gaussian estimation problems. It is based on a set of random samples with weights, called particles, for representing a posterior density function. Estimates are computed based on these samples and weights. The posterior probability density function (PDF) of the state is approximated using the following equation :

$$p(\mathbf{x}_t|\mathbf{z}_t) \approx \sum_{i=1}^{N_s} w_t^i \delta(\mathbf{x}_t - \mathbf{x}_t^i) \tag{5.1}$$

Algorithm 1 Generic Particle Filter

GENERIC PF(N)

```
1  Sample N particles from initial pdf
2  repeat
3          Get z_t
4          for i ← 1 to N
5              do get x_i^t from p(x_t|x_{t-1})
6                  Calculate w̃_t^i = w_{t-1}^i p(z_t|x_t^i)
7          Calculate total weight k
8          for i ← 1 to N
9              do normalize w_t^i = k^{-1} w̃_t^i
10         if N_eff < N_T
11           then Resample
12         Estimate state x_t = (1/N) Σ_{i=1}^N x_t^i
13         Increment t
14     until stop
```

where $\mathbf{z}_t$ are the observations, $\mathbf{x}_t^i$ is the i-th sampling point or particle of the posterior probability and w_t^i is the weight of the particle, all at time t. As the number of samples N_s becomes very large, the representaion becomes equivalent to the usual functional description of the posterior. The weights are modified at each time step using the relation

$$w_t^i \propto w_{t-1}^i \frac{p(\mathbf{z}_t|\mathbf{x}_t^i)p(\mathbf{x}_t^i|\mathbf{x}_{t-1}^i)}{q(\mathbf{x}_t|\mathbf{x}_{t-1}^i, \mathbf{z}_t)} \tag{5.2}$$

In practice, it is often convenient to choose the importance density to be the prior

$$q(\mathbf{x}_t|\mathbf{x}_{t-1}^i, \mathbf{z}_t) = p(\mathbf{x}_t|\mathbf{x}_{t-1}^i) \tag{5.3}$$

Substituting Equation 5.3 into Equation 5.2 then gives

$$w_t^i \propto w_{t-1}^i p(\mathbf{z}_t|\mathbf{x}_t^i) \tag{5.4}$$

One problem with a naive implementation of these ideas is degeneracy: after a few iterations, all but one particle will have negligible weight. A brute force method to avoid this is to use a very large number of particles but this creates a computational burden. Alternatively, the degeneracy can be detected when the effective number of particles $N_{eff} = 1/\Sigma_{i=1}^{N_s}(w_t^i)^2$ falls below some threshold N_T. It can then corrected by generating a new set $\{\mathbf{x}_t^i\}_{i=1}^{N_s}$via a resampling algorithm. Detailed derivations and further explanation can be found in [143]. A generic particle filter algorithm is given in Algorithm 1.

Figure 5.2 illustrates how a particle filter can used for tracking a person. Here, WiFi and wireless sensor nodes provide position likelihood information and a simple

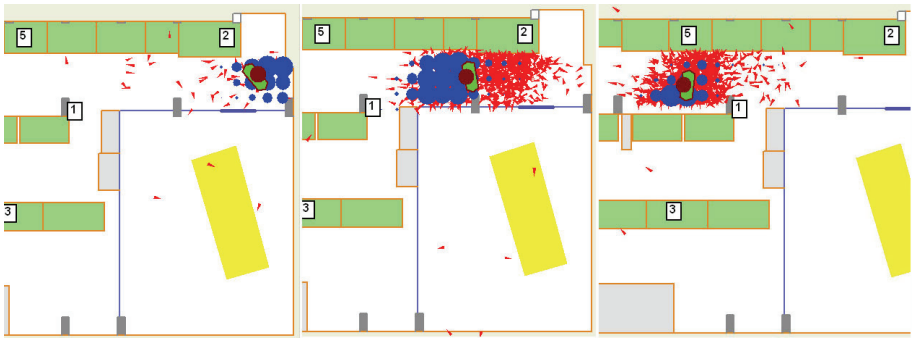

Figure 5.2: Example Particle Filter Behavior: Sequence of particle posterior distributions at $t = 1s$,$t = 20s$, and $t = 30s$. The blue circles represent the likelihood function, in this case from RF signal strength measurements. ([239], p. 157)

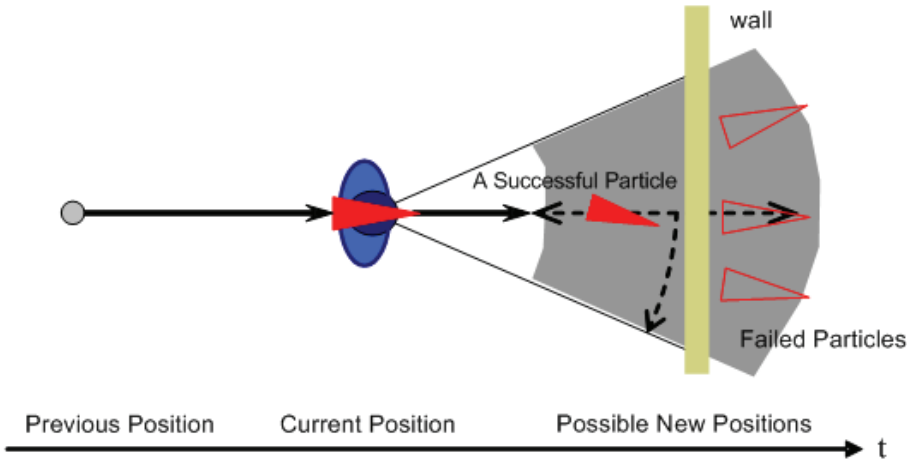

Figure 5.3: Particle Transition Near Obstacles: If a particle tries to move to an impossible location, e.g., across walls defined in the map, it will be killed off. ([239], p. 135)

motion model using only heading measurements from a magnetometer drive the prediction sampling step. The figure shows a sequence of posterior distributions, likelihood functions and state estimates at $t = 1$s, $t = 20$s and $t = 30$s.

For indoor positioning, building plans are very useful information that can be used to enhance location accuracy and reduce uncertainty of walking trajectories. Particle Filters can take into account building plan information during the indoor positioning process with a technique called Map Filtering [159, 239]. Map Filtering implements a fairly straightforward idea. New particles should not occupy impossible positions given the map constraints. For example, particles are not allowed to cross directly through walls. Particles that transition through such obstacles are deleted from the set of particles or are downweighted, as depicted in Figure 5.3.

Algorithm 2 Backtracking Particle Filter

BPF($N, tail$)

```
 1  Sample N particles from initial pdf
 2  tailcount ← 0
 3  repeat
 4          Get z_t
 5          for i ← 1 to N
 6              do get x_i^t from p(x_t|x_{t-1})
 7                  Calculate w̃_t^i = p(z_t|x_t^i)
 8          Calculate total weight k
 9          for i ← 1 to N
10              do normalize w_t^i = k^{-1} w̃_t^i
11          if N_eff < N_T
12            then Resample and inherit state history
13          Estimate state x̃_t = (1/N) Σ_{i=1}^N x_t^i
14          if tailcount ≥ tail
15            then x̃_{t-tail} = (1/N) Σ_{i=1}^N x_{t-tail}^i
16          Increment tailcount
17          Increment t
18      until stop
```

Backtracking Particle Filter

The Backtracking Particle Filter (BPF) is a technique for refining state estimates based on particle trajectory histories [238]. The incorporation of the Map Filtering technique allows the BPF to exploit long-range geometrical constraints. If some particles x_t^i are not valid at some time t, the previous state estimates back to x_{t-k} can be refined by removing the invalid particle trajectories. This is based on assumption that an invalid particle is the result of a particle that follows an invalid trajectory or path. Therefore, recalculation of the previous state estimation $\hat{x}_{t-k}$ without invalid trajectories will produce better estimates. In order to enable backtracking, each particle has to remember its state history or trajectory.

The BPF implementation for PDR is as follows. Figure 5.4(a) shows a typical phenomenon when a standard Particle Filter is used for Dead Reckoning. It illustrates posterior density of particles in four time steps. The position estimates and the ground truth are shown in the image as well. Map Filtering categorizes some particles as invalid at the 3rd step and the invalid particles are not subsequently resampled. Figure 5.4(b) shows how the Backtracking Particle Filter is used for removing the invalid trajectories. Figure 5.4(c) illustrates the recalculated state estimates after backtracking. It can be seen that under conditions like these, backtracking can improve state estimates relative to a normal PF.

The pseudocode above describes the complete BPF algorithm for state refine-

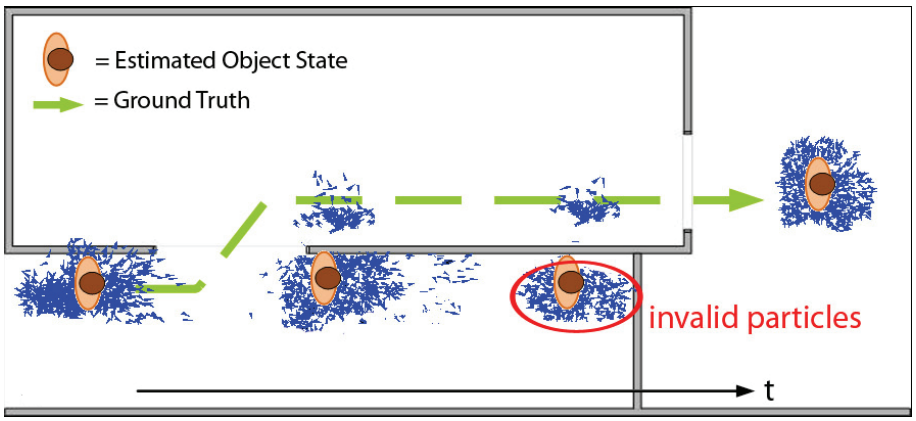

(a) Detecting invalid particles during PDR with Map Filtering

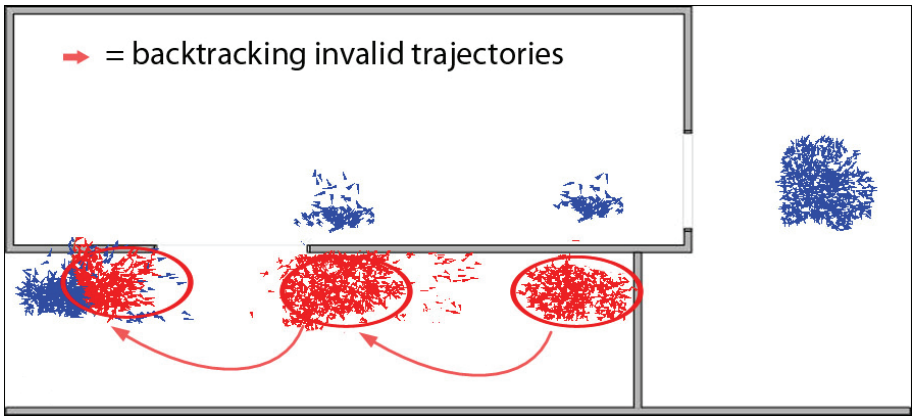

(b) Backtracking the invalid trajectories

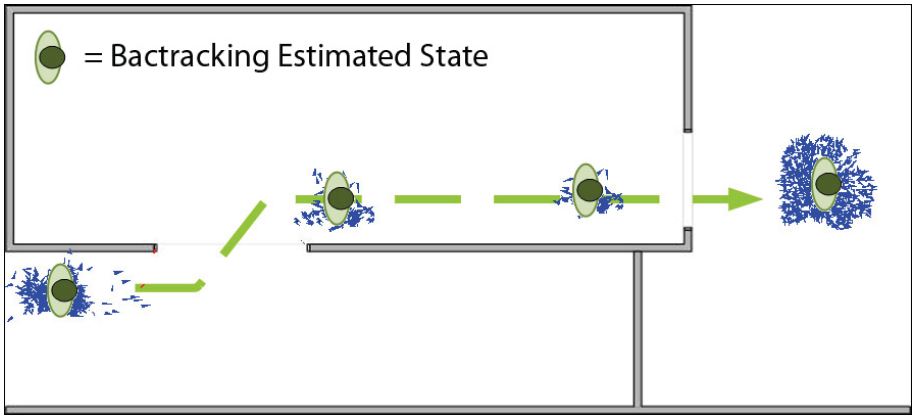

(c) Backtracking estimated states

Figure 5.4: BPF with Map Filtering. [30]

ment. The main features of the BPF can be seen in steps 6, 12, and 15 of the pseudocode. During *prediction sampling* in step 5, a new particle is sampled from the transition PDF $p(x_t|x_{t-1})$. In step 12, the *resampling step* is followed by inheritance of the state history. This *inheritance step* will enable the backtracking of invalid trajectories and also the calculation of the backtracking state. The *tail* value for the *backtracking* state calculation (step 15) is established empirically. The value is optimized manually by considering several parameters, most notably building plans dimension and trial duration.

Implementation for PDR

Implementing Particle Filters and Map Filtering with PDR displacement estimates can improve the accuracy of position estimates. It works especially well for PDR in indoor positioning scenarios where building plan information is available. Particle Filter and Map Filtering can be used to reduce the error accumulation by filtering the trajectory uncertainty. Note that with the infrastructureless assumption, no use was made of any likelihood measurements such as those depicted in Figure 5.2 and derived from UWB, WiFi or WSN RSSI measurements. Consequently, the likelihood calculation step found in most PF implementations is skipped.

Particle Filtering for PDR is implemented by incorporating displacement estimates into the particle transition function. Constraints defined in the map prevent impossible particle movements, such as crossing walls or other obstacles defined in the building plan. For each stride[2], a new particle position x_t^i is generated from the stride length and stride azimuth (heading) estimated from the foot-inertial calculations and is governed by the following transition function:

$$\mathbf{x}_t^i = \begin{bmatrix} x_t^i \\ y_t^i \end{bmatrix} = \begin{bmatrix} x_{t-1}^i + s_t^i cos(\theta_t^i) \\ y_{t-1}^i + s_t^i sin(\theta_t^i) \end{bmatrix} \tag{5.5}$$

where s_t^i is the stride length of the i-th particle at time t, sampled from normal distribution $N(s_t, \sigma_s)$, with mean stride length s_t and standard deviation σ_s. s_t is set to the foot-inertial-calculated stride length estimate and σ_s is set to a fixed value around 5% of the stride length (about 15 cm for a typical adult stride). The particle heading θ_t^i is sampled from a normal distribution $N(\theta_t, \sigma_{\theta t})$ with a mean stride heading θ_t and standard deviation $\sigma_{\theta t}$. $\sigma_{\theta t}$ is set to a fixed percentage (10%) of the inertially-calculated stride-to-stride heading change[3]. The net effect is that in straight segments, the particles remain on their previous course and that during turns, the particle cloud tends to spread out. The particle cloud also tends to spread out along the down-track direction.

The new particle position, which is determined by the transition function, should not be an impossible one. For example, movement across walls should not occur. If a

[2]Since the motion sensor is on one foot only, the PDR algorithm calculates the distance between footfalls for the same foot. This is the definition of a stride. For adults, one normal stride is between 1.2 and 2.0 m in length.

[3]More sophisticated step length and heading error models were proposed in [149] for simulation purposes. These models are overkill for the particle filtering done here.

particle attempts to cross such an obstacle, the particle weight is changed according to the following rule:

$$w_t^i = \begin{cases} 0, & \textit{if new particle moves to impossible location} \\ 1/N_s, & \textit{otherwise} \end{cases} \tag{5.6}$$

where N_s is the number of particles. For the first few failed attempts, the particle is downweighted and returned to its original position. After a predetermined number of attempts, the particle along with its history are removed from the particle set.

In addition to a basic wall-crossing rule, a more global rule with respect to the building perimeter was also suggested by the author and implemented. The idea is that GPS availability can provide a quite strong indication whether one is indoors or outdoors. The GPS receiver's signal strength or quality values, the number of tracked satellites, the carrier lock state or similar measurements can be used to synthesize an indoor/outdoor indicator. Particles that are on the inside of the building when GPS signals are still available are penalized. Conversely, those that are outside when GPS signals are not available are also penalized. The net effect of this rule is that it prevents the particle cloud from breaking up into isolated clusters inside and outside the building and that diverge away from each other. This logic was implemented in the transition function for the sake of expediency. It could have just as well been implemented in the PF likelihood application step.

5.4 Experiments

5.4.1 Tools

An Xsens MTi motion sensor was solidly attached to one shoe and inertial data were collected during walks along paths in and out of two representative office buildings. A tablet PC was used to log raw measurements from the MTi. These were then post-processed with the Xsens API and Matlab, generating raw PDR stride length and azimuth tables using the algorithms described in Chapter 4. Ground truth information was generated manually based on surveyed reference points and time stamps. For the sake of expediency, a synthetic, binary GPS availability flag was generated manually based on the ground truth path. The start position was set to a surveyed point and the initial azimuth was set so that the direction of travel from the starting point was approximately correct. No GPS position updates were used for any of the experiments. The stride length and direction, availability flag and ground truth data were then used as input to the MF software. Two thousand particles were used during the filtering. In these experiments, only 2D maps were used. Consequently, some walls on adjacent floors were removed to allow freer particle movement in certain locations, for example up winding stairwells.

The MF code, developed by Dr. Martin Klepal and Widyawan of the Cork Institute of Technology, was originally used for wireless positioning research [239]. As the code was not open source, the two collaborators modified their C++ source code to read in the PDR displacement and error estimates as well as the GPS flag data

provided by the author. The new transition function plus support features (such as statistical analysis and replay functions) were also added. They also implemented the BPF idea proposed by the author by maintaining the histories of every individual particle in the filter. Electronic building plans supplied by the author were converted into their application's internal format (based on SVG and XML).

5.4.2 Liaison Experiments

The first set of experiments was carried out in the context of a collaboration between the WearIT@Work and Liaison EU IP projects [46]. The tests were conducted in a small, one-storey office building at one Liaison partner's locations. They lasted approximately 10 minutes for around ∼400 strides and had a start/end point outdoors. The dimensions of the test area were around 52 m x 52 m.

The PDR displacement and azimuth data were analyzed on their own, with a standard Particle Filter with Map Filtering, and with the BPF technique. Each approach was in turn evaluated with different levels of building plan detail. The trajectory evolution over time with external wall map information is shown in Figure 5.5. In red color is the PDR trajectory and the black color represent the ground truth. As expected, the PDR trajectory error grows over time. This can be seen in some part of the trajectory which lie outside the wall boundaries. Figure 5.5 also shows PF+PDR trajectory and BPF+PDR trajectory both using Map Filtering. The trajectories are better since they are constrained by the external wall information. The sequence of figures show how increasing the level of building plan detail can influence the positioning trajectories. Figure 5.6(a) shows the trajectory with an escape map and Figure 5.7(a) with a detailed building plan. The BPF that can take advantage of trajectory histories and long-range (geometrical) constraint information yields excellent positioning performance (1.32 m mean 2D error) with detailed building plan information. More significantly, the BPF using only outlines of external walls yields substantially improved positioning performance (1.89 m mean 2D error) relative to a PDR-only, no map base case (8.04 m mean 2D error). This result is achieved via the elimination of the largest azimuth blunders. Furthermore, the combination PDR measurements and a Particle Filter performs approximately 4 to 5 times better compared to PDR measurements alone. PDR+BPF performance improves steadily with the level of map detail level (1.82 m, 1.5 m, and 1.32 m 2D mean error). In contrast, PDR+PF performance improves only if the detail level increases significantly (i.e. from external wall map to detail map). The positioning accuracy is summarized in Table 5.1. The analysis of the probability density function (depicted in figures 5.5(b), 5.6(b) and 5.7(b)) show that the estimation errors of the fusion solution follow a log-normal distribution. This distribution was selected based on a maximum likelihood fit of the error data to various distributions (normal, log-normal, Rayleigh, Rician). The log-normal fits had highest likelihood. In contrast, the PDR-only errors are more scattered and show a multimodal histogram.

In [187], a Fréchet distribution was fit to PDR trajectory errors, apparently for the first time. No explanation for this choice of distribution was given in that pub-

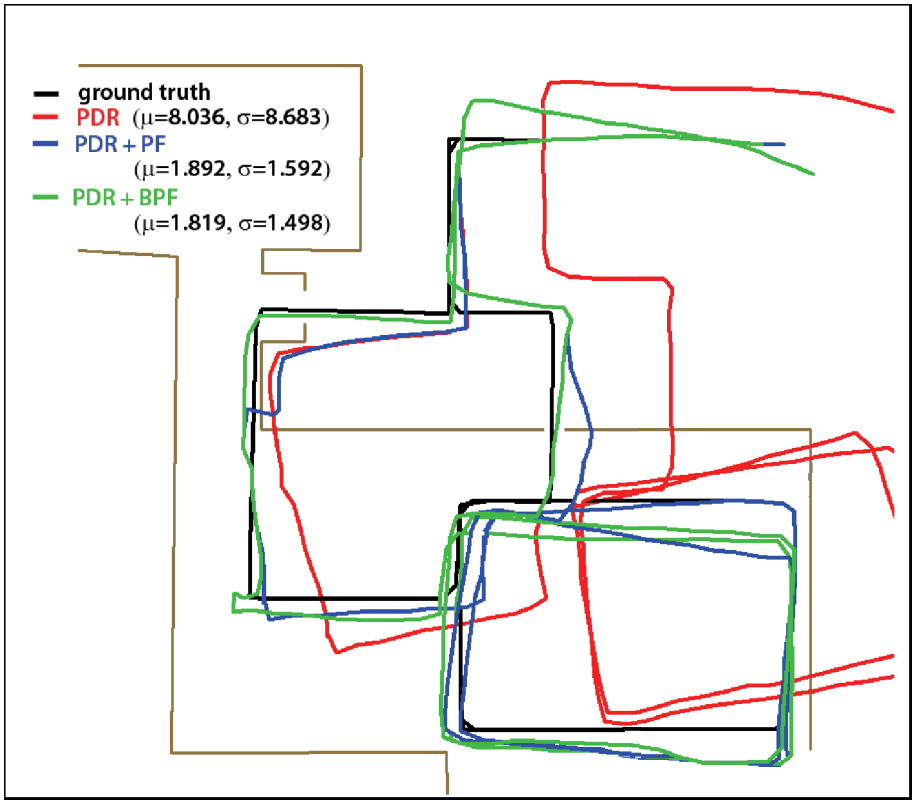

(a) Estimated trajectories

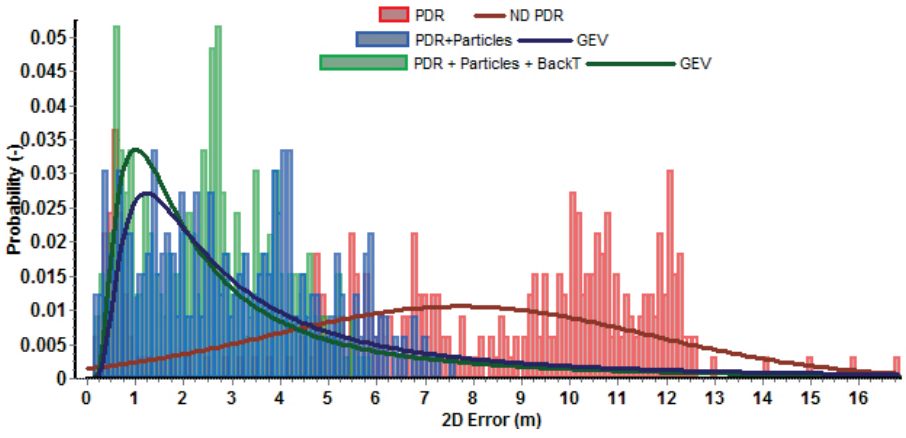

(b) Position error PDFs

Figure 5.5: Liaison positioning results using external wall plan

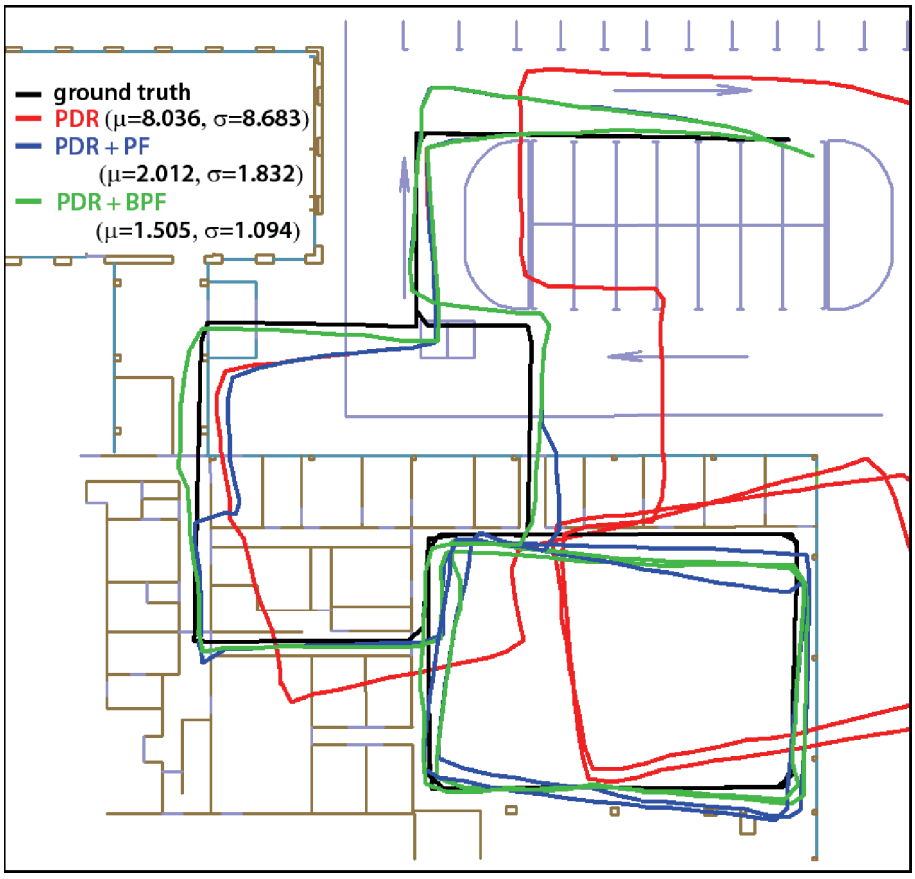

(a) Estimated trajectories

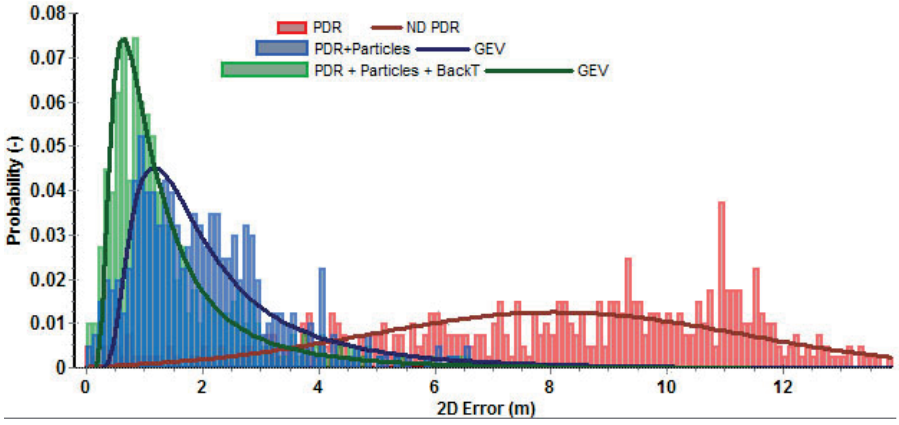

(b) Position error PDFs

Figure 5.6: Liaison positioning results using building escape plan

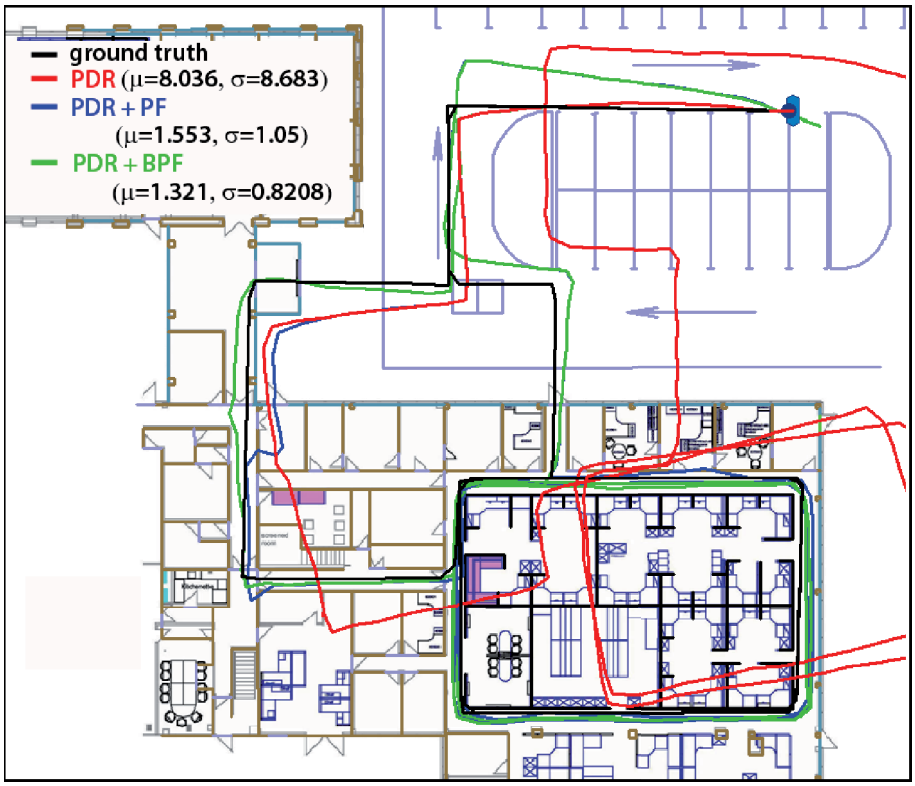

(a) Estimated trajectories

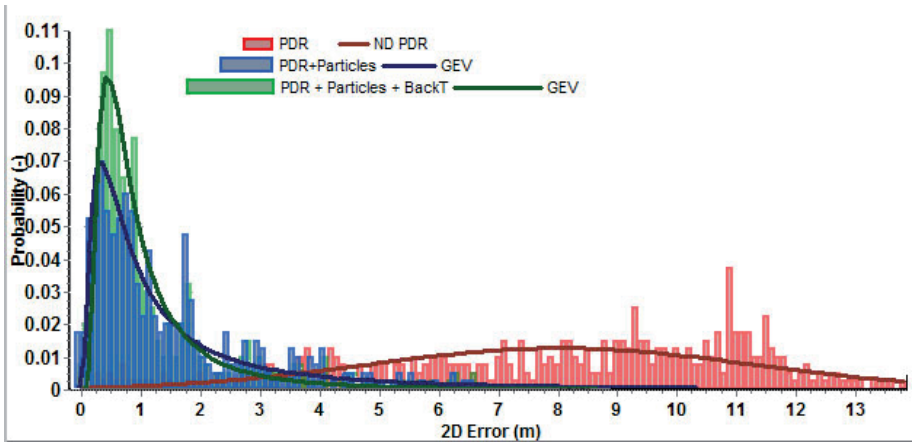

(b) Position error PDFs

Figure 5.7: Liaison positioning results using detailed building plan

Table 5.1: Liaison Experiments Positioning Accuracy

	PDR	**PDR+PF**	**PDR+BPF**
External Wall Map	μ =8.036 σ =8.683	μ =1.892 σ =1.592	μ =1.819 σ =1.498
Escape Map	μ =8.036 σ =8.683	μ =2.012 σ =1.832	μ =1.505 σ =1.094
Detail Map	μ =8.036 σ =8.683	μ =1.553 σ =1.05	μ =1.321 σ =0.821

lication. However, the Fréchet type (a subclass of the Generalized Extreme Value distribution [106]) may be related to the Fréchet distance, which can be used for calculating the similarity between two curves [60, 19]. The author speculates that depending on the type of drift and shape of the test path, this type of distribution may be a better choice that the log-normal distribution. Also, there may be a theoretical link between the Fréchet distribution and the (potentially unbounded) difference between ground truth paths and drifty estimated paths. However, investigating these conjectures is beyond the scope of this dissertation.

5.4.3 TZI Experiments

This walk lasted around 10 minutes (∼330 strides) and mimicked a reconnaissance mission during a fire. The start point was outdoors and the path included two loops in and out of the building. The end point was indoors. The overall dimensions of the test-bed were approximately 60 m x 60 m in an L-shaped building wing. The path included a straight, ground-level outdoor segment plus two flights of staircases to the first floor. The PDR displacement and azimuth data were analyzed on their own, with a standard Particle Filter with Map Filtering, and with the BPF technique. Each filter approach was in turn evaluated with two different levels of building plan detail.

The basic PDR trajectory which does not take advantage of any geometrical information is shown in red in Figure 5.8. As expected, the PDR trajectory error grows over time. This can be easily seen as some part of the trajectory already lie outside the wall boundaries before the end of the experiment. A number of heading/azimuth jumps are also apparent. Figures 5.9(a) and 5.10(a) show PF+PDR and BPF+PDR trajectories respectively both using Map Filtering. These trajectories are far better than the PDR one since they are constrained by the building plan information.

The positioning errors for this experiment are summarized in Table 5.2. The BPF which takes advantage of trajectory histories and long-range (geometrical) constraint information yields excellent positioning performance (0.74 m mean 2D error) with detailed building plan information. More significantly, the BPF using only outlines of external walls yields substantially improved positioning performance (2.56 m mean 2D error) relative to a PDR-only, no map base case (7.74 m mean 2D

Figure 5.8: TZI ground truth and uncorrected PDR trajectory: Building Floor Plan, Ground Truth (black line) and PDR path (red line). The blue shape on the lower left is an overhead view of a person standing at the start position.

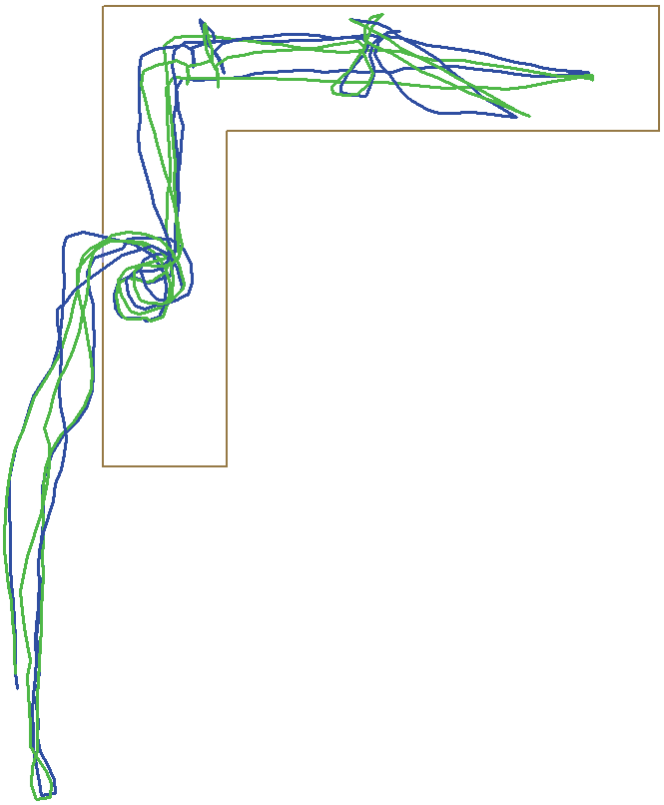

(a) Estimated trajectories

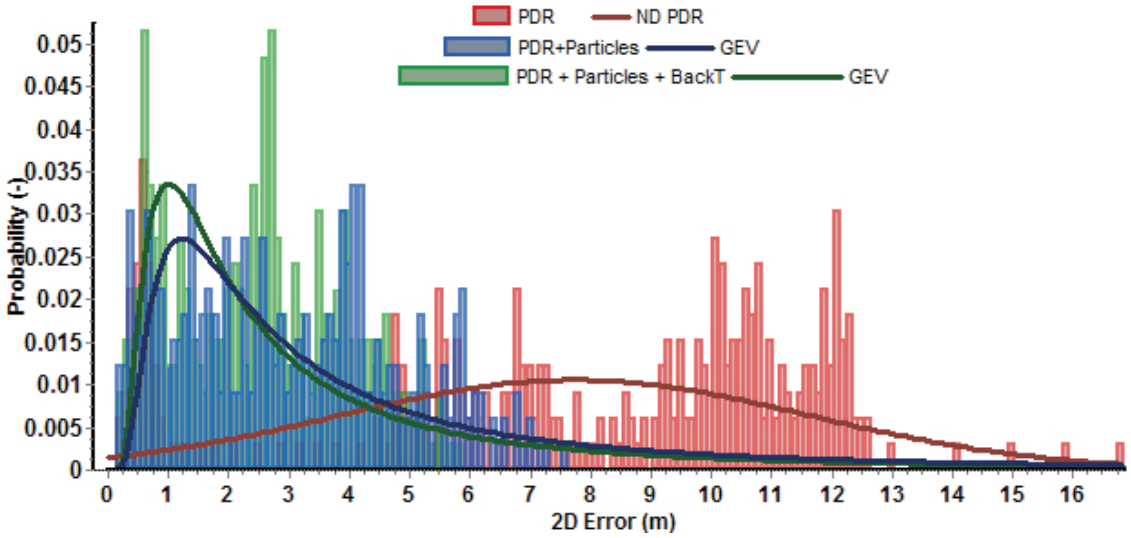

(b) Position error PDFs

Figure 5.9: TZI positioning results using external wall plan

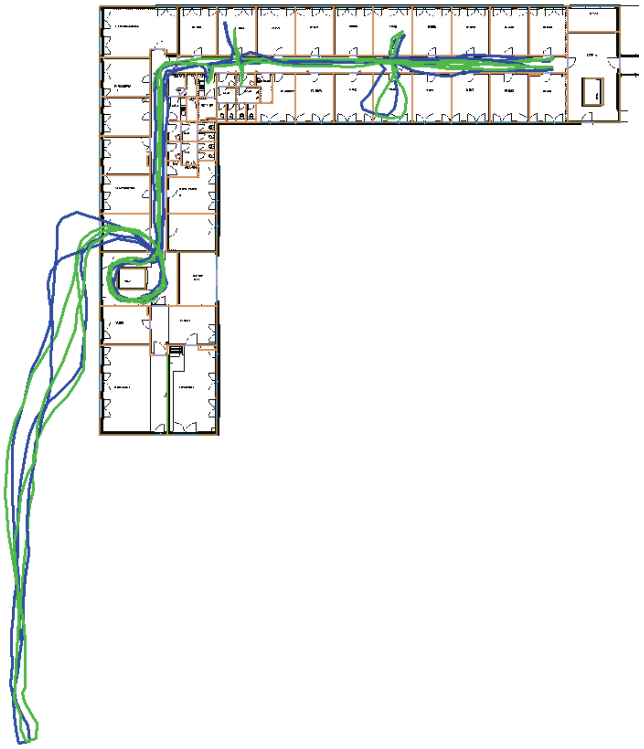

(a) Estimated trajectories

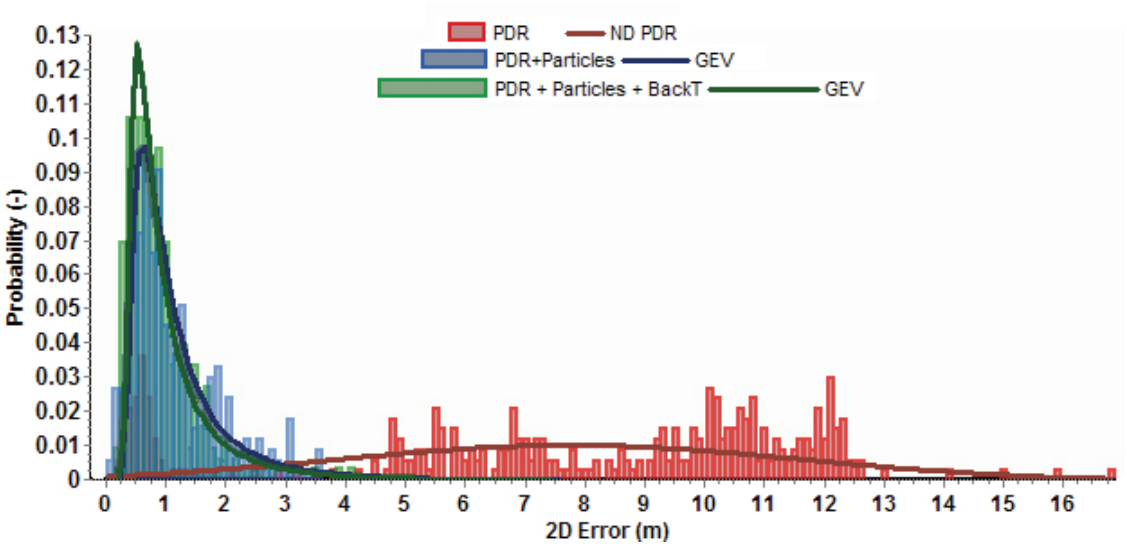

(b) Position error PDFs

Figure 5.10: TZI positioning results using detailed plan

Table 5.2: TZI Experiments Positioning Error

	PDR	**PDR+PF**	**PDR+BPF**
External Wall Map	μ =7.738 σ =8.741	μ =3.103 σ =2.939	μ =2.557 σ =2.606
Detail Wall Map	μ =7.738 σ =8.741	μ =1.083 σ =0.8431	μ =0.7432 σ =0.6046

error). This result is achieved via the elimination of the largest azimuth blunders. It is clear that increasing the level of building plan detail positively influences the quality of the positioning.

The analysis of the probability density function (depicted in Figure 5.9(b) and 5.10(b)) show that the estimation errors of the fusion solution again follow the log-normal distribution. The PDR base case estimation errors again yield a scattered, multimodal histogram.

The time course of the errors is shown in Figure 5.11. The time stamping of the ground truth and the alignment of the measurements to the ground truth were accurate to about 1 second and to about 50 cm. Some of the error spikes in Figures 5.11(a) and 5.11(b) may be due to this misalignment. Therefore the presented error statistics can be considered pessimistic.

5.4.4 Altitude Changes

Since it is possible to obtain quite accurate height change information using the foot-inertial technique, error in the vertical positions were also calculated. The vertical profile of a typical experiment through the TZI location was shown in Section 4.4. Recall that the occurrence of upward and downward steps were clearly visible but only after detrending was performed. This is also true for the tests done at the Liaison partner's location, see Figure 5.12.

As no 3D map information was used to constrain vertical displacements, no map filtering along the vertical axis was performed. However, a simple "altitude quantization" heuristic was used to improve accuracy along this axis. If the stride to stride height change was much less than twice a standard step height, or approximately 2 x 20 cm, then the assumption is that there was no altitude change. The outcome of using this heuristic is very accurate altitude change estimates, as shown in Figure 5.13. A more sophisticated and flexible heuristic might take advantage of the relatively standard relationships between the stair riser and tread dimensions.

A more general approach would be to combine these foot-inertial height change estimates with measurements from other sensors. Outdoors, it is of course possible to fuse barometer measurements with GPS and PDR altitude estimates for pedestrian navigation, as described in [131]. This has been shown to work up or down slopes as well as over staircases. More interestingly, it is possible to fuse (differential) barometric measurements with vertical acceleration measurements obtained from an IMU [216]. Modern MEMS pressure sensors (such as the VTI product [5]) have

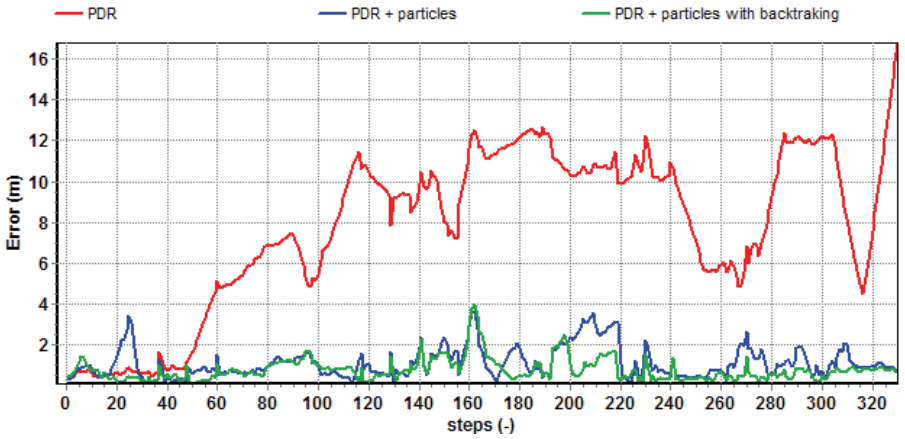

(a) Position error vs steps with detail wall map

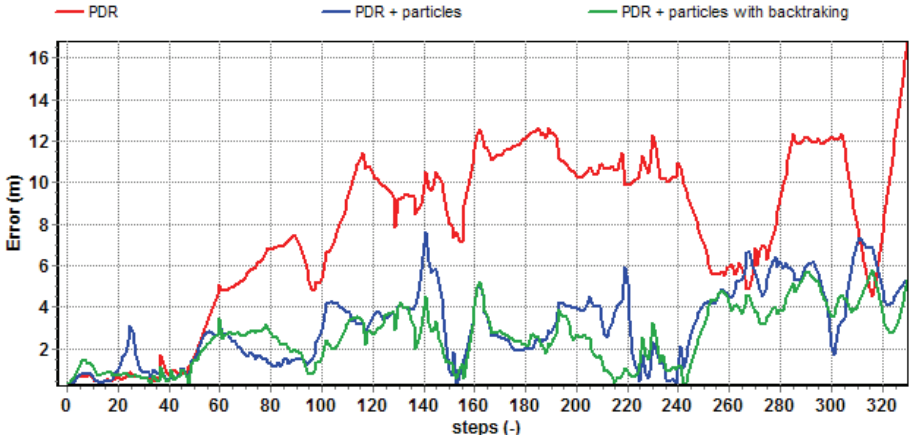

(b) Position error vs steps with external wall map

Figure 5.11: Position Error Dynamics using Map Matching

sufficient resolution to pick out very fine altitude changes, so that even variations due to leg squats (about 50 cm) can be detected. For general-purpose end applications, this approach could become very interesting, e.g., in cellular telephone handsets. For first responder applications, however, local differential barometric corrections would be required to mitigate the effects of perturbations from temperature differentials, air currents and pressure waves. Differential corrections could be provided by deployable sensor nodes but these would have to be in the same building room or corridor as the first responder whose altitude is being estimated. As discussed in Subsection 2.1.5, deployable sensor nodes unfortunately present their own set of additional practical problems.

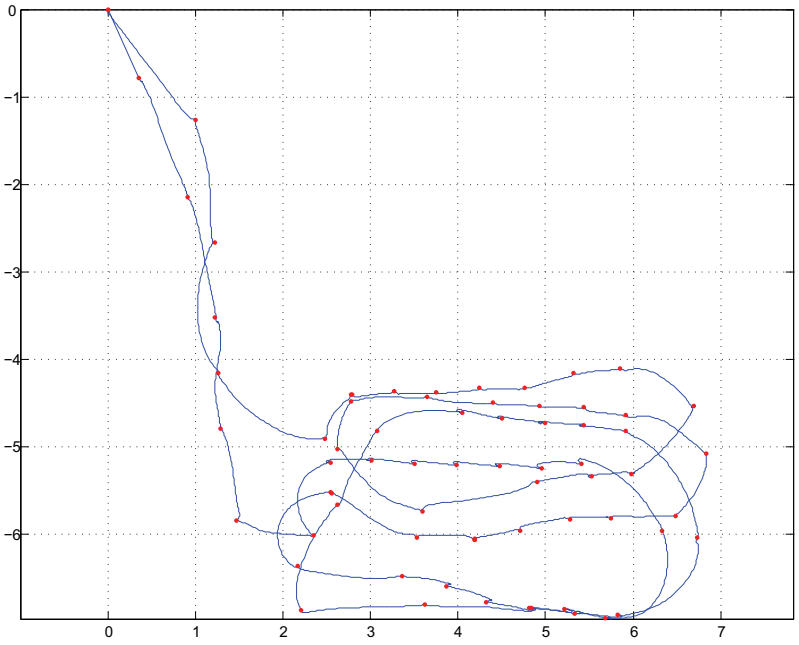

(a) Top View

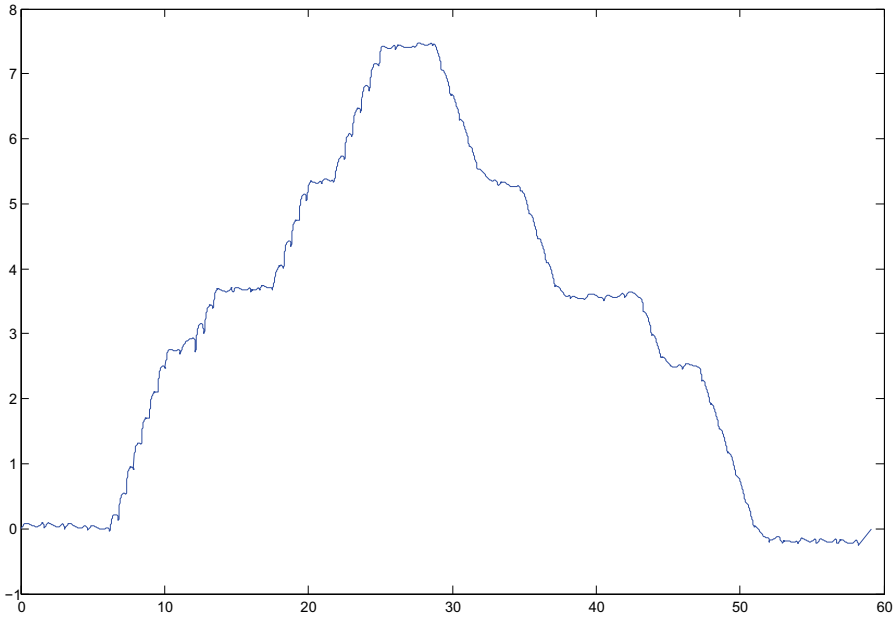

(b) Vertical Trajectory

Figure 5.12: Liaison Stairwell Test. In (a), the axes are x and y position in meters. Plot (b) shows the detrended vertical channel versus distance over ground. Both scales are in meters.

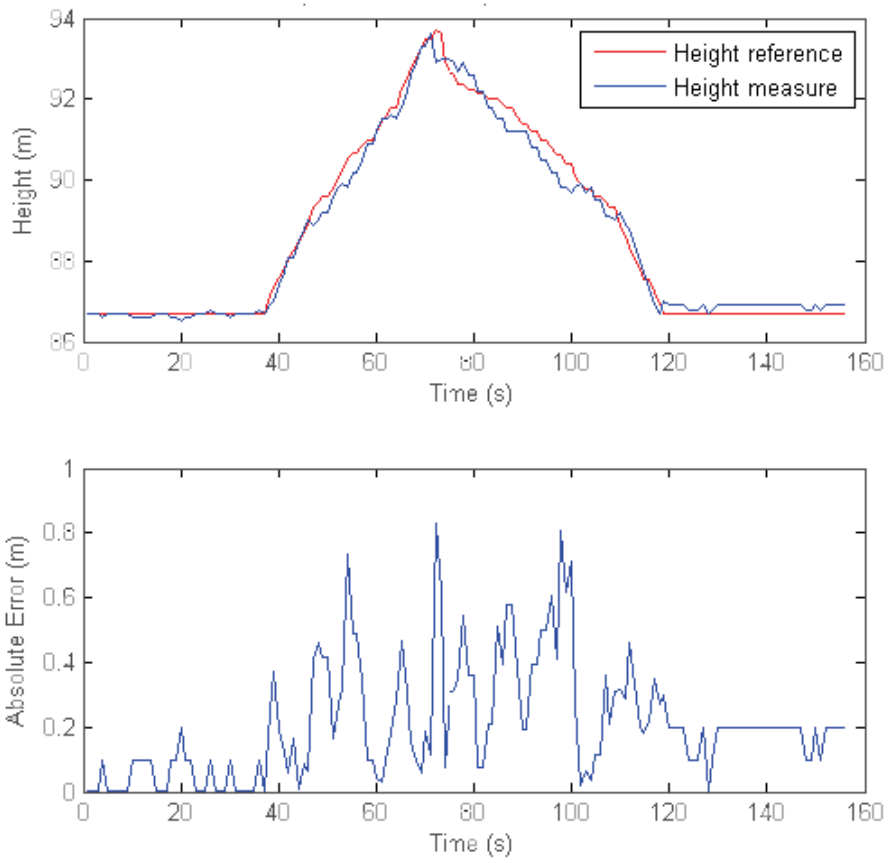

Figure 5.13: Liaison stairwell altitude change plot. The step height quantization heuristic has been applied.

5.5 Summary

As pointed out at the beginning of this chapter, regardless of the sensor fusion algorithm sophistication or of future advances in MEMS gyro technology, there will always remain a certain amount of heading error in the foot-inertial PDR positioning approach. This is due to the extreme operating conditions experienced by the IMU and to the short-term, high dynamics of the foot. As demonstrated in this chapter, these heading errors can be effectively mitigated with building map information. Other pedestrian dead reckoning systems would also benefit from this type of map filtering approach. For example, the distorted indoor tests trajectories using an occurrential PDR system (e.g., with the Honeywell DRM used in [151]) are analogous to the ones used here and could be corrected using map information.

A framework for fusing Pedestrian Dead Reckoning and building plans information was proposed and evaluated with different levels of building plan detail. The implementation was based on an existing code base and the basic method above is not especially novel. However, the novel Backtracking Particle Filter using a minimum level of map detail provides a significant performance improvement relative to a PDR-only, no map base case and a slight advantage relative to the basic Particle Filter. When only minimum building plan detail is available, the largest heading blunders are eliminated via the long-range geometrical constraints exploited by the BPF. Future experiments will determine if these very encouraging results can be reproduced for more erratic paths and for paths through larger spaces such as parking garages or warehouses.

These results have a substantial practical significance since the estimated level of positioning performance would certainly be useful in emergency/rescue scenarios. Also, the minimum level of building plan detail required by the approach is probably not difficult to obtain, e.g., from overhead aerial imagery or from cadastre databases. In the future, detailed building plan information might be made systematically accessible to police, fire and public safety organizations in the form of standardized, electronic search and rescue maps [11]. In principle, building automation and security systems could be leveraged to store map information as well as to provide rough localization information [92, 223]. Finally, indoor building plans could be constructed "on the fly" using additional wearable imaging and active ranging devices plus SLAM (Simultaneous Localization and Mapping) algorithms [219].

Chapter 6

Conclusion

6.1 Contributions of Research

The following contributions were made to the state-of-the-art:

1. The relative merits of different techniques for pedestrian positioning, and in particular first responder positioning, were highlighted and accompanied by an extensive and complete survey of previous research in this domain.

2. Headgear mounting of IMUs for occurrential PDR was shown to be an alternative to body-mounted sensors for straight-ahead walking. The practical significance of the result lies in the possibility of accompanying the IMU with other sensors on the headgear such as GPS antennae. This makes tight coupling between occurrential PDR, inertial and GPS systems possible.

3. The neural-network based step length estimator was shown to be at least as accurate as other systems reported elsewhere. A biomechanically-inspired explanation for the accuracy of the estimator was proposed.

4. For the foot-inertial technique, distance over ground estimation performance was shown to be consistently below the 2% error level in controlled tests. This was accomplished using the generic orientation estimation filter supplied with the IMU. Vertical displacement estimates, after detrending, were shown to be qualitatively correct and useful for, e.g., floor determination.

5. Omni-directional capability of the foot-inertial technique was demonstrated. This is an important result for the application of the technique to first responder scenarios where locomotion patterns can be far from regular.

6. The accurate alignment of foot-mounted IMUs was identified as a major issue for the practical use of these systems. This issue has been for the most part ignored in previous research.

7. It was shown how magnetic disturbances can be easily identified and matched to "cultural objects" in the environment. It was proposed that these could be

used in applications where the environment can be surveyed ahead of time. A map of these feature could then be used for positioning purposes.

8. It was shown that map-filtering with minimal building plan information can mitigate most of the major heading blunders that occur during indoor paths with the foot-inertial technique and the generic orientation filter. To accomplish this, a PDR heading error model was established.

9. Some specific features for incorporation into a Kalman filter for foot-mounted sensors were identified. Quaternion parameterization of attitude, the incorporation magnetic perturbation in the state, and facilities for fast kinematic alignment (e.g., using multipath-robust GPS, local positioning systems, or map filtering) are among these.

6.2 Limitations of Research

The most significant limitations of this research are as follows:

1. For the helmet-mounted PDR approach, it remains to be shown that the direction of gaze can be separated from the direction of walking and also that walking patterns other than just straight ahead can be modeled effectively. If this cannot be done, then the technique will be of quite limited practical use.

2. Few multiuser tests were done. There was no reason to expect any user-dependent changes in foot-inertial positioning performance due to the way the inertial calculations work. In fact none were encountered. Normally, a few systematic tests with a small number of users and over very precise ground truths (i.e., predefined paths marked on the ground) could have been done to confirm this. Unfortunately, it was not yet practical to do so. The foot-inertial approach (using the XKF filter) was not stable enough to generate meaningful test result statistics (especially for position error) since the heading often had unpredictable behavior, and indoors in particular.

3. The map filtering method for correcting PDR heading errors remains to be tested on a wider range of building geometries and walking patterns.

4. Designing and tuning the Kalman filter (an UKF) for the foot-inertial PDR approach turned out to be very difficult and it was not possible to create a working filter in the time-frame of this thesis. This was due in part to the author's limited experience in the specialized areas of inertial navigation, sensor fusion filters and MEMS sensor error modeling and to a lack of local expertise.

6.3 Papers in preparation

Two publications that follow on directly from the material presented in this thesis are currently in preparation:

1. "*UKF for Foot-Inertial Dead Reckoning*", by S. Beauregard is in preparation for submission to ION GNSS 2009. This will report on the author's further work on a custom sensor fusion filter that was outlined in Section 4.7.

2. "*Map-Filtering for Position Aiding of Foot-Inertial PDR*", by S. Beauregard, M. Klepal and Widyawan, is planned for a major navigation conference. The idea is to extent the concepts presented in Chapter 5 and use map-based position estimates as position updates to the foot-inertial Kalman filter (the topic of paper #1) . The goal is to determine if these position updates can supplement GNSS fixes for the purpose of fast kinematic alignment of the foot-mounted IMU.

6.4 Future work

There are a number of avenues for future work that follow on from the results presented here. In the author's opinion, the most important are 1) obtaining accurate position fixes for the purpose of aligning the foot-mounted IMU and 2) on-the-fly indoor map construction. These are explained in some detail in the sections below. Additional future work that is not so closely related to the present thesis but is nonetheless worth mentioning are as follows:

- Given the IMU temperature sensitivity problem described in the previous chapters, it may not be very practical to attach an IMU to the exterior of the first responder's boot (see Fig. 4.1(e)). With the latest MEMS inertial sensors, it is possible to build a 6-DoF IMU on single small circuit board and mount it in the sole or heel of a shoe (Fig. 4.1(f)). In this location, the IMU will never likely be exposed to temperatures beyond what the fireman's feet can bear so compensation is easier than if the IMU were mounted outside the shoe.

- In [41], it was proposed that an RF transmitter on one boot send a continuous wave signal, that the other boot would receive this, and a phase resolver would track range changes. It was shown through simulation that such foot-to-foot range measurements would provide additional information to help to stabilize a foot-inertial estimation filter.

6.4.1 Vehicle-to-Door GPS

As discussed in Chapter 4, accurate position fixes are required not only for navigation initialization but also for proper kinematic alignment of INSs, particularly for

ones using low-cost sensors. As there may be very little time or distance between the first responder's egress from a fire vehicle and his entry into a building, providing a position fix in these conditions may be beyond the state of the art in GNSS algorithms. Results from tests done by Draper Lab on their latest PDR systems showed that most of their position errors could be traced to spurious GPS fixes at building entry [217]. Similar conclusions were drawn from simulation studies by Mezentsev et al. [149], in this case for step length calibration purposes. Current GNSS research is trying to address this need for accurate positioning in urban canyons and close to buildings. Interesting possibilities exist for using helmet-mounted GPS antennas and IMUs in tightly-coupled or deeply-coupled configurations in this context. Recent carrier-phase derived velocity estimation techniques [55] (as opposed to Doppler or delta position fix derived estimates) could be leveraged to provide velocity updates to a helmet-mounted INSs but the techniques will likely have to be modified to work in multipath conditions.

If 2D plans of the immediate surroundings of an incident are available, these might be exploited via map filtering. For example, an accurate position estimate could be provided when passing through a narrow passage (e.g, a door or gate) depicted on a georeferenced site map. Three-dimensional outdoor plans might also be used to mitigate GNSS multipath effects via corrections based on 3D RF signal propagation modeling (e.g., ray tracing [76, 113, 237]). This could be used to improve position estimates in urban canyons and close to buildings where rescue operations often take place.

6.4.2 On-the-Fly Map Construction

As demonstrated in Chapter 5, it is clear that even coarse map information can greatly assist positioning by bounding DR drift. There are several potential methods for building up map information as the user (i.e., a first responder) moves through an unknown space. The simplest possible is to construct building maps based on the history of estimated traveled paths of first responders [218, 85][1]. Of course, the accuracy of such maps is completely dependent on the quality of the path data generated by the initial non-map-assisted traverses through the space to be mapped. In the course of this thesis, the author began working with short-range radar technology, principally as a replacement for the laser line scanners which will likely not work well in fires with smoke, mist or vapour. The idea is to use conventional SLAM (Simultaneous Localization and Mapping) algorithms with radar range measurements and PDR-based "odometry" to reconstruct an interior map on-the-fly. Hybrid computer vision and INS approaches could be used in a similar fashion [64].

Maps of the insides of buildings could in theory be constructed using indoor-to-outdoor wireless communication links and by exploiting RF multipath diversity phenomena (i.e., reflections), some geometrical assumptions and nonlinear filters to

[1]The American firm TRX Systems uses this technique. See `http://www.trxsystems.com/map-building/` (last visited 22 May 2009).

reconstruct the positions of reflecting surfaces, i.e., walls [84, 168]. This approach requires quite large transmission bandwidths in order to extract the channel impulse response in sufficiently fine detail. This kind of inverse RF modeling approach probably cannot be easily followed with standard, off-the-shelf RF transceivers, e.g., Tetra public safety radios, which have fairly limited transmission bandwidths.

Bibliography

[1] "Dynastream SpeedMax Technology White Paper," last visited 5 March 2009. [Online]. Available: http://www.dynastream.com/datafiles/SpeedMaxWhitePaperv4_1.pdf

[2] "Garmin Foot Pod introduction press release," last visited 5 March 2009. [Online]. Available: http://www.garmin.com/pressroom/outdoor/081006.html

[3] "Nike+ product description," last visited 5 March 2009. [Online]. Available: http://www.apple.com/ipod/nike/run.html

[4] "Pelote project results page," last visited 5 March 2009. [Online]. Available: http://labe.felk.cvut.cz/~pelote/results/pena.htm

[5] "SCP1000-D01(E)/D11(E) pressure sensor Application Note," VTI Technologies, last visited 3 March 2009. [Online]. Available: http://www.vti.fi/en/products/pressure-sensors/pressure_sensors/

[6] "Suunto foot pod product description," last visited 5 March 2009. [Online]. Available: http://www.suuntowatches.com/Suunto-Foot-POD.pro

[7] "Thermal imaging helmet camera product flyer," Rosenbauer International AG. Last visited 6 March 2009. [Online]. Available: http://www.rosenbauer.com/tools/cms_media.php?mid=5779&pdf=true

[8] "Return-path guidance system," DoD Army Small Business Innovation Research (SBIR) Contract Award DAAB07-03-C-E802, December 19 2003, last visited 3 March 2009. [Online]. Available: http://www.dodsbir.net/awards/

[9] "Handheld positioning/navigation system for urban and indoor environments," CERDEC Request For Proposal A04-103, U.S. Army Small Business Innovation Research (SBIR) Office, May 3 2004, last visited 3 March 2009. [Online]. Available: http://www.dodsbir.net/sitis/archives_display_topic.asp?Bookmark=10808

[10] "Land Warrior & Stryker Warrior Programs," *Defense Update: International Online Defense Magazine*, no. 5, 2004. [Online]. Available: http://www.defense-update.com/features/du-4-04/land-warrior-2.htm

[11] "Proposal of standard for rescue maps," Helsinki University of Technology, Automation Technology Laboratory (FI), Tech. Rep., July 31 2004, building Presence through Localization for Hybrid Telematic Systems (PeLoTe), Deliverable 2.4.

[12] "Individual soldier/vehicle situational awareness feasible now with existing military equipment," *Signal*, 2008, magazine published by the Armed Forces Communications and Electronics Association (AFCEA). Last visited 3 March 2009. [Online]. Available: http://www.afcea.org/signal/documents/rockwell_2.pdf

[13] A. Abdelhamied, S. Winslow, and C. Kane, "Navigation in a GPS-denied environment: Phase 1 final technical report," Office of Naval Research (ONR), Technical Report BAA 06-007, April 10 2007, created under contract by Mercury Data Systems 4214 Beechwood Drive Suite 105 Greensboro, NC 27410. Last visited 3 March 2009. [Online]. Available: http://www.dtic.mil/cgi-bin/GetTRDoc?AD=ADA465423&Location=U2&doc=GetTRDoc.pdf

[14] A. Aboshosha and A. Zell, "Disambiguating robot positioning using laser and geomagnetic signatures," in *Proceedings of 8th Conference on Intelligent Autonomous Systems (IAS-8)*, F. C. Groen, Ed. Amsterdamm, The Netherlands: IOS Press, Pittsburg, USA, March 10-13 2004.

[15] G. Abwerzger, B. Ott, and E. Wasle, "Demonstrating a GPS/EGNOS/LORAN-C navigation system in difficult environments as part of the ESA project SHADE," in *European Radio Navigation Systems and Services (EURAN) Conference*, Munich, Germany, June 2004.

[16] K. Alanen, L. Wirola, J. Kappi, and J. Syrjarinne, "Inertial sensor enhanced mobile RTK solution using low-cost assisted GPS receivers and Internet-enabled cellular phones," in *Proceedings of IEEE/ION PLANS 2006*, San Diego, California, April 25-27 2006, pp. 920 – 926.

[17] S. Alban, D. Akos, and S. Rock, "Performance analysis and architectures for INS-aided GPS tracking loops," in *Proceedings of the 2003 National Technical Meeting of the Institute of Navigation*, Anaheim, California, January 22 - 24 2003, pp. 611 – 622.

[18] J. Ali and F. Jiancheng, "Alignment of strapdown inertial navigation system: A literature survey spanned over the last 14 years," 2005, last visited 3 March 2009. [Online]. Available: http://www.bloodyaxes.com/kalmanlib/StrapdownAlignment.pdf

[19] H. Alt, C. Knauer, and C. Wenk, "Matching polygonal curves with respect to the Fréchet distance," in *Proceedings of the 18th Annual Symposium on Theoretical Aspects of Computer Science (STACS '01)*, A. Ferreira and H. Reichel, Eds. London, UK: Springer-Verlag, 2001, pp. 63–74.

[20] D. Alvarez, R. C. Gonzalez, A. Lopez, and J. C. Alvarez, "Comparison of step length estimators from weareable accelerometer devices," in *Proceedings of the 28th Annual International Conference of the IEEE Engineering in Medicine and Biology Society (EMBS '06)*, New York City, USA, August 30 - September 3 2006, pp. 5964–5967.

[21] V. Amendolare, D. Cyganski, R. J. Duckworth, S. Makarov, J. Coyne, H. Daempfling, and B. Woodacre, "WPI precision personnel locator system: Inertial navigation supplementation," in *Proc. IEEE/ION Position, Location and Navigation Symposium*, Monterey, CA, May 5-8 2008, pp. 350–357.

[22] K. Aminian, P. Robert, E. Jequier, and Y. Schutz, "Estimation of speed and incline of walking using neural network," in *IEEE Instrumentation and Measurement Technology Conference (IMTC/94)*, Hamamatsu, May 10-12 1994, pp. 160–162.

[23] M. Angermann, M. Khider, and P. Robertson, "Towards operational systems for continuous navigation of rescue teams," in *IEEE/ION Position, Location and Navigation Symposium (PLANS '08)*, Monterey, CA, May 2008, pp. 153–158.

[24] P.-O. Astrand, K. Rodahl, H. A. Dahl, and S. B. Stromme, *Textbook of Work Physiology: Physiological Bases of Exercise*, 4th ed., H. A. Dahl and S. B. Stromme, Eds. Leeds, UK: Human Kinetics Europe Ltd, June 2003.

[25] R. Babu and J. Wang, "Improving the quality of IMU-derived Doppler estimates for ultra-tight GPS/INS integration," in *GNSS 2004*, Rotterdam, The Netherlands, May 16-19 2004.

[26] ——, "Ultra-tight integration of pseudolites with INS," in *IEEE/ION Position, Location, And Navigation Symposium (PLANS '06)*, San Diego, CA, May 25-27 2006, pp. 705–714.

[27] K. Bakhru, "A seamless tracking solution for indoor and outdoor position location," in *IEEE 16th International Symposium on Personal, Indoor and Mobile Radio Communications (PIMRC)*, vol. 3, Berlin, Germany, September 11-14 2005, pp. 2029–2033.

[28] J. Bancroft, G. Lachapelle, M. Cannon, and M. Petovello, "Twin IMU-HSGPS integration for pedestrian navigation," in *21st International Technical Meeting of the Satellite Division of the Institute of Navigation (ION GNSS '08)*. Savannah, GA: The Institute of Navigation, September 16-19 2008, pp. 1377 – 1387.

[29] J. Barnes, C. Rizos, J. Wang, D. Small, G. Voigt, and N. Gambale, "Locata: A new positioning technology for high precision indoor and outdoor positioning," in *16th International Technical Meeting of the Satellite Division of the Institute*

of Navigation (ION GPS/GNSS '03), Portland, Oregon, September 9-12 2003, pp. 1119 – 1128.

[30] S. Beauregard, Widyawan, and M. Klepal, "Indoor PDR performance enhancement using minimal map information and particle filters," in *IEEE/ION Position, Location and Navigation Symposium (PLANS'08)*, May 5-8 2008, pp. 141–147.

[31] S. Beauregard, "Mobile Discovering System (MDS): Final Report," International University Bremen, Bremen, Germany, Tech. Rep., September 2005, (unpublished).

[32] ——, "Mobile Discovering System (MDS): Navigation Algorithms and Experiments," International University Bremen, Bremen, Germany, Tech. Rep., April 2005, (unpublished).

[33] ——, "A Helmet-Mounted Pedestrian Dead Reckoning System," in *3rd International Forum on Applied Wearable Computing (IFAWC '06)*, O. Herzog, H. Kenn, M. Lawo, P. Lukowicz, and G. Tröster, Eds. Bremen, Germany: VDE Verlag, March 15-16 2006, pp. 79–89.

[34] S. Beauregard and H. Haas, "Pedestrian Dead Reckoning: A Basis for Personal Positioning," in *3rd Workshop on Positioning, Navigation and Communication (WPNC'06)*. Hannover, Germany: Shaker Verlag, March 16 2006, pp. 27–35.

[35] D. Bernstein and A. Kornhauser, "An introduciton to map matching for personal navigation assistants," New Jersey TIDE Center, Technical Report, 1996.

[36] J. E. Bertram and A. Ruina, "Multiple walking speed-frequency relations are predicted by constrained optimization." *Journal of Theoretical Biology*, vol. 209, no. 4, pp. 445–453, April 2001.

[37] S. D. Billings, L. R. Pasion, and D. W. Oldenburg, "Inversion of magnetics for UXO discrimination and identification," in *UXO Forum*, Orlando, FL, September 3-6 2002.

[38] J. Bird and D. Arden, "Simulation of updating requirements for MEMS-based inertial navigation," in *CASI 14th Symposium on Navigation*. Montreal, Canada: Canadian Aeronautics and Space Institute, April 28-30 2003.

[39] C. M. Bishop, *Neural Networks for Pattern Recognition*. Oxford University Press, 1999.

[40] M. Boronowsky, O. Herzog, P. KnackfuSS, and M. Lawo, "WearIT@Work - Towards Real Life Industrial Applications of Wearable Computing," in *4th International Forum on Applied Wearable Computing (IFAWC)*, O. Herzog, H. Kenn, M. Lawo, P. Lukowicz, and T. Stiefmeier, Eds. Tel Aviv, Israel: VDE Verlag, March 12 – 13 2007, pp. 1 – 12.

[41] T. J. Brand and R. E. Phillips, "Foot-to-foot range measurements as an aid to personal navigation," in *ION 59th Annual Meeting / CIGTF 22nd Guidance Test Symposium*, Albuquerque, NM, June 23-25 2003.

[42] F. Brännström, "Positioning techniques alternatives to GPS," Master's Thesis, Luleå University of Technology, June 2002.

[43] D. Büchel and P.-Y. Gilliéron, "Navigation pédestre àă l'intérieur des bâtiments," *Géomatique Suisse*, vol. 1, pp. 664–668, 2004.

[44] A. Cappozzo, "The mechanics of human walking," in *Adaptability of Human Gait*, A. E. Patla, Ed. North-Holland, Elsevier Sciences Publishers B.V., 1991, pp. 167–186.

[45] G. A. Cavagna and R. Margaria, "Mechanics of walking," *Journal of Applied Physiology*, vol. 21, pp. 271–278, 1966.

[46] R. Challamel, P. Tome, D. Harmer, and S. Beauregard, "Performance assessment of indoor location technologies," in *IEEE/ION Position, Location and Navigation Symposium (PLANS '08)*, Monterey, CA, May 5-8 2008, pp. 624–632.

[47] P. Chewputtanagul and D. Jackson, "A road recognition system using GPS/GIS integrated system," *TENCON 2004. 2004 IEEE Region 10 Conference*, vol. D, pp. 225–228, Nov. 2004.

[48] H. S. Cobb, "GPS pseudolites: Theory, design, and applications," Ph.D. dissertation, Stanford University, September 1997.

[49] J. Collin, O. Mezentsev, and G. Lachapelle, "Indoor positioning system using accelerometry and high accuracy heading sensors," in *16th International Technical Meeting of the Satellite Division of the Institute of Navigation (ION GPS/GNSS) (Section C3).* Portland, OR: The Institute of Navigation, September 9-12 2003.

[50] F. Comblet, F. Peyret, C. Ray, J. M. Bonnin, and Y. M. Le Roux, "The LoCoSS project of GIS ITS Bretagne: Status and Perspectives," in *7th International Conference on ITS Telecommunications (ITST '07)*, Sophia Antipolis, France, June 6-8 2007, pp. 1–6.

[51] D. Cyganski, J. Duckworth, S. Makarov, W. Michalson, J. Orr, V. Amendolare, J. Coyne, H. Daempfling, J. Farmer, D. Holl, S. Kulkarni, H. Parikh, and B. Woodacre, "WPI precision personnel locator system," in *National Technical Meeting of the Institute of Navigation (ION NTM)*, San Diego, California, January 22 - 24 2007, pp. 806 – 814.

[52] H. Dejnabadi, B. Jolles, E. Casanova, P. Fua, and K. Aminian, "Estimation and visualization of sagittal kinematics of lower limbs orientation using body-fixed sensors," *IEEE Transactions on Biomedical Engineering*, vol. 53, no. 7, pp. 1385–1393, July 2006.

[53] A. Dempster, "QZSS's Indoor Messaging System: GNSS Friend or Foe?" *Inside GNSS*, pp. 37 – 40, January / February 2009.

[54] L. Dickmann, "Pedestrian Dead Reckoning," Universität Bremen, Techniques of Digital Media Course Project Report, March 2007.

[55] W. Ding, "Integration of MEMS INS with GPS carrier phase derived velocity: A new approach," in *20th International Technical Meeting of the Satellite Division of the Institute of Navigation (ION GNSS '07)*, Fort Worth, Texas, September 25 - 28 2007, pp. 2085 – 2093.

[56] W. Ding, J. Wang, and C. Rizos, "Improving covariance based adaptive estimation for GPS/INS integration," in *12th IAIN Congress and 2006 Int. Symp. on GPS/GNSS*, Jeju, Korea, October 18-20 2006, pp. 259–264.

[57] M. Dippold, "Personal Dead Reckoning with Accelerometers," in *3rd International Forum on Applied Wearable Computing (IFAWC '06)*, O. Herzog, H. Kenn, M. Lawo, P. Lukowicz, and G. Tröster, Eds. Bremen, Germany: TZI Universität Bremen, 2006, pp. 177–182.

[58] J. M. Donelan, R. Kram, and A. D. Kuo, "Mechanical work for step-to-step transitions is a major determinant of the metabolic cost of human walking," *The Journal of Experimental Biology*, vol. 205, pp. 3717 – 3727, 2002.

[59] A. Doucet, N. de Freitas, and N. Gordon, Eds., *Sequential Monte Carlo Methods in Practice*, ser. Statistics for Engineering and Information Science. Wien: Springer-Verlag, 2001.

[60] T. Eiter and H. Mannila, "Computing discrete Fréchet distance," Technische Universität Wien, Vienna, Austria, Tech. Rep. CD-TR 94/64, April 25 1994.

[61] J. Elwell, "Personal inertial navigator," Charles Stark Draper Laboratory, Inc., Tech. Rep., 1994, (Cited in Elwell 1999).

[62] ——, "Inertial navigation for the urban warrior," in *SPIE Conference on Digitization of the Battlespace IV*, ser. SPIE proceedings series, R. Suresh, Ed., vol. 3709, Orlando, FL, April 7-8 1999, pp. 196–204, (Also published as Draper Lab Report no. P-3716).

[63] L. Fang, P. Antsaklis, L. Montestruque, M. McMickell, M. Lemmon, Y. Sun, H. Fang, I. Koutroulis, M. Haenggi, M. Xie, and X. Xie, "Design of a wireless assisted pedestrian dead reckoning system - the NavMote experience," *IEEE Transactions on Instrumentation and Measurement*, vol. 54, no. 6, pp. 2342–2358, December 2005.

[64] G. Farley and M. Chapman, "An alternate approach to GPS denied navigation based on monocular SLAM techniques," in *National Technical Meeting of the Institute of Navigation (ION NTM '08)*, San Diego, California, January 25-28 2008, pp. 810–.

[65] M. G. Farley and M. D. Chapman, "Monocular SLAM: Alternative navigation for GPS-denied areas," *GPS World*, pp. 42–49, September 2008.

[66] T. Faulkner and S. Chestnut, "Impact of rapid temperature change on firefighter tracking in GPS-denied environments using inexpensive MEMS IMUs," in *National Technical Meeting of the Institute of Navigation (ION NTM '08)*, San Diego, California, January 2008, p. 828.

[67] C. Fischer, K. Muthukrishnan, M. Hazas, and H. Gellersen, "Ultrasound-aided pedestrian dead reckoning for indoor navigation," in *First ACM international workshop on Mobile entity localization and tracking in GPS-less environments (MELT '08)*. New York, NY, USA: ACM, 2008, pp. 31–36, co-located with the 14th Annual International Conference on Mobile Computing and Networking (MobiCom 2008).

[68] R. Fontana, *Experimental results from an ultra wideband precision geolocation system*, ser. Ultra-Wideband, Short-Pulse Electromagnetics 5. New York: Klewer Academic, 2002, vol. 2, ch. 4, pp. 215–223.

[69] R. J. Fontana, "Advances in ultra wideband indoor geolocation systems," in *Proceedings of the 3rd IEEE Workshop on Wireless Local Area Networks*, Newton, Massachusetts, September 27-28 2001.

[70] R. J. Fontana and S. J. Gunderson, "Ultra-wideband precision asset location system," in *IEEE Conference on Ultra Wideband Systems and Technologies*, Baltimore, MD, May 21-23 2002, pp. 147–150.

[71] E. Foxlin, "Pedestrian tracking with shoe-mounted inertial sensors," *IEEE Computer Graphics and Applications*, vol. 25, no. 6, pp. 38–46, 2005.

[72] K. Fyfe, "Motion analysis system," U.S. Patent 5,955,667, 1999.

[73] S. Ganesan, "Differential GPS for object tracking: Kinematic and static tests," International University Bremen, Graduate guided research project report, January 2005, Supervised by S. Beauregard and H. Haas.

[74] G. Gao and G. Lachapelle, "INS-assisted high sensitivity GPS receivers for degraded signal navigation," in *Proceedings of the 19th International Technical Meeting of the Satellite Division of the Institute of Navigation (ION GNSS)*, Fort Worth, Texas, September 26 - 29 2006, pp. 2977 – 2989.

[75] *Forerunner 205/305 Owner's Manual*, Garmin Ltd., last visited 6 March 2009. [Online]. Available: http://www8.garmin.com/manuals/984_OwnersManual.pdf

[76] A. J. Gavin, S. Scarda, K. Sheridan, and J. I. Herrero, "Polaris: A software tool to support GNSS-based application design," in *IGS Workshop and Symposium 2004*. Berne, Switzerland: International GPS Service, March 1-5 2004.

[77] A. Gelb, J. Joseph F. Kasper, J. Raymond A. Hash, C. F. Price, and J. Arthur A. Sutherland, *Applied Optimal Estimation*, A. Gelb, Ed. Cambridge, Massachusetts: The M.I.T. Press, 1974.

[78] G. L. Godha, S. and M. Cannon, "Integrated GPS/INS system for pedestrian navigation in a signal degraded environment," in *19th International Technical Meeting of the Satellite Division of the Institute of Navigation (ION GNSS '06)*. Fort Worth, Texas: The Institute of Navigation, September 26 - 29 2006.

[79] M. S. Grewal and A. P. Andrews, *Kalman Filtering: Theory and Practice Using MATLAB*, 3rd ed. New York, Chichester: John Wiley & Sons, 2008.

[80] M. S. Grewal, L. R. Weill, and A. P. Andrews, *Global Positioning Systems, Inertial Navigation and Integration*. New York: John Wiley & Sons, 2001.

[81] P. D. Groves, G. W. Pulford, C. A. Littlefield, D. L. Nash, , and C. J. Mather, "Inertial navigation versus pedestrian dead reckoning: Optimizing the integration," in *20th International Technical Meeting of the Satellite Division of the Institute of Navigation (ION GNSS '07)*, Fort Worth, Texas, September 25 - 28 2007, pp. 2043 – 2055.

[82] W. Guinon, "Bio-Kinematic Navigation," Charles Stark Draper Laboratory, Inc., Cambridge, MA, Tech. Rep., December 1998, (Cited in Elwell 1999).

[83] ——, "BKN distance travelled accuracy," Charles Stark Draper Laboratory, Inc., Cambridge, MA, Tech. Rep., May 1998, (Cited in Elwell 1999).

[84] D. Gustafson, J. Elwell, and J. Soltz, "Innovative indoor geolocation using RF multipath diversity," in *IEEE/ION Position, Location, And Navigation Symposium (PLANS '06)*, San Diego, California, April 25-27 2006, pp. 904–912.

[85] R. K. Harle and A. Hopper, "Using personnel movements for indoor autonomous environment discovery," in *Proceedings of the First IEEE International Conference on Pervasive Computing and Communications (PERCOM '03)*. Washington, DC, USA: IEEE Computer Society, 2003, p. 125.

[86] D. Harmer, M. Russell, E. Frazer, T. Bauge, S. Ingram, N. Schmidt, B. Kull, A. Yarovoy, A. Nezirovic, L. Xia, V. Dizdarevic, and K. Witrisal, "Europcom: Emergency ultrawideband radio for positioning and communications," in *IEEE International Conference on Ultra-Wideband (ICUWB '08)*, vol. 3, Hannover, Germany, September 10-12 2008, pp. 85–88.

[87] J. Hartikainen and S. Särkkä, *Optimal filtering with Kalman filters and smoothers - a Manual for Matlab toolbox EKF/UKF*, 1st ed., Department of Biomedical Engineering and Computational Science, Helsinki University of Technology, Helsinki, Finland, February 2008, last visited 3 March 2009. [Online]. Available: http://www.lce.hut.fi/research/mm/ekfukf/

[88] M. Hassan-Ali and K. Pahlavan, "A new statistical model for site-specific indoor radio propagation prediction based on geometric optics and geometric probability," *IEEE Transactions on Wireless Communications*, vol. 1, no. 1, pp. 112–124, January 2002.

[89] D. Herold, L. Griffiths, and T. Y. Fung, "Lightweight, high-bandwidth conformal antenna system for ballistic helmets," in *IEEE Military Communications Conference (MILCOM)*, Orlando, FL, October 29-31 2007, pp. 1–6.

[90] S. Hicks, "Advanced cruise missile guidance system description," in *Proceedings of the IEEE 1993 National Aerospace and Electronics Conference (NAECON 1993)*, vol. 1, Dayton, Ohio, USA, May 1993, pp. 355–361.

[91] J. M. Hill, I. F. Progri, and W. R. Michalson, "Techniques for reducing the near-far problem in indoor geolocation systems," in *National Technical Meeting of the Institute of Navigation (ION NTM '01)*, Long Beach, CA, January 22 - 24 2001, pp. 860 – 865.

[92] D. G. Holmberg, W. D. Davis, S. J. Treado, and K. A. Reed, "Building Tactical Information System for Public Safety Officials. Intelligent Building Response (iBR)," U.S. Department of Commerce, National Institute of Standard and Technology, Building and Fire Research Laboratory, Gaithersburg, MD 20899-8600, Technical Report NISTIR 7314, January 2006, last visited 3 March 2009. [Online]. Available: http://fire.nist.gov/bfrlpubs/fire06/art044.html

[93] J. C. Hughes, J. Banks, A. Kerkhoff, B. Tolman, and J. Wyant, "Submillimeter precision GPS survey system at the Holloman high speed test track," in *19th International Technical Meeting of the Satellite Division of the Institute of Navigation (ION GNSS '06)*, Fort Worth, Texas, September 26-29 2006, pp. 2743 – 2753.

[94] L. J. Hutchings, "Rotational sensor system," U.S. Patent 6,305,221, October 23, 2001.

[95] P. Hwang, R. Young, J. Marek, J. Bruckner, J. Jantzen, and B. Kaspar, "DARPA SNIPER: A demonstration of tightly-coupled GPS/IMU/LORAN integration for low-power portable applications," in *Proceedings of the 55th Annual Meeting of the Institute of Navigation.* Alexandria, VA: Institute of Navigation ION, June 28-30 1999, pp. 123 – 132.

[96] *IAAF Track and Field Facilities Manual - Marking Plan 400m Standard Track*, International Association of Athletics Federations, Monaco, 2008, last visited 2 March 2009. [Online]. Available: http://www.iaaf.org/competitions/technical/regulations/index.html

[97] H. Isshiki, T. Sugiyama, H. Yasuda, A. Uchiyama, T. Saito, T. Hujino, T. Nanbu, H. Iwahashi, and T. Kimura, "Theory of indoor GPS by using reradiated GPS signal," in *Proceedings of the 2002 National Technical Meeting of the Institute of Navigation*, The Catamaran Resort Hotel, San Diego, California, January 28-30 2002, pp. 587 – 597.

[98] M. Jadaliha, A. Shahri, and M. Mobed, "A new pedestrian navigation system based on low-cost IMU," in *The 5th International Conference on Ubiquitous Robots and Ambient Intelligence (URAI 2008)*, Korea University, Seoul, Korea, November 20-22 2008.

[99] A. Johnson and J. Montgomery, "Overview of terrain relative navigation approaches for precise lunar landing," in *IEEE Aerospace Conference*, March 2008, pp. 1–10.

[100] T. Judd, "A personal dead reckoning module," in *10th International Technical Meeting of the Satellite Division of the Institute of Navigation (ION GPS '97)*. Kansas City, MO: Institute of Navigation, September 16-19 1997.

[101] T. Judd and T. Vu, "Use of a new pedometric dead reckoning module in GPS denied environments," in *IEEE/ION Position, Location and Navigation Symposium (PLANS '08)*, Monterey, CA, May 2008, pp. 120–128.

[102] S. Julier, J. Uhlmann, and H. Durrant-Whyte, "A new approach for filtering nonlinear systems," in *Proceedings of the American Control Conference*, vol. 3, Seattle, WA, June 21-23 1995, pp. 1628–1632.

[103] M. Kanli, "Limitations of pseudolite systems using off-the-shelf GPS receivers," in *The 2004 International Symposium on GNSS/GPS*, Sydney, Australia, December 6-8 2004.

[104] J. Kappi, J. Syrjarinne, and J. Saarinen, "MEMS-IMU based pedestrian navigator for handheld devices," in *14th International Technical Meeting of the Satellite Division of the Institute of Navigation (ION GPS '01)*, Salt Lake City, UT, September 11-14 2001, pp. 1369 – 1373.

[105] P. W. Kasameyer, L. Hutchings, M. F. Ellis, and R. Gross, "MEMS-based INS tracking of personnel in a GPS-denied environment," in *18th International Technical Meeting of the Satellite Division of the Institute of Navigation (ION GNSS '05)*, Long Beach, California, September 13-16 2005, pp. 949 – 955.

[106] R. Katz, "Background on extreme value theory with emphasis on climate applications," Short Course on Statistics of Extremes in Climate Change,

Michigan State University, 2008, last visited 3 March 2009. [Online]. Available: http://www.isse.ucar.edu/staff/katz/docs/pdf/msulect1.pdf

[107] C. Kee, D. Yun, B. Parkinson, S. Pullen, and T. Lagenstein, "Centimeter-accuracy indoor navigation using GPS-like pseudolites," *GPS World*, vol. 12, no. 11, pp. 14–22, September 2001.

[108] J. T. Kelly, "Warfighter Awareness: DAGRs and Radios," *GPS World*, vol. 18, no. 8, pp. 30–35, August 2007.

[109] T. J. Kennedy, "Workshop on precision personnel location and tracking summary report," CTC Inc., Public Safety Technology Center, Tech. Rep., August 7-8 2006, last visited 3 March 2009. [Online]. Available: http://www.ece.wpi.edu/Research/PPL/Workshops/2006/PDF/CTCFinalReport.pdf

[110] J. Kim and S. Sukkarieh, "Improving the real-time efficiency of inertial SLAM and understanding its observability," in *IEEE/RSJ International Conference on Intelligent Robots and Systems (IROS '04)*, vol. 1, Sendai, Japan, September 28 - October 2 2004, pp. 21–26.

[111] Y. Kim, B.-T. Yoon, I.-J. Yoon, and Y. Kim, "Read range measurement and estimation of 900-MHz-band mobile radiofrequency identification (mRFID) system," *Microwave and Optical Technology Letters*, vol. 48, no. 11, pp. 2753–2755, August 2007.

[112] M. Klann, T. Riedel, H. Gellersen, C. Fischer, M. Oppenheim, P. Lukowicz, G. Pirkl, K. Kunze, M. Beuster, M. Beigl, O. Visser, and M. Gerling, "LifeNet: An Ad-hoc Sensor Network and Wearable System to Provide Firefighters with Navigation Support," in *Adjunct Proc. Ubicomp 2007*, Innsbruck, Austria, September 16-19 2007.

[113] M. Klepal, "Novel approach to indoor electromagnetic wave propagation modelling," Ph.D. dissertation, Faculty of Electrical Engineering, Czech Technical University in Prague, Prague, Czech Republic, July 2003.

[114] M. Kourogi and T. Kurata, "A method of personal positioning based on sensor data fusion of wearable camera and self-contained sensors," in *IEEE Conference on Multisensor Fusion and Integration for Intelligent Systems (MFI2003)*, Tokyo, 2003, pp. 287–292.

[115] B. Krach and P. Roberston, "Cascaded estimation architecture for integration of foot-mounted inertial sensors," in *IEEE/ION Position, Location and Navigation Symposium (PLANS '08)*, Monterey, CA, May 5-8 2008, pp. 112–119.

[116] B. Krach and P. Robertson, "Integration of foot-mounted inertial sensors into a Bayesian location estimation framework," in *5th Workshop on Positioning, Navigation and Communication (WPNC'08)*, Hannover, Germany, March 27 2008, pp. 55–61.

[117] E. Kraft, "A quaternion-based unscented Kalman filter for orientation tracking," in *Sixth International Conference on Information Fusion*, vol. 1, Cairns, Queenland, Australia, July 8-11 2003, pp. 47–54.

[118] A. D. Kuo, "A simple model of bipedal walking predicts the preferred speed-step length relationship," *Journal of Biomechanical Engineering*, vol. 123, pp. 264 – 269, June 2001.

[119] ——, "The six determinants of gait and the inverted pendulum analogy: A dynamic walking perspective," *Human Movement Science*, vol. 26, no. 4, pp. 617–656, August 2007.

[120] P. Labbé, D. Arden, L. Li, and Y. Ge, "Self-aware / Situation aware - Integrated Handhelds for Dispersed Civil and Military Urban Operations," *Inside GNSS*, vol. 2, no. 2, pp. 34–45, March - April 2007, last visited 3 March 2009. [Online]. Available: http://www.insidegnss.com/auto/igm_034-045.pdf

[121] G. Lachapelle, H. Kuusniemi, D. Dao, G. MacGougan, and M. Cannon, "HSGPS signal analysis and performance under various indoor conditions," *Journal of the Institute of Navigation*, vol. 51, no. 1, pp. 29–42, Spring 2004.

[122] G. Lachapelle, O. Mezentsev, J. Collin, and G. MacGougan, "Pedestrian and vehicular navigation under signal masking using integrated HSGPS and self-contained sensor technologies," in *11th World Conference, International Association of Institutes of Navigation*, Berlin, October 21-24 2003.

[123] G. Lachapelle, "Pedestrian navigation with high sensitivity GPS receivers and MEMS," *Personal and Ubiquitous Computing*, vol. 11, no. 6, pp. 481–488, 2007.

[124] ——, "GNSS-based indoor location technologies," in *International Symposium on GPS/GNSS*, Sydney, Australia, December 6-8 2004.

[125] ——, "GNSS indoor location technologies," *Journal of Global Positioning Systems*, vol. 3, no. 1-2, pp. 2–11, 2004, last visited 3 March 2009. [Online]. Available: http://plan.geomatics.ucalgary.ca/papers/gnss04_sydney_dec04_gl%20keynote_footers.pdf

[126] Q. Ladetto, "In Step with INS: Navigation for the Blind, Tracking Emergengy Crews," *GPS World*, vol. 13, no. 10, pp. 30–38, October 2002.

[127] ——, "Capteurs et algorithmes pour la localization autonome en mode pedestre," Ph.D. Thesis, École Polytechnique Fédérale de Lausanne, Lausanne, Switzerland, January 2003.

[128] Q. Ladetto, V. Gabaglio, and B. Merminod, "Two different approaches for augmented GPS pedestrian navigation," in *International Symposium on Location Based Services for Cellular Users (Locellus)*, Munich, Germany, February 5-7 2001.

[129] Q. Ladetto, V. Gabaglio, B. Merminod, P. Terrier, and Y. Shutz, "Human walking analysis assisted by DGPS," in *GNSS 2000*, Edinburgh, Scotland, May 1-4 2000.

[130] Q. Ladetto and B. Merminod, "Digital magnetic compass and gyroscope integration for pedestrian navigation," in *9th Saint Petersburg International Conference on Integrated Navigation Systems*, Saint Petersburg, Russia, May 27-29 2002.

[131] Q. Ladetto, J. van Seeters, S. Sokolowsi, Z. Sagan, and B. Merminod, "Digital magnetic compass and gyroscope for dismounted soldier position and navigation," in *NATO-RTO Meeting: Military Capabilities enabled by Advances in Navigation Sensors*. Istanbul, Turkey: NATO Research and Technology Agency, Sensors & Electronics Panel, October 14-16 2002.

[132] D. Landis, T. Thorvaldsen, B. Fink, P. Sherman, and S. Holmes, "A deep integration estimator for urban ground navigation," in *Proc. IEEE/ION Position, Location, And Navigation Symposium (PLANS)*, San Diego, CA, April 25–27, 2006, pp. 927–932.

[133] J. Lebaric and A.-T. Tan, "Ultra-wideband conformal helmet antenna," in *Asia-Pacific Microwave Conference*, Sydney, Australia, December 3-6 2000, pp. 1477–1481.

[134] H. K. Lee, J. Wang, C. Rizos, and D. Grejner-Brzezinska, "Analysing the impact of integrating pseudolite observables into a GPS/INS system," *Journal of Surveying Engineering*, pp. 95–103, May 2004.

[135] E. Lenz, "Networked transport of RTCM via Internet protocol (NTRIP)," in *FIG Working Week 2004*. Athens: International Federation of Surveyors, May 22-27 2004.

[136] H. Leppäkoski, J. Kappi, J. Syrjärinne, and J. Takala, "Error analysis of step length estimation in pedestrian dead reckoning," in *ION GPS 2002*. Portland, OR: The Institute of Navigation, September 24 -27 2002, pp. 1136 – 1142.

[137] H. Leppäkoski, J. Syrjärinne, and J. Saarinen, "Personal positioning using wireless assisted GPS with low-cost INS," in *ION GPS 2001*. Salt Lake City, UT: Institute of Navigation, September 11-14 2001, pp. 1361 – 1368.

[138] R. Levi and T. Judd, "Dead reckoning navigation system using accelerometer to measure foot impacts," US Patent 5 583 776, 1996.

[139] J. Li, G. Taylor, and D. B. Kidner, "Accuracy and reliability of map-matched GPS coordinates: the dependence on terrain model resolution and interpolation algorithm," *Computers & Geosciences*, vol. 31, no. 2, pp. 241 – 251, 2005, geospatial Research in Europe: AGILE

2003. [Online]. Available: http://www.sciencedirect.com/science/article/B6V7D-4F2V526-1/2/bf7b27e3acbf397669564d9d718fdc38

[140] W. Lindstrot, "The differential global positioning service RASANT (Radio Aided Satellite Navigation Technique)," Satellitenpositionierungsdienst der deutschen Landesvermessung (SAPOS), Tech. Rep., 2003.

[141] P. H. Madhani, P. Axelrad, K. Krumvieda, and J. Thomas, "Application of successive interference cancellation to the GPS pseudolite near-far problem," *IEEE Transactions on Aerospace and Electronic Systems*, vol. 39, no. 2, pp. 481–488, April 2003.

[142] J. D. Martin, J. Krösche, and S. Boll, "Dynamic GPS-position correction for mobile pedestrian navigation and orientation," in *3rd Workshop on Positioning, Navigation and Communication (WPNC'06)*, Hannover, Germany, March 2006.

[143] S. Maskell and N. Gordon, "A Tutorial on Particle filters for On-line Nonlinear/Non-Gaussian Tracking," in *The IEEE Seminar on Target Tracking: Algorithms and Applictions*, 2001, vol. 2, pp. 2/1 –2/15.

[144] C. Mather, P. Groves, and M. Carter, "A man motion navigation system using high sensitivity GPS, MEMS IMU and auxiliary sensors," in *Proceedings of ION GNSS*. Savannah, Georgia: Institute of Navigation, September 2006.

[145] D. McCrady, R. Goldberg, and T. Pfister, "RF ranging for indoor tracking and positioning," in *WPI / CTC Technology Workshop on Precision Personnel Location and Tracking*. Worcester Polytechnic Institute, August 7-8 2006, last visited 3 March 2009. [Online]. Available: http://www.ece.wpi.edu/Research/PPL/Workshops/2006/PDF/ITT.pdf

[146] H. B. Menz, S. R. Lord, and R. C. Fitzpatrick, "Acceleration patterns of the head and pelvis when walking on level and irregular surfaces," *Gait and Posture*, vol. 18, no. 1, pp. 35–46, August 2003.

[147] M. Meurer, S. Heilmann, D. Reddy, T. Weber, and P. Baier, "A signature based localization technique relying on covariance matrices of channel impulse responses," in *2nd Workshop on Positioning, Navigation and Communication (WPNC'05) and 1st Ultra-Wideband Expert Talk (UET'05)*, Hannover, Germany, March 17 2005, pp. 31 –40.

[148] O. Mezentsev, "Sensor aiding of HSGPS pedestrian navigation," Ph.D. Thesis, University of Calgary, Department of Geomatics Engineering, Calgary, Alberta, March 2005, also published as Tech Report UCGE 20212.

[149] O. Mezentsev, G. Lachapelle, and J. Collin, "Pedestrian dead reckoning – a solution to navigation in GPS signal degraded areas?" *Geomatica*, vol. 59, no. 2, pp. 175 – 182, 2005.

[150] L. Miller, P. F. Wilson, N. P. Bryner, M. H. Francis, J. R. Guerrieri, D. W. Stroup, and L. Klein-Berndt, "RFID-assisted indoor localization and communication for first responders," in *Proceedings of the 10th Annual International Symposium on Advanced Radio Technologies*, Boulder, Colorado, March 2006, pp. 83–91, NTIA Special Publication SP-06-438. Last visted 3 March 2009. [Online]. Available: http://www.antd.nist.gov/wctg/RFID/ISART06-Assisted-LocCom.pdf

[151] L. E. Miller, "Indoor navigation for first responders: A feasibility study," Wireless Communications Technologies Group, Advanced Networking Technologies Division, Information Technology Laboratory, National Institute of Standards and Technology, Tech. Rep., February 2006, last visited 3 March 2009. [Online]. Available: http://www.antd.nist.gov/wctg/RFID/Report_indoornav_060210.pdf

[152] M. Modsching, R. Kramer, M. Riebeck, A. Stark, K. ten Hagen, and J. Kawalek, "Field trial on the efficiency and user experience of GPS based state of the art navigational systems for pedestrians," in *Proc. 4th Workshop on Positioning, Navigation and Communication (WPNC '07)*, Hannover, Germany, March 22 2007, pp. 129–134.

[153] M. Munchy, D. Boulanger, P. Ulrich, and M. Bouiflane, "Magnetic mapping for the detection and characterization of UXO: Use of mulit-sensor fluxgate 3-axis magnetometers and methods of interpretation," *Journal of Applied Geophysics*, vol. 61, no. 3-4, pp. 168–183, March 2007.

[154] I. T. Nabney, *Netlab: Algorithms for Pattern Recognition*, ser. Advances in Pattern Recognition. London: Springer-Verlag, 2002.

[155] *NAVIndoor Specification*, Naviva, Espoo, Finland, http://www.naviva.fi.

[156] E. Nebot and H. Durrant-Whyte, "Initial calibration and alignment of an inertial navigation unit," in *Fourth Annual Conference on Mechatronics and Machine Vision in Practice*. Toowoomba, Queensland, Australia: IEEE, September 22-25 1997, pp. 175–180.

[157] H. Niwa, K. Kodaka, Y. Sakamoto, M. Otake, S. Kawaguchi, K. Fujii, Y. Kanemori, and S. Sugano, "GPS-based indoor positioning system with multi-channel pseudolite," in *Proc. IEEE International Conference on Robotics and Automation ICRA 2008*, Pasadena, CA, May 19-23 2008, pp. 905–910.

[158] A. Nummela, T. Keränen, and L. Mikkelsson, "Factors related to top running speed and economy," *International Journal of Sports Medicine*, vol. 28, no. 8, pp. 655–661, August 2007.

[159] S. M. Oh, S. Tariq, B. Walker, and F. Dellaert, "Map-based priors for localization," in *IEEE/RSJ International Conference on Intelligent Robots and Systems (IROS '04)*, Sendai, Japan, September 28 - October 2 2004.

[160] L. Ojeda and J. Borenstein, "Non-GPS navigation with the personal dead-reckoning system," in *Society of Photo-Optical Instrumentation Engineers (SPIE) Conference Series*, vol. 6561, May 2007.

[161] L. Ojeda, H. Chung, and J. Borenstein, "Precision calibration of fiber-optics gyroscopes for mobile robot navigation," in *Proc. IEEE International Conference on Robotics and Automation (ICRA '00)*, vol. 3, San Francisco, CA, April 24-28 2000, pp. 2064–2069.

[162] L. Ojeda and J. Borenstein, "Non-GPS navigation for emergency responders," in *2006 International Joint Topical Meeting: "Sharing Solutions for Emergencies and Hazardous Environments"*, Salt Lake City, Utah, USA, February 12-15 2006.

[163] ——, "Non-GPS navigation for security personnel and first responders," *The Journal of Navigation*, vol. 60, pp. 391–407, 2007.

[164] G. Opshaug, "Leapfrog navigation system," in *Proceedings of the 15th International Technical Meeting of the Satellite Division of the Institute of Navigation (ION GPS 2002)*, Portland, Oregon, September 24-27 2002, pp. 357 – 362.

[165] B. Ott, E. Wasle, G. Abwerzger, P. Branco, and R. Nicole, "Special handheld based applications in difficult environment - SHADE," in *NAVITEC 2004*, Noordwijk, The Netherlands, December 2004 2004.

[166] K. Pahlavan, P. Krishnamurthy, and A. Beneat, "Wideband radio propagation modeling for indoor geolocation applications," *IEEE Communications Magazine*, vol. 36, no. 4, pp. 60–65, April 1998.

[167] K. Pahlavan, X. Li, and J. Makela, "Indoor geolocation science and technology," *IEEE Communications Magazine*, vol. 40, no. 2, pp. 112–118, February 2002.

[168] K. Pahlavan, F. O. Akgul, M. Heidari, A. Hatami, J. M. Elwell, and R. D. Tingley, "Indoor geolocation in the absence of direct path," *IEEE Wireless Communications*, vol. 13, no. 6, pp. 50–58, December 2006.

[169] W. Pelgrum, "New potential of low-frequency radionavigation in the 21st century," Ph.D. Thesis, Delft University of Technology, November 2006.

[170] O. Perrin, P. Terrier, Q. Ladetto, B. Merminod, and Y. Schutz, "Improvement of walking speed prediction by accelerometry and altimetry, validated by satellite positioning." *Med Biol Eng Comput*, vol. 38, no. 2, pp. 164–168, March 2000.

[171] M. G. Petovello, O. Mezentsev, G. Lachapelle, and M. E. Cannon, "High sensitivity GPS velocity updates for personal indoor navigation using inertial navigation systems," in *16th International Technical Meeting of the Satellite Division of the Institute of Navigation (ION GPS/GNSS '03)*. Portland, OR: The Institute of Navigation, September 9-12 2003, pp. 2886 – 2896.

[172] I. Petrovski, I. Surouvtcev, T. Petrovskaia, K. Okano, M. Ishii, H. Torimoto, K. Suzuki, M. Toda, and J. Akita, "Precise navigation indoor," in *SICE 2004 Annual Conference*, vol. 2, Sapporo, Japan, August 2004, pp. 1739–1744.

[173] S. Pourtakdoust and H. G. Asl, "An adaptive unscented Kalman filter for quaternion-based orientation estimation in low-cost AHRS," *Aircraft Engineering and Aerospace Technology: An International Journal*, vol. 79, no. 5, pp. 485–493, 2007.

[174] N. B. Priyantha, A. Chakraborty, and H. Balakrishnan, "The Cricket Location-Support System," in *6th ACM International Conference on Mobile Computing and Networking (MOBICOM)*, Boston, MA, August 2000.

[175] I. F. Progri and W. R. Michalson, "An investigation of a DSSS-OFDM-CDMA-FDMA indoor geolocation system," in *Proc. Position Location and Navigation Symposium (PLANS)*, April 26-29 2004, pp. 662–670.

[176] I. Progri, "A MC-CDMA indoor geolocation system," in *IEEE 16th International Symposium on Personal, Indoor and Mobile Radio Communications (PIMRC)*, vol. 4, Berlin, Germany, September 11-14 2005, pp. 2535–2542.

[177] I. F. Progri, W. R. Michalson, J. Orr, and D. Cyganski, "A system for tracking and locating emergency personnel inside buildings," in *13th International Technical Meeting of the Satellite Division of the Institute of Navigation (ION GPS '00)*, Salt Lake City, UT, September 19-22 2000, pp. 560–568.

[178] I. F. Progri, W. R. Michalson, J. Wang, and M. C. Bromberg, "Indoor geolocation using FCDMA pseudolites: Signal structure and performance analysis," *Navigation*, vol. 54, no. 3, pp. 241 – 256, 2007.

[179] D. L. Pérez, "Measuring round trip times for distance estimation between WLAN nodes," Master's Thesis, Cork Institute of Technology, Cork, Ireland, August 2006.

[180] M. Rabinowitz and J. Spilker, "The Rosum television positioning technology," in *Proceedings of the ION 59th Annual Meeting and CIGTF 22nd Guidance Test Symposium*, Albuquerque, New Mexico, June 23-25 2003, pp. 528 – 541.

[181] A. L. Randall and R. C. Walter, "Overview of the small unit operations situational awareness system," in *IEEE Military Communications Conference (MILCOM)*, vol. 1, October 2003, pp. 169–173.

[182] J. Rantakokko and P. Händel, "Positioning of incident responders scenarios, user requirements and technological enablers," in *Precision Indoor Personnel Location and Tracking for Emergency Responders, Technology Workshop*, Worcester Polytechnic Institute, Worcester, MA, August 6-7 2007.

[183] J. Rantakokko, P. Händel, F. Eklöf, B. Boberg, M. Junered, D. Akos, I. Skog, H. Bohlin, F. Neregaard, F. Hoffmann, D. Andersson, M. Jansson, and P. Stenumgaard, "Positioning of emergency personnel in rescue operations - Possibilities and vulnerabilities with existing techniques and identification of needs for future R&D," Royal Institute of Technology (KTH), Stockholm, Sweden., Tech. Rep. TRITA-EE 2007:037, July 2007.

[184] H. E. Rauch, F. Tung, and C. T. Striebel, "Maximum likelihood estimates of linear dynamic systems," *AIAA Journal*, vol. 3, no. 8, pp. 1445–1450, 1965.

[185] V. Renaudin, B. Merminod, and M. Kasser, "Optimal data fusion for pedestrian navigation based on UWB and MEMS," in *IEEE/ION Position, Location and Navigation Symposium (PLANS '08)*, Monterey, CA, May 5-8 2008, pp. 341–349.

[186] V. Renaudin, O. Yalak, and P. Tomé, "Hybridization of MEMS and Assisted GPS for pedestrian navigation," *Inside GNSS*, pp. 34–42, January - February 2007. [Online]. Available: http://infoscience.epfl.ch/record/100277/files/IGM0207_Renaudin_WM.pdf

[187] V. Renaudin, O. Yalak, P. Tomé, and B. Merminod, "Indoor Navigation of Emergency Agents," *European Journal of Navigation*, vol. 5, no. 3, pp. 36–45, 2007.

[188] G. Retscher, "An intelligent multi-sensor system for pedestrian navigation," *Journal of Global Positioning Systems*, vol. 5, no. 1-2, pp. 110–118, 2006.

[189] B. Ristic, S. Arumpalampam, and N. Gordon, *Beyond the Kalman Filter: Particle Filters for Tracking Applications*, ser. Radar Library. Norwood, MA: Artech House Publishers, February 2004.

[190] C. Rizos, "Pseudolite augmentation of GPS," in *Workshop on Geolocation Technology to Support UXO Geophysical Investigations*, Annapolis, Maryland, USA, June 1-2 2005.

[191] P. Rosenrot and J. Wall, "The relationship between velocity, stride time, support time and swing time during normal walking," *Journal of Human Movement Studies*, vol. 6, pp. 323–335, 1980.

[192] J. Rouiller, D. Perrottet, Q. Ladetto, and B. Merminod, "Faciliter le déplacement des aveugles avec une carte numérique et une interface vocale," *Mensuration, Photogrammétrie, Génie rural*, pp. 517–521, August 2002.

[193] S. I. Roumeliotis, G. S. Sukhatme, and G. A. Bekey, "Circumventing dynamic modeling: Evaluation of the error-state Kalman filter applied to mobile robot localization," in *IEEE International Conference on Robotics and Automation (ICRA '99)*, vol. 2, Detroit, MI, May 10-15 1999, pp. 1656–1663.

[194] R. Rowe, P. Duffett-Smith, M. Jarvis, and N. Graube, "Enhanced GPS: The tight integration of received cellular timing signals and GNSS receivers for ubiquitous positioning," in *IEEE/ION Position, Location and Navigation Symposium (PLANS)*, Monterey, CA, May 2008, pp. 838–845.

[195] J. Saarinen, J. Suomela, S. Heikkila, M. Elomaa, and A. Halme, "Personal navigation system," in *Proc. IEEE/RSJ International Conference on Intelligent Robots and Systems (IROS 2004)*, vol. 1, Sendai, Japan, September 28 - October 2 2004, pp. 212–217.

[196] A. Sabatini, "Quaternion based strap-down integration method for applications of inertial sensing to gait analysis," *Medical & Biological Engineering & Computing (Med. Biol. Eng. Comput.)*, vol. 43, no. 1, pp. 94 – 101, 2005.

[197] K. Sagawa, H. Inooka, and Y. Satoh, "Non-restricted measurement of walking distance," in *IEEE International Conference on Systems, Man, and Cybernetics*, vol. 3, 2000, pp. 1847–1852 vol.3.

[198] C. Savarese, J. Rabaey, and J. Beutel, "Location in distributed ad-hoc wireless sensor networks," in *Proceedings of the IEEE International Conference on Acoustics, Speech, and Signal Processing, 2001. (ICASSP '01)*, vol. 4, 2001, pp. 2037–2040.

[199] R. D. Schraft, H. Rust, and H. R. Gehringer, "Sensors for the object detection in environments with high heat radiation and photoresist or diffuse visibility," in *The Sixth International Symposium Experimental Robotics VI*, ser. Lecture Notes in Control and Information Sciences, P. I. Corke and J. Trevelyan, Eds., vol. 250. Sydney, Australia: Springer, March 26-28 1999, pp. 69–78.

[200] P. Shan Hung and T. Chung Su, "Map-matching algorithms of GPS vehicle navigation systems," Geographic Information System Research Center, Reng Chia University, Tech. Rep., 1998.

[201] P. Sherman, A. Kourepenis, S. Holmes, H. Girolamo, G. Zimmer, and S. Sokolowski, "Personal navigation for the warfighter," in *Joint Navigation Conference (JNC)*, Orlando, FL, April 11-15 2005, sponsored by: DoD. (Draper Report no. P-4351).

[202] P. Sherman, A. Kourepenis, M. Matranga, M. McConley, J. Scudiere, T. Thorvaldsen, H. Girolamo, and S. Sokolowski, "Precision positioning system - autonomous GPS-denied navigation for the dismounted soldier," in *WPI Indoor Personnel Location and Tracking for Emergency Responders, Third Annual*

Technology Workshop, Worcester Polytechnic Institute, Worcester, MA, August 4-5 2008.

[203] P. Sherman and S. Holmes, "Personal navigation system," Draper Laboratory, Cambridge, MA, Final Report for June 2002 - April 2005, October 2005.

[204] S. Shin, C. Park, J. Kim, H. Hong, and J. Lee, "Adaptive step length estimation algorithm using low-cost MEMS inertial sensors," in *IEEE Sensors Applications Symposium (SAS '07)*, San Diego, California, USA, February 6-8 2007, pp. 1–5.

[205] J. Skaloud, *Navigation Techniques*, École Polytechnique Fédérale de Lausanne, Lausanne, Switzerland, June 2007, Graduate course notes.

[206] W. Soehren and W. Hawkinson, "A prototype personal navigation system," in *IEEE/ION Position, Location, And Navigation Symposium (PLANS '06)*, San Diego, CA, April 25-27 2006, pp. 539–546.

[207] W. E. Soehren, C. T. Bye, and C. L. Keyes, "Navigation system, method and software for foot travel," U.S. Patent 6 522 266, February 18, 2003.

[208] A. Soloviev and F. van Graas, "Utilizing multipath reflections in deeply integrated GPS/INS architecture for navigation in urban environments," in *IEEE/ION Position, Location and Navigation Symposium (PLANS)*, Monterey, CA, May 2008, pp. 383–393.

[209] I. Spassov, "Algorithms for map-aided autonomous indoor pedestrian positioning and navigation," Ph.D. dissertation, Ecole Polytechnique Federale de Lausanne (EPFL), Lausanne, Switzerland, November 2007.

[210] R. Stirling, "Development of a pedestrian navigation system using shoe-mounted sensors," M.Sc. Thesis, Department of Mechanical Engineering, University of Alberta, Calgary, Alberta, Canada, Spring 2004.

[211] R. Stirling, J. Collin, K. Fyfe, and G. Lachapelle, "An innovative shoe-mounted pedestrian navigation system," in *The European Navigation Conference (GNSS '03)*, Graz, Austria, April 22-25 2003.

[212] R. Stirling, K. Fyfe, and G. Lachapelle, "Evaluation of a new method of heading estimation for pedestrian dead reckoning using shoe-mounted sensors," *The Journal of Navigation*, vol. 58, pp. 31–45, 2005.

[213] O. Strauss, F. Comby, and M. Aldon, "Multibeam sonar image matching for terrain-based underwater navigation," *OCEANS '99 MTS/IEEE. Riding the Crest into the 21st Century*, vol. 2, pp. 882–887 vol.2, 1999.

[214] L. Sweeney, Jr., "Comparative benefits of various automotive navigation and routing technologies," in *IEEE Position Location and Navigation Symposium (PLANS)*, Atlanta, Georgia, April 22-26 1996, pp. 415–421.

[215] J. Syrjärinne, "Use of GPS in cellular phone industry," CGSIC Meeting Presentation, September 2001, Nokia Mobile Phones, Research and Technology Access.

[216] M. Tanigawa, H. Luinge, L. Schipper, and P. Slycke, "Drift-free dynamic height sensor using MEMS IMU aided by MEMS pressure sensor," in *5th Workshop on Positioning, Navigation and Communication (WPNC '08)*, Hannover, Germany, March 27 2008, pp. 191–196.

[217] D. Taylor, "Tracking first responders in GPS-denied environments using low-cost IMUs," in *WPI Indoor Personnel Location and Tracking for Emergency Responders, Third Annual Technology Workshop*, Worcester Polytechnic Institute, Worcester, MA, August 4-5 2008.

[218] C. Teolis, "TRX sentinel," in *WPI Indoor Personnel Location and Tracking for Emergency Responders, Third Annual Technology Workshop*, Worcester Polytechnic Institute, Worcester, MA, August 4-5 2008.

[219] S. Thrun, W. Burgard, and D. Fox, *Probabilistic Robotics*, ser. Intelligent Robotics and Autonomous Agents. Cambridge, Massachusetts: The MIT Press, 2005.

[220] A. N. Tikhonov and V. A. Arsenin, *Solution of Ill-posed Problems*. Washington: Winston & Sons, 1977.

[221] D. Titterton and J. Weston, *Strapdown Inertial Navigation Technology*, 2nd ed., ser. Progress in Astronautics and Aeronautics. The American Institute of Aeronautics and Astronautics, 2004, vol. 207.

[222] P. Tomé, F. Bonzon, B. Merminod, and K. Aminian, "Improving pedestrian dynamics modelling using fuzzy logic," in *4th International conference on pedestrian and evacuation dynamics (PED2008)*, 2008. [Online]. Available: www.ped2008.com

[223] S. J. Treado, A. Vinh, D. Holmberg, and M. Galler, "Building information for emergency responders," in *11th World Multi-Conference on Systemics, Cybernetics and Informatics (WMSCI 2007).*, N. Callaos, W. Lesso, C. Zinn, and H. Yang, Eds., vol. 3, Orlando, FL, July 8-11 2007, pp. 1–6, Held jointly with the 13th International Conference on Information Systems Analysis and Synthesis (ISAS 2007).

[224] E. Vildjiounaite, E.-J. Malm, J. Kaartinen, and P. Alahuhta, "Location estimation indoors by means of small computing power devices, accelerometers, magnetic sensors, and map knowledge," in *Pervasive 2002*, ser. Lecture Notes in Computer Science, F. Mattern and M. Naghshineh, Eds. Springer-Verlag Berlin Heidelberg, 2002, vol. 2414/2002, pp. 211–224.

[225] M. Vossiek, T. Schafer, and D. Becker, "Regenerative backscatter transponder using the switched injection-locked oscillator concept," in *IEEE MTT-S International Microwave Symposium Digest*, Atlanta, GA, June 15-20 2008, pp. 571–574.

[226] A. Waegli, "Trajectory analysis in sports by satellite and inertial navigation," Ph.D. dissertation, École Polytechnique Fédérale de Lausanne (EPFL), Lausanne, Switzerland, December 2008.

[227] H.-h. Wang, C.-r. Zhai, X.-q. Zhan, and D.-e. Song, "The research and geometric analysis of indoor positioning using multiple pseudolites signals," in *Congress on Image and Signal Processing (CISP '08)*, D. Li and G. Deng, Eds., vol. 5, Sanya, Hainan, China, May 27-30 2008, pp. 203–207.

[228] J. Wang, "Pseudolite applications in positioning and navigation: Progress and problems," *Journal of Global Positioning Systems*, vol. 1, no. 1, pp. 48–56, 2002.

[229] J. Wang, R. Babu, D. Li, F. Chan, and J. Choi, "Integrating GPS/INS/PL for robust positioning: The challenging issues," *Coordinates*, vol. 3, no. 7, pp. 12–19, 2007.

[230] Q. Wang, C. Rizos, Y. Li, and S. Li, "Application of a sigma-point Kalman filter for alignment of MEMS-IMU," in *IEEE/ION Position, Location and Navigation Symposium (PLANS '08)*, Monterey, CA, May 5-8 2008, pp. 44–52.

[231] A. Warnasch and A. Killen, "Low cost, high G, micro electro-mechanical systems (MEMS), inertial measurement unit (IMU) program," in *IEEE Position Location and Navigation Symposium (PLANS '02)*, 2002, pp. 299–305.

[232] E. Wasle, G. Abwerzger, P. Branco, and R. Nicole, "SHADE - System Architecture," in *The European Navigation Conference (GNSS 2004)*, Rotterdam, The Netherlands, May 2004.

[233] J. R. A. Watson, "High-sensitivity GPS L1 signal analysis for indoor channel modelling," MSc Thesis, Department of Geomatics Engineering, University of Calgary, Calgary, Canada, April 2005, Published as UCGE Report No. 20215.

[234] R. Watson, "GNSS-based indoor tracking: Approaches, developments, and test," in *WPI / CTC Technology Workshop on Precision Personnel Location and Tracking.* Worcester Polytechnic Institute, August 7-8 2006.

[235] N. Weber, S. Moedl, and M. Hackner, "A novel signal processing approach for microwave Doppler speed sensing," in *IEEE MTT-S International Microwave Symposium Digest*, vol. 3, Seattle, WA, June 2-7 2002, pp. 2233–2235.

[236] F. Weimann, J. Seybold, and B. Hofmann-Wellenhof, "Development of a pedestrian navigation system for urban and indoor environments," in *European Navigation Conference (GNSS '07)*, Geneva, Switzerland, May 29 - April 1 2007.

[237] J. P. Weiss, P. Axelrad, A. G. Dempster, C. Rizos, and S. Lim, "Estimation of simplified reflection coefficients for improved modeling of urban multipath," in *Proceedings of the 63rd Annual Meeting of the Institute of Navigation*, Cambridge, Massachusetts, April 23-25 2007, pp. 635–643.

[238] Widyawan, M. Klepal, and S. Beauregard, "A backtracking particle filter for fusing building plans with PDR displacement estimates," in *Proc. 5th Workshop on Positioning, Navigation and Communication (WPNC)*, Hannover, Germany, March 27-27 2008, pp. 207–212.

[239] Widyawan, M. Klepal, and D. Pesch, "A Bayesian Approach for RF-based Indoor Localisation," in *Proceedings of the 4th International Symposium on Wireless Communication Systems (ISWCS)*, Oct. 2007, pp. 133–137.

[240] Widyawan, M. Klepal, and S. Beauregard, "A novel backtracking particle filter for pattern matching indoor localization," in *1st ACM international workshop on Mobile entity localization and tracking in GPS-less environments (MELT '08)*, New York, NY, USA, 2008, pp. 79–84, co-located with the 14th Annual International Conference on Mobile Computing and Networking (MobiCom 2008).

[241] P. Wilson, D. Prashanth, and H. Aghajan, "Utilizing RFID signaling scheme for localization of stationary objects and speed estimation of mobile objects," in *IEEE International Conference on RFID*, Grapevine, TX, March 26-28 2007, pp. 94–99.

[242] S. Winslow, C. Kane, and A. Abdelhamied, "Concept of operations document," Office of Naval Research (ONR), Technical Report BAA 06-007, April 10 2007, created under contract by Mercury Data Systems 4214 Beechwood Drive Suite 105 Greensboro, NC 27410.

[243] O. Woodman and R. Harle, "Pedestrian localisation for indoor environments," in *Proceedings of the 10th international conference on Ubiquitous computing (UbiComp '08)*, Seoul, Korea, September 21-24 2008, pp. 114–123.

[244] W. M. Wynn, C. P. Frahm, P. J. Carroll, R. H. Clark, J. Wellhoner, and M. J. Wynn, "Advanced superconducting gradiometer/magnetometer arrays and a novel signal processing technique," *IEEE Transactions on Magnetics*, vol. MAG-11, no. 2, pp. 701–707, March 1975.

[245] Y. Yi, D. Grejner-Brzezinska, C. Toth, J. Wang, and C. Rizos, "GPS + INS + pseudolites," *GPS World*, vol. 14, no. 7, pp. 42–49, July 2003.

[246] H. Zhang, M. Petovello, and M. Cannon, "Performance comparison of kinematic GPS integrated with different tactical level IMUs," in *National Technical Meeting of the Institute of Navigation (ION NTM)*, San Diego, CA, January 24-26 2005, pp. 270–275.

[247] N. I. Ziedan, *GNSS Receivers for Weak Signals*, ser. GNSS Technology and Applications Series. Norwood, MA: Artech House Inc., 2006.